arXiv:1611.08030v1 [physics.flu-dyn] 23 Nov 2016

4-wave dynamics in kinetic wave turbulence

Sergio Chibbaro [a], Giovanni Dematteis[b], Lamberto Rondoni[b,c,d]

[a]*Sorbonne University, UPMC Univ Paris 06, CNRS, UMR 7190, Institut Jean Le Rond d'Alembert, F-75005 Paris, France;* [b]*Dipartimento di Scienze Matematiche, Politecnico di Torino;* [b]*Graphene@PoliTO Lab, Politecnico di Torino, Corso Duca degli Abruzzi 24, I-10129 Torino, Italy;* [d]*INFN, Sezione di Torino, Via P. Giuria 1, I-10125, Torino, Italy*

Abstract

A general Hamiltonian wave system with quartic resonances is considered, in the standard kinetic limit of a continuum of weakly interacting dispersive waves with random phases. The evolution equation for the multimode characteristic function Z is obtained within an "interaction representation" and a perturbation expansion in the small nonlinearity parameter. A frequency renormalization is performed to remove linear terms that do not appear in the 3-wave case. Feynman-Wyld diagrams are used to average over phases, leading to a first order differential evolution equation for Z. A hierarchy of equations, analogous to the Boltzmann hierarchy for low density gases is derived, which preserves in time the property of random phases and amplitudes. This amounts to a general formalism for both the N-mode and the 1-mode PDF equations for 4-wave turbulent systems, suitable for numerical simulations and for investigating intermittency.

Keywords: Weak wave turbulence, Kinetic theory, Intermittency

1. Introduction

Wave Turbulence theory (WT) concerns the dynamics of dispersive waves that interact nonlinearly over a wide range of scales[1]. In general the nonlinear interaction can be considered small, allowing a perturbative analysis and then an asymptotic closure for statistical observables[2]. Sometimes one then talks about Weak Wave Turbulence (WWT). Until recently, most of the attention was given the energy spectrum, which is governed by a kinetic equation. Wave turbulence also provides exact solutions of the kinetic equation, which are related to equipartition, Rayleigh-Jeans solution, or stationnary cascade, Kolmogorov-Zakharov solutions[3]. Many physical phenomena are studied within this general framework, for instance gravity [4, 5, 6], capillary or Alvèn waves [7, 8, 9, 10], non-linear optics[11] and elastic plates [12, 13, 14].

In the last years, many experiments and numerical simulations were performed to verify the predictions of WT. The picture is relatively clear in the case of the capillary waves on a fluid surface (water, ethanol, liquid hydrogen or liquid helium): both experiments and numerical simulations confirm the Kolmogorov-Zakharov spectrum predicted by WT in this case. For other cases, *e.g.* surface gravity waves or waves in vibrating elastic plates, the picture is more complicated: both numerics and experiments showed deviations from theoretical predictions, and the presence of intermittency [15, 16, 17]. This was unexpected, since WT appears as a mean-field theory, based on an initial "quasi-gaussianinty", which was thought to prevent sensible deviations from gaussianity.

In order to address this issue, a more detailed WT formalism for non-gaussian wavefields has been developed [18, 19, 20, 1]. In particular, the 3-wave and 4-wave resonant systems have been studied and a Peierls equation for the N-particles probability density function (PDF) has been proposed. These works have also clarified the different assumptions needed for the statistical closure.

Nevertheless, the Peierls equation does not guarantee preservation of the independence of phases and amplitudes[1]. Furthermore, Ref.[21] demonstrated for 3-wave resonant systems that previous works missed the normalization of the wave amplitudes necessary for a finite spectrum in the infinite-box limit, in which an amplitude density arises as a function of the continuous variable $\mathbf{k}$. For such a density to remain finite, the original amplitudes must be normalized by a factor scaling as $1/V$, where V is the volume of the box. Therefore, the Peierls equations for multimode PDF's are not the leading-order asymptotic equations of the continuum limit of weakly interacting, incoherent waves. This observation led to new multimode equations, that are simpler than Peierls equation and, importantly, that have exponential form solutions excluded by Peierls equation. The property of preserving exponential solutions implies a law of large numbers (LLN) for the quantity called empirical spectrum at times $\tau > 0$, which is analogous to the propagation of chaos of the BBGKY hierarchy in the kinetic theory of gases. This LLN implies that the empirical spectrum satisfies the wave-kinetic closure equations for nearly every initial realization of random phases and amplitudes (RPA), without necessity of averaging. Just as the Boltzmann hierarchy has factorized solutions for factorized initial conditions, so does the kinetic wave hierarchy for all multi-point spectral correlation functions. An H-theorem corresponding to positive entropy variation holds as well.

On the other hand, [21] showed using these multimode equations that the 1-mode PDF equations of Refs.[18, 19, 20] are correct, if the initial wave modes have statistically-independent RPA.

The present work addresses the cases with 4-waves interactions, because most of the known violations of gaussianity arise in gravity waves and in vibrating elastic plates, which are 4-wave resonant systems. We will show that a treatment analogous to that of Ref.[21] leads to the previously lacking leading-order equations for the evolution of 4-wave resonant systems, hence it sheds light also on the issue of WT intermittency. In particular, we are going to use the correct normalization of amplitudes, for a generic 4-wave resonant Hamiltonian system.

This work is organized as follows. Below, we describe our models and, for sake of consistency, where possible we use the notation of Ref.[21]. Section 2 discusses the probabilistic properties of RPA fields. The main results of this paper are reported in section 3-4, where the multimode equations are derived and discussed. This is done first in Section 3 for the spectral generating functional and correlation functions, and then in Section 4 for the PDF generating functions and correlation functions. Technical details are provided in Appendix A, Appendix B and Appendix C. Appendix C briefly explains the diagrams used to calculate the averages. Section 5 summarizes our results.

1.1. Model and notation

Similarly to [21], we consider a complex wavefield $u(\mathbf{x}, t)$ in a d-dimensional periodic cube with side L. This field is a linear combination of the canonical coordinates and momenta. It is assumed that there is a maximum wavenumber $k_{\max}$, to avoid ultraviolet divergences. This can be achieved by a lattice regularization with spacing $a = L/M$, for some large integer M, so that $k_{\max} = \pi/a$. The location variable x then ranges over the physical space

$$\Lambda_L = a\mathbb{Z}_M^d, \tag{1}$$

with the usual notation $\mathbb{Z}_M$ for the field of integers, modulo M. This space has volume $V = L^d$. The dual space of wavenumbers is

$$\Lambda_L^* = \frac{2\pi}{L}\mathbb{Z}_M^d \tag{2}$$

with $k_{\min} = 2\pi/L$. The total number of modes is $N = M^d$, so that $V = Na^d$. The following index notation will be used:

$$u^\sigma(\mathbf{x}) = \begin{cases} u(\mathbf{x}) & \sigma = +1 \\ u^*(\mathbf{x}) & \sigma = -1 \end{cases} \tag{3}$$

[1] Or better: [18], Section 5, and [1], Section 11.4, argue that the property of Random Phases and Amplitudes (see Section 2) is preserved in a somewhat weaker form.

for u and its complex-conjugate u^*. Likewise, we adopt the convention for (discrete) Fourier transform:

$$A^\sigma(\mathbf{k}) = \frac{1}{N}\sum_{\mathbf{x}\in\Lambda_L} u^\sigma(\mathbf{x},t)\exp(-i\sigma\mathbf{k}\cdot\mathbf{x}) \tag{4}$$

so that $A^+(\mathbf{k})$ and $A^-(\mathbf{k})$ are complex conjugates. This quantity converges to the continuous Fourier transform $\frac{1}{L^d}\int_{[0,L]^d} d^dx\ u^\sigma(\mathbf{x},t)\exp(-i\sigma\mathbf{k}\cdot\mathbf{x})$ in the limit $a\to 0$. The discrete inverse transform is

$$u^\sigma(\mathbf{x}) = \sum_{\mathbf{k}\in\Lambda_L^*} A^\sigma(\mathbf{k})\exp(i\sigma\mathbf{k}\cdot\mathbf{x}). \tag{5}$$

The dynamics is assumed to be canonical Hamiltonian, with a 4^{th} power term in the Hamiltonian density (energy per volume) describing 4-wave interactions. As in [3] and with lattice regularization, we write:

$$H = H_0 + \delta H\ , \quad H_0 = \frac{1}{2}\sum_{\mathbf{k}\in\Lambda^*}\omega_{\mathbf{k}}|A_{\mathbf{k}}|^2 \tag{6}$$

Taking the most general Hamiltonian with any kind of 4-wave interactions, [3], one can write $\delta\mathcal{H}$ in the symmetrized compact form:

$$\delta H = \epsilon\sum_{1234}\mathcal{H}_{1234}^{\sigma_1\sigma_2\sigma_3\sigma_4}\ A_1^{\sigma_1}A_2^{\sigma_2}A_3^{\sigma_3}A_4^{\sigma_4}\ \delta_{1234} \tag{7}$$

with the coefficients satisfying the general relations:

$$(\mathcal{H}_{1234}^{\sigma_1\sigma_2\sigma_3\sigma_4})^* = \mathcal{H}_{1234}^{-\sigma_1-\sigma_2-\sigma_3-\sigma_4}\ , \quad \mathcal{H}_{1234}^{\sigma_1\sigma_2\sigma_3\sigma_4} = \mathcal{H}_{\Pi(1234)}^{\Pi(\sigma_1\sigma_2\sigma_3\sigma_4)}. \tag{8}$$

$\Pi\in S^4$ represents any permutation of the four elements. Introducing further notation:

$$\begin{aligned}
&\underline{\sigma}\doteq(\sigma_1,\sigma_2,\sigma_3,\sigma_4)\ , \qquad \underline{\mathbf{k}}\doteq(\mathbf{k}_1,\mathbf{k}_2,\mathbf{k}_3,\mathbf{k}_4)\ , \qquad \delta_{\underline{\sigma}\cdot\underline{\mathbf{k}},\mathbf{0}} = \delta_{\sigma_1\mathbf{k}_1+\sigma_2\mathbf{k}_2+\sigma_3\mathbf{k}_3+\sigma_4\mathbf{k}_4,\mathbf{0}}\\
&\omega_1\doteq\omega(\mathbf{k}_1)\ , \qquad A_1\doteq A(\mathbf{k}_1)\ , \qquad \sum_1\doteq\sum_{\sigma_1=\pm1}\sum_{\mathbf{k}_1\in\Lambda^*}
\end{aligned} \tag{9}$$

the Hamiltonian can be written as:

$$H = \frac{1}{2}\sum_1\omega_1 A_1^{\sigma_1}A_1^{-\sigma_1} + \epsilon\sum_{1234}\mathcal{H}_{\underline{\mathbf{k}}}^{\underline{\sigma}}\ A_1^{\sigma_1}A_2^{\sigma_2}A_3^{\sigma_3}A_4^{\sigma_4}\ \delta_{\underline{\sigma}\cdot\underline{\mathbf{k}},\mathbf{0}} \tag{10}$$

which leads to

$$\frac{\partial A_{\mathbf{k}}^\sigma}{\partial t} = i\sigma\omega_{\mathbf{k}}A_{\mathbf{k}}^\sigma + \epsilon\sum_{234}\mathcal{L}_{\mathbf{k}234}^{\sigma\sigma_2\sigma_3\sigma_4}A_2^{\sigma_2}A_3^{\sigma_3}A_4^{\sigma_4}\delta_{-\mathbf{k}+\sigma_2\mathbf{k}_2+\sigma_3\mathbf{k}_3+\sigma_4\mathbf{k}_4,\mathbf{0}} \tag{11}$$

where

$$\mathcal{L}_{\mathbf{k}234}^{\sigma\sigma_2\sigma_3\sigma_4}\doteq 4i\sigma\mathcal{H}_{\mathbf{k}234}^{(-\sigma)\sigma_2\sigma_3\sigma_4}. \tag{12}$$

Changing $\mathbf{k}\to\mathbf{k}_1$ and introducing the interaction representation[2] $A_{\mathbf{k}}^\sigma = a_{\mathbf{k}}^\sigma e^{i\sigma\omega_{\mathbf{k}}t}$, one obtains[3]:

$$\begin{aligned}
\frac{\partial a_1}{\partial t} \quad = \quad & \epsilon\sum_{234}\mathcal{L}_{1234}^{+\sigma_2\sigma_3\sigma_4}a_2^{\sigma_2}a_3^{\sigma_3}a_4^{\sigma_4}\\
& \times\exp\left[i\left(-\omega_1+\sigma_2\omega_2+\sigma_3\omega_3+\sigma_4\omega_4\right)t\right]\delta_{-\mathbf{k}_1+\sigma_2\mathbf{k}_2+\sigma_3\mathbf{k}_3+\sigma_4\mathbf{k}_4,\mathbf{0}}
\end{aligned} \tag{13}$$

[2] Such a representation eliminates the fast linear oscillations, giving a variable $a_{\mathbf{k}}^\sigma$ that does not oscillate on fast scales.

[3] In our derivation, for simplicity and no loss of generality, we consider $\sigma=+1$. Trivially, the equations with $\sigma=-1$ are redundant, because obtained by complex conjugation of the ones with $\sigma=+1$. From now a_1 stands for a_1^+.

With notation [21]:

$$\begin{aligned} \mathcal{L}_{1234} &\doteq \mathcal{L}_{1234}^{+\sigma_2\sigma_3\sigma_4}\,, \qquad \omega_{234}^1 \doteq -\sigma_1\omega_1 + \sigma_2\omega_2 + \sigma_3\omega_3 + \sigma_4\omega_4 \\ \delta_{234}^1 &\doteq \delta_{-\sigma_1\mathbf{k}_1+\sigma_2\mathbf{k}_2+\sigma_3\mathbf{k}_3+\sigma_4\mathbf{k}_4,\mathbf{0}} \end{aligned} \tag{14}$$

the dynamical equation of motion with 4-wave interactions now reads:

$$\dot{a}_1 = \epsilon \sum_{234} \mathcal{L}_{1234} a_2^{\sigma_2} a_3^{\sigma_3} a_4^{\sigma_4} \exp\left(i\omega_{234}^1 t\right) \delta_{234}^1 \tag{15}$$

2. Fields with random phases and amplitudes

In derivations of wave kinetic equations, it is often assumed that initial fields have Fourier coefficients with random statistically independent phases and amplitudes (RPA). This property is expected to be preserved in time, in some suitable sense, in the wave-kinetic limit.

Let N complex-valued random variables $a_{\mathbf{k}}$, $\mathbf{k} \in \Lambda_L^*$ be the Fourier coefficients of a random field:

$$u_L(\mathbf{x}) = \sum_{\mathbf{k}\in\Lambda_L^*} a_{\mathbf{k}} \exp(i\mathbf{k}\cdot\mathbf{x}). \tag{16}$$

Here $a_{\mathbf{k}}$ corresponds to $a_{\mathbf{k}}^+$, i.e. $A_{\mathbf{k}}^+$ in the previous section (no distinction need be made between the two at time $t = 0$). It will be crucial in the following to work with normalized variables

$$\widetilde{a}_{\mathbf{k}} = \left(\frac{L}{2\pi}\right)^{d/2} a_{\mathbf{k}} \tag{17}$$

which are assumed to remain finite in the large-box limit $L \to \infty$. This normalization is sufficient for the spectrum of the random field to be well defined in that limit, as first pointed out in [21]. It is convenient to write the complex variables in polar coordinates (action-angle variables, or amplitudes and phases)

$$a_{\mathbf{k}} = \sqrt{J_{\mathbf{k}}} e^{i\varphi_{\mathbf{k}}} = \sqrt{J_{\mathbf{k}}} \psi_{\mathbf{k}}^{\mu_{\mathbf{k}}} \tag{18}$$

with normalized action defined by

$$\widetilde{J}_{\mathbf{k}} = \left(\frac{L}{2\pi}\right)^{d} J_{\mathbf{k}}. \tag{19}$$

We denote by $s_{\mathbf{k}}$ and $\xi_{\mathbf{k}}$ for possible values of the random variables $\widetilde{J}_{\mathbf{k}} \in \mathbb{R}^+$ and $\psi_{\mathbf{k}} = e^{i\varphi_{\mathbf{k}}} \in S^1$.

$$d\mu(s,\xi) = \prod_{\mathbf{k}\in\Lambda_L^*} ds_{\mathbf{k}} \frac{|d\xi_{\mathbf{k}}|}{2\pi} \tag{20}$$

suitably normalized. The N-mode joint probability density function $\mathcal{P}^{(N)}(s,\xi)$ is defined with respect to the Liouville measure, such that the average of the random variable $f_{\tilde{J}_\psi}(s,\xi)$ is given by

$$\langle f_{\tilde{J}_\psi} \rangle = \int d\mu(s,\xi)\, \mathcal{P}^{(N)}(s,\xi) f(s,\xi) \tag{21}$$

where the integral is over (s,ξ) in the product space $\left(\mathbb{R}^+\right)^N \times \left(S^1\right)^N$.

As in Ref.[21], the field $u_L(\mathbf{x})$ is called a *random-phase field* (RP) if for all $\mathbf{k} \in \Lambda_L^*$ the $\psi_{\mathbf{k}} = e^{i\varphi_{\mathbf{k}}}$ are independent and identically distributed (i.i.d.) random variables, uniformly distributed over the unit circle S^1 in the complex plane. For the joint PDF, this is equivalent to:

$$\mathcal{P}^{(N)}(s,\xi) = \mathcal{P}^{(N)}(s) \tag{22}$$

Note that an RP $u_L(\mathbf{x})$ is a homogeneous random field on Λ_L, statistically invariant under space-translations by the finite group $a\mathbb{Z}^d_M$. In the limit $L \to \infty$ the field $u_L(\mathbf{x})$ defined with appropriately chosen $\tilde{J}_{\mathbf{k},L}$ will converge to a homogeneous random field $u(\mathbf{x})$ invariant under translations by $a\mathbb{Z}^d$. The standard definition of the spectrum $n(\mathbf{k}) = \lim_{L\to\infty}(L/2\pi)^d\langle|a_{\mathbf{k},L}|^2\rangle$ implies that one must choose

$$\lim_{L\to 0}\langle\tilde{J}_{\mathbf{k}_L,L}\rangle = n(\mathbf{k}), \tag{23}$$

for $\mathbf{k} \in \Lambda^* = [-k_{\max}, +k_{\max}]^d$, where $\mathbf{k}_L = \frac{\mathbf{k}L}{2\pi}(\mathrm{mod}\, M)\cdot\frac{2\pi}{L} \in \Lambda^*_L$ converges to $\mathbf{k}$ as $L = aM \to \infty$ (for fixed a). So, $u_L(\mathbf{x})$ converges in distribution to a homogeneous field $u(\mathbf{x})$ with spectrum $n(\mathbf{k})$.

Let $u_L(\mathbf{x})$ be a *random-phase and amplitude field* (RPA) if $u_L(\mathbf{x})$ is RP and if also $\tilde{J}_{\mathbf{k}}$ are mutually independent random variables for all $\mathbf{k} \in \Lambda^*_L$. This is equivalent to the factorization of the N-mode PDF into a product of 1-mode PDF's:

$$\mathcal{P}^{(N)}(s) = \prod_{\mathbf{k}\in\Lambda^*_L} P(s_{\mathbf{k}};\mathbf{k}). \tag{24}$$

All homogeneous Gaussian random fields are RPA. Conversely, for any sequence of RPA fields satisfying condition (23) the spatial field $u_L(\mathbf{x})$ converges in distribution to the homogeneous Gaussian field with mean zero and spectrum $n(\mathbf{k})$ as $L \to \infty$ [22]. Here we note only that

$$u_L(\mathbf{x}) = \left(\frac{2\pi}{L}\right)^{d/2}\sum_{\mathbf{k}\in\Lambda^*_L}\sqrt{\tilde{J}_{\mathbf{k},L}}\exp(i\mathbf{k}\cdot\mathbf{x} + i\varphi_{\mathbf{k}}) \tag{25}$$

is a sum of N independent variables scaled by $1/\sqrt{N}$. It is important to emphasize that the Fourier coefficients $\widetilde{a}_{\mathbf{k},L}$ can remain far from Gaussian in this limit. In physical space also there are non-vanishing cumulants for large but finite L.

Let us define the characteristic functional, containing information about the statistical distribution of amplitudes and phases:

$$\mathcal{Z}_L(\lambda,\mu) = \left\langle \exp\left[\int d\mathbf{k}(i\lambda_{\mathbf{k}}J_{\mathbf{k}} + i\mu_{\mathbf{k}}\phi_{\mathbf{k}})\right]\right\rangle \tag{26}$$

A most important result for RPA fields is that the *empirical spectrum*

$$\widehat{n}_L(\mathbf{k}) = \left(\frac{2\pi}{L}\right)^d\sum_{\mathbf{k}_1\in\Lambda^*_L}\tilde{J}_{\mathbf{k}_1,L}\delta^d(\mathbf{k}-\mathbf{k}_1), \quad \mathbf{k}\in\Lambda^* \tag{27}$$

converges under the condition (23) to the deterministic spectrum $n(\mathbf{k})$ with probability going to 1 in the limit $L \to \infty$ (weak LLN). One can show that $\int d^dk\ \lambda(\mathbf{k})\ \widehat{n}_L(\mathbf{k})$ converges in probability to $\int d^dk\ \lambda(\mathbf{k})n(\mathbf{k})$ for every bounded, continuous λ. This is sufficient to infer that the amplitude characteristic function defined in (26) satisfies

$$\lim_{L\to\infty}\mathcal{Z}_L(\lambda) = \exp\left(i\int d^dk\ \lambda(\mathbf{k})n(\mathbf{k})\right) \tag{28}$$

with $n(\mathbf{k})$ the deterministic spectrum. The LLN means that for RPA fields the empirical spectrum $\widehat{n}_L(\mathbf{k})$ coincides with $n(\mathbf{k})$ at large L for almost every realization of the random phases and amplitudes.

Notice that for the above result one does not actually need the full independence assumption in RPA, but it suffices that

$$\lim_{L\to\infty}[\mathcal{N}^{(2)}_L(\mathbf{k}_1,\mathbf{k}_2) - \mathcal{N}^{(1)}_L(\mathbf{k}_1)\mathcal{N}^{(1)}_L(\mathbf{k}_2)] = 0, \tag{29}$$

where the M-th order correlation functions are defined as

$$\mathcal{N}^{(M)}_L(\mathbf{k}_1,...,\mathbf{k}_M) = \langle\widehat{n}_L(\mathbf{k}_1)\cdots\widehat{n}_L(\mathbf{k}_M)\rangle. \tag{30}$$

Property (29) is analogous to Boltzmann's *Stosszahlansatz* for his kinetic equation. Under this assumption, the M-th order correlations that exist will factorize in the large-box limit [23, 24]:

$$\lim_{L\to\infty} \mathcal{N}_L^{(M)}(\mathbf{k}_1, ..., \mathbf{k}_M) = \prod_{m=1}^{M} n(\mathbf{k}_m). \tag{31}$$

Our results indicate that properties RP and (23,29) for the initial wave field, suffice for the wave kinetic equation and for the LLN for the empirical spectrum to hold at positive times.

RPA fields whose Fourier amplitudes possess the full independence property satisfy the even stronger LLN for the *empirical 1-mode PDF*

$$\widehat{P}_L(s;\mathbf{k}) = \left(\frac{2\pi}{L}\right)^d \sum_{\mathbf{k}_1\in\Lambda_L^*} \delta(s - \tilde{J}_{\mathbf{k}_1})\delta^d(\mathbf{k}-\mathbf{k}_1). \tag{32}$$

Assume that the limiting random variables $\tilde{J}_{\mathbf{k}} = \lim_{L\to\infty} \tilde{J}_{\mathbf{k}_L,L}$ of an RPA field exist and have PDF's $P(s;\mathbf{k})$ which are continuous in $\mathbf{k}$. Then, the random functions $\widehat{P}_L(s;\mathbf{k})$ converge to $P(s;\mathbf{k})$ with probability approaching 1 as $L\to\infty$. This implies the previous LLN for the spectrum, since $\widehat{n}_L(\mathbf{k}) = \int_0^\infty ds\, s\widehat{P}_L(s;\mathbf{k})$ and $n(\mathbf{k}) = \int_0^\infty ds\, sP(s;\mathbf{k})$. Although the "empirical PDF" defined in (32) is mathematically very convenient, it is not a PDF for finite L. It is therefore more intuitive to use an alternative definition

$$\widehat{P}_L(s;\Delta) = \frac{1}{N_L(\Delta)} \sum_{\mathbf{k}\in\Lambda_L^*\cap\Delta} \delta(s-\tilde{J}_{\mathbf{k}}), \tag{33}$$

for any open set $\Delta\subset\Lambda^*$ and with $N_L(\Delta)$ the number of elements in $\Lambda_L^*\cap\Delta$. This quantity is nearly the same as $\frac{1}{|\Delta|}\int_\Delta d^dk\ \widehat{P}_L(s;\mathbf{k})$ for large L but it has the advantage that it defines a probability measure in s for each fixed Δ and L. Definition (33) also has a simple intuitive meaning, since it represents the instantaneous distribution of amplitudes of the large number of Fourier modes that reside in the set Δ for large box-size L. Under the same assumptions as above, it follows with probability going to 1 that

$$\lim_{L\to\infty} \widehat{P}_L(s;\Delta) = \frac{1}{|\Delta|}\int_\Delta d^dk\ P(s;\mathbf{k}) \equiv P(s;\Delta). \tag{34}$$

Strict independence is not necessary for this to hold; factorization of *multimode PDF*'s for $\mathbf{k}_1, ..., \mathbf{k}_M \in \Lambda^*$ is required:

$$\mathcal{P}_L^{(M)}(s_1, ..., s_M; \mathbf{k}_1, ..., \mathbf{k}_M) = \langle \delta(s_1 - \tilde{J}_{\mathbf{k}_{1,L},L}) \cdots \delta(s_M - \tilde{J}_{\mathbf{k}_{M,L},L})\rangle. \tag{35}$$

The factorization property for all pairs of distinct $\mathbf{k}_1, \mathbf{k}_2 \in \Lambda^*$

$$\lim_{L\to\infty} [\mathcal{P}_L^{(2)}(s_1, s_2; \mathbf{k}_1, \mathbf{k}_2) - \mathcal{P}_L^{(1)}(s_1;\mathbf{k}_1)\mathcal{P}_L^{(1)}(s_2;\mathbf{k}_2)] = 0 \tag{36}$$

suffices for the LLN for the empirical PDF and also the factorization of the multi-mode PDF's

$$\lim_{L\to\infty} \mathcal{P}_L^{(M)}(s_1, ..., s_M; \mathbf{k}_1, ..., \mathbf{k}_M) = \prod_{m=1}^{M} P(s_m;\mathbf{k}_m) \tag{37}$$

for all integers $M > 2$ and distinct $\mathbf{k}_1, ..., \mathbf{k}_M \in \Lambda^*$. The asymptotic independence is considerably weaker than RPA, permitting statistical dependence between Fourier modes at finite L. In the following, we show that properties (31), (37) are preserved by the limiting kinetic hierarchies of WT.

3. Multimode hierarchy equations

In this section we formally derive the multimode kinetic equations for the 4-wave dynamics of our system, analogously to Ref.[21]. Our analysis differs from those of Refs.[18, 19] mainly because of the nonlinear frequency shift, and because of the $L\to\infty$ and $\epsilon\to 0$ limits [21].

The action-angle variables (amplitudes and phases) for linear dynamics are defined as $J_{\mathbf{k}} = |A^{\sigma}_{\mathbf{k}}|^2$ and $\varphi_{\mathbf{k}} = \sigma \arg(A^{\sigma}_{\mathbf{k}})$, so that $A^{\sigma}_{\mathbf{k}} = \sqrt{J_{\mathbf{k}}}\psi^{\sigma}_{\mathbf{k}}$, where $\psi_{\mathbf{k}} = \exp(i\varphi_{\mathbf{k}})$. Then, the Liouville measure μ conserved by the Hamiltonian flow can be written as

$$d\mu = \prod_{\mathbf{k}} dQ_{\mathbf{k}} dP_{\mathbf{k}} = \prod_{\mathbf{k}} \frac{1}{i} dA^{+}_{\mathbf{k}} dA^{-}_{\mathbf{k}} = \prod_{\mathbf{k}} \frac{1}{i} da^{+}_{\mathbf{k}} da^{-}_{\mathbf{k}} = \prod_{\mathbf{k}} dJ_{\mathbf{k}} d\varphi_{\mathbf{k}} \tag{38}$$

The canonical momenta and coordinates are given by real and imaginary parts of $A^{\sigma}_{\mathbf{k}} = \frac{1}{\sqrt{2}}(P_{\mathbf{k}} + i\sigma Q_{\mathbf{k}})$, and $A^{\sigma}_{\mathbf{k}}$ and $a^{\sigma}_{\mathbf{k}}$ are linked by the simple rotation in the complex plane used to obtain (13). The generating function of amplitudes and phases for finite box-size L is as in [21]:

$$\mathcal{Z}_L[\lambda, \mu, T] \doteq \left\langle \exp\left(\sum_{\mathbf{k}\in\Lambda^*_L} \lambda_{\mathbf{k}} J_{\mathbf{k}}(T) \right) \prod_{\mathbf{k}\in\Lambda^*_L} \psi^{\mu_{\mathbf{k}}}_{\mathbf{k}}(T) \right\rangle \tag{39}$$

$$\lambda_{\mathbf{k}} \in \mathbb{R}, \quad \mu_{\mathbf{k}} \in \mathbb{Z} \qquad \forall \mathbf{k} \in \Lambda^*_L$$

3.1. Power Series Expansion in the Dynamical Equation

3.1.1. The frequency shift

Let us perturbatively expand the solution of Eq.(15) in ϵ at finite L. As explained in [21] and [1], we consider an intermediate time between the "linear time", that is the wave period, and the "nonlinear time" that represents the time scale of evolution of the wave amplitude statistics. To consider the long-time behavior of the wave field expanding in ϵ the solution of the dynamical equation, we need to renormalize the frequency [18, 1]. The equation for the order zero in ϵ has a constant solution:

$$a^{(0)}_1(T) = a_1(0), \tag{40}$$

Thus, the terms like $\sum_{234} \mathcal{L}_{1234} a^{(0)}_2 a^{(0)}_3 a_4 \exp\left(i\omega^1_{234} t\right) \delta^1_{234}$, for $\mathbf{k}_2 = \mathbf{k}_3$, $\sigma_2 = -\sigma_3$ and $\mathbf{k}_4 = \mathbf{k}_1$, play the role of linear terms in a_1, responsible for fast oscillations. We want to remove all terms of this kind, using an interaction representation and a frequency renormalization [18]:

$$\sum_{234}{}^{**} \doteq \sum_{\sigma_2\sigma_3\sigma_4} \sum_{\mathbf{k}_2\mathbf{k}_3\mathbf{k}_4} \delta_{\sigma_2,\sigma_1} \delta_{\sigma_3,-\sigma_4} \delta_{\mathbf{k}_2,\mathbf{k}_1} \delta_{\mathbf{k}_3,\mathbf{k}_4} + (2 \leftrightarrow 3) + (2 \leftrightarrow 4) \tag{41}$$

$$\sum_{234}{}^{*} \doteq \left(\sum_{\sigma_2\sigma_3\sigma_4} \sum_{\mathbf{k}_2\mathbf{k}_3\mathbf{k}_4} - \sum_{234}{}^{**} \right) \tag{42}$$

Recalling Eq.(15), we can write:

$$\begin{aligned} \dot{a}_1 &= \epsilon \left(\sum_{234}{}^{*} + \sum_{234}{}^{**} \right) \mathcal{L}^{+\sigma_2\sigma_3\sigma_4}_{1234} a^{\sigma_2}_2 a^{\sigma_3}_3 a^{\sigma_4}_4 \exp\left(i\omega^1_{234} t\right) \delta^1_{234} \\ &= \epsilon \sum_{234}{}^{*} \mathcal{L}^{+\sigma_2\sigma_3\sigma_4}_{1234} a^{\sigma_2}_2 a^{\sigma_3}_3 a^{\sigma_4}_4 \exp\left(i\omega^1_{234} t\right) \delta^1_{234} + i\,\Omega_1\, a_1 + \epsilon^2 \mathcal{D}_1 a_1 \end{aligned} \tag{43}$$

where

$$i\Omega_1 \doteq \epsilon \sum_{\sigma_2=\pm 1} \sum_{\mathbf{k}_2} \mathcal{L}^{++\sigma_2-\sigma_2}_{1122} \left|a^{(0)}_2\right|^2 + (2 \leftrightarrow 3) + (2 \leftrightarrow 4) \tag{44}$$

and $\mathcal{D}_1 = O(1)$. Introducing a new interaction representation with

$$b_{\mathbf{k}} = a_{\mathbf{k}} e^{-i\Omega_{\mathbf{k}} t} \tag{45}$$

Eq.(43) becomes:

$$\dot{b}_1 = \epsilon \sum_{234}{}^{*} \mathcal{L}^{+\sigma_2\sigma_3\sigma_4}_{1234}\, b^{\sigma_2}_2 b^{\sigma_3}_3 b^{\sigma_4}_4\, e^{i\tilde{\omega}^1_{234} t}\, \delta^1_{234} + \epsilon^2 \mathcal{D}_1 b_1 \tag{46}$$

where the renormalized frequency with a shift is given by [18, 1]:

$$\tilde{\omega}_{\mathbf{k}} \doteq \omega_{\mathbf{k}} + \Omega_{\mathbf{k}} \tag{47}$$

3.1.2. 2^{nd} order equations

Considering an intermediate time between the linear and the nonlinear time ($\frac{2\pi}{\tilde{\omega}_{\mathbf{k}}} << T << \frac{2\pi}{\epsilon^2\tilde{\omega}_{\mathbf{k}}}$), the solution of Eq.(46) to second order in ϵ is:

$$b_{\mathbf{k}}(T) = b_{\mathbf{k}}^{(0)}(T) + \epsilon b_{\mathbf{k}}^{(1)}(T) + \epsilon^2 b_{\mathbf{k}}^{(2)}(T) + O(\epsilon^3) \tag{48}$$

which implies

$$b_1^{(0)}(T) = b_1(0) \tag{49}$$

$$b_1^{(1)}(T) = \sum_{234}{}^{*} \mathcal{L}_{1234} b_2^{(0)} b_3^{(0)} b_4^{(0)} \Delta_T(\tilde{\omega}_{234}^1)\delta_{234}^1 \tag{50}$$

$$\begin{aligned} b_1^{(2)}(T) = & \sum_{234567}{}^{*} \mathcal{L}_{1234}\mathcal{L}_{4567}\, b_2^{(0)} b_3^{(0)} b_5^{(0)} b_6^{(0)} b_7^{(0)} E_T\left(\tilde{\omega}_{234}^1 \tilde{\omega}_{23567}^1\right) \delta_{234}^1 \delta_{567}^4 \\ & + (4 \leftrightarrow 3) + (4 \leftrightarrow 2) + \int_0^T \mathcal{D}_1 b_1^{(0)} dt \end{aligned} \tag{51}$$

where

$$\Delta_T(x) \doteq \int_0^T \exp(ixt)dt\ , \quad E_T(x,y) \doteq \int_0^T \Delta_t(x-y)\exp(iyt)dt \tag{52}$$

and

$$\begin{aligned} \sum_{234567}{}^{**} \ \doteq \ & \sum_{\sigma_2\sigma_3\ldots\sigma_7} \sum_{\mathbf{k}_2\mathbf{k}_3\ldots\mathbf{k}_7} \delta_{\sigma_2,\sigma_1}\delta_{\sigma_3,-\sigma_4}\delta_{\sigma_4,\sigma_5}\delta_{\sigma_6,-\sigma_7} \\ & \times\delta_{\mathbf{k}_2,\mathbf{k}_1}\delta_{\mathbf{k}_3,\mathbf{k}_4}\delta_{\mathbf{k}_4,\mathbf{k}_5}\delta_{\mathbf{k}_6,\mathbf{k}_7} + (2 \leftrightarrow 3) + (2 \leftrightarrow 4) \\ & + (5 \leftrightarrow 6) + (5 \leftrightarrow 7) + (2 \leftrightarrow 3, 5 \leftrightarrow 6) + (2 \leftrightarrow 4, 5 \leftrightarrow 6) \\ & + (2 \leftrightarrow 3, 5 \leftrightarrow 7) + (2 \leftrightarrow 4, 5 \leftrightarrow 7) \end{aligned} \tag{53}$$

$$\sum_{234567}{}^{*} \ \doteq \ \left(\sum_{\sigma_2\sigma_3\ldots\sigma_7} \sum_{\mathbf{k}_2\mathbf{k}_3\ldots\mathbf{k}_7} - \sum_{234567}{}^{**} \right) \tag{54}$$

$$\mathcal{D}_1 \doteq \sum_{\sigma_2=\pm 1} \sum_{\mathbf{k}_2} \mathcal{L}_{1122}^{++\sigma_2-\sigma_2} \left(b_2^{(0)} b_2^{(1)*} + b_2^{(1)} b_2^{(0)*} \right) + (2 \leftrightarrow 3) + (2 \leftrightarrow 4) \tag{55}$$

3.2. Phase averaging: Feynman-Wyld Diagrams

In this section we essentially follow the computations in Appendix of [19]. An expansion like (48) for the original normal variables $A_{\mathbf{k}}$ may be written as

$$A_{\mathbf{k}}(T) = A_{\mathbf{k}}^{(0)}(T) + \epsilon A_{\mathbf{k}}^{(1)}(T) + \epsilon^2 A_{\mathbf{k}}^{(2)}(T) + O(\epsilon^3) \tag{56}$$

where:

$$b_{\mathbf{k}}^{(i)} = A_{\mathbf{k}}^{(i)} e^{-i\tilde{\omega}t}, \quad i = 0, 1, 2 \tag{57}$$

and a similar expansion Equation (56) leads to:

$$J_{\mathbf{k}}(T) = |A_{\mathbf{k}}(T)|^2 = |b_{\mathbf{k}}(T)|^2 \doteq J_{\mathbf{k}}^{(0)} + \epsilon J_{\mathbf{k}}^{(1)} + \epsilon^2 J_{\mathbf{k}}^{(2)} + O(\epsilon^3) \tag{58}$$

Definition (39) shows that $\mathcal{Z}_L$ satisfies the simmetry:

$$\mathcal{Z}_L\left[\lambda, \mu, T\right] = \mathcal{Z}_L^*\left[\lambda, -\mu, T\right] \tag{59}$$

Therefore, writing

$$\mathcal{Z}_L\left[\lambda, \mu, T\right] = \chi_L\left\{\lambda, \mu, T\right\} + \chi_L^*\left\{\lambda, -\mu, T\right\} \tag{60}$$

one eventually gets:

$$\chi_L\left\{\lambda,\mu,T\right\}=\chi_L\left\{\lambda,\mu,0\right\}+\left\langle\prod_{\mathbf{k}\in\Lambda_L^*}e^{\lambda_{\mathbf{k}}J_{\mathbf{k}}^{(0)}}\left[\epsilon\mathcal{J}_1+\epsilon^2\left(\mathcal{J}_2+\mathcal{J}_3+\mathcal{J}_4+\mathcal{J}_5\right)\right]\right\rangle_J \tag{61}$$

where [19]:

$$\mathcal{J}_1\doteq\Big\langle\prod_{\mathbf{k}}\psi_{\mathbf{k}}^{(0)\mu_{\mathbf{k}}}\sum_1\Big(\lambda_1+\frac{\mu_1}{2J_1^{(0)}}\Big)b_1^{(1)}b_1^{(0)*}\Big\rangle_\psi \tag{62}$$

$$\mathcal{J}_2\doteq\frac{1}{2}\Big\langle\prod_{\mathbf{k}}\psi_{\mathbf{k}}^{(0)\mu_{\mathbf{k}}}\sum_1\Big(\lambda_1+\lambda_1^2J_1^{(0)}-\frac{\mu_1^2}{4J_1^{(0)}}\Big)|b_1^{(1)}|^2\Big\rangle_\psi \tag{63}$$

$$\mathcal{J}_3\doteq\Big\langle\prod_{\mathbf{k}}\psi_{\mathbf{k}}^{(0)\mu_{\mathbf{k}}}\sum_1\Big(\lambda_1+\frac{\mu_1}{2J_1^{(0)}}\Big)b_1^{(2)}b_1^{(0)*}\Big\rangle_\psi \tag{64}$$

$$\mathcal{J}_4\doteq\Big\langle\prod_{\mathbf{k}}\psi_{\mathbf{k}}^{(0)\mu_{\mathbf{k}}}\sum_1\Big(\frac{1}{2}\lambda_1^2+\frac{\mu_1}{4J_1^{(0)2}}(\frac{\mu_1}{2}-1)+\frac{\lambda_1\mu_1}{2J_1^{(0)}}\Big)(b_1^{(1)}b_1^{(0)*})^2\Big\rangle_\psi \tag{65}$$

$$\begin{aligned}\mathcal{J}_5\doteq\frac{1}{2}\Big\langle\prod_{\mathbf{k}}\psi_{\mathbf{k}}^{(0)\mu_{\mathbf{k}}}\sum_{1\neq2}\Big(&\lambda_1\lambda_2(b_1^{(1)}b_1^{(0)*}+b_1^{(1)*}b_1^{(0)})b_2^{(1)}b_2^{(0)*}\\&+(\lambda_1+\frac{\mu_1}{4J_1^{(0)}})\frac{\mu_2}{J_2^{(0)}}(b_2^{(1)}b_2^{(0)*}-b_2^{(1)*}b_2^{(0)})b_1^{(1)}b_1^{(0)*}\Big)\Big\rangle_\psi\end{aligned} \tag{66}$$

The averages over phases and amplitudes have been separated. Furthermore,

$$\chi_L\left\{\lambda,\mu,0\right\}\doteq\left\langle\prod_{\mathbf{k}}\exp\left[\lambda_{\mathbf{k}}J_{\mathbf{k}}^{(0)}\right]\right\rangle_J \tag{67}$$

3.2.1. Rules for phase-averaging

The terms in the perturbative solution of the equation of motion can be represented by Wyld diagram expansions [18, 21, 25, 26]. The main rules for such diagrams and for averages over phases follow.

Rule 1 **How to build the basic diagrams**

The various contributions are represented by tree diagrams illustrated in Figs. 1-3, for the zeroth-, first- and second-order terms, that we call "basic diagrams".

- Lines: a solid line labeled by an integer j represents factor $b_j^{(0)}$; dashed line indicates the absence of such a factor. An arrow added to a solid line, pointing away from j, indicates $\sigma_j=+1$ (source); if the arrow points toward j, it corresponds to $\sigma_j=-1$ (sink).
- Vertices: the vertex labelled 1234 represents $\mathcal{L}_{1234}^{\sigma_1,\sigma_2,\sigma_3,\sigma_4}e^{\tilde{\omega}_{234}^1t}\delta_{234}^1$ with $\sigma_1=+1$ when the arrow points out of the vertex and $\sigma_1=-1$ when the arrow points into the vertex. The times at each vertex are ordered causally, with the latest times at the root of the tree, labelled by 1. Integrating from time 0 to T, one gets the various contributions to the perturbative solution.

Figure 1: $b_1^{(0)+}$ and $b_1^{(0)-}$

For completeness, observe that:

$$b_1^{(1)}(T)=\sum_{234}{}^*\,\mathcal{L}_{1234}b_2^{(0)}b_3^{(0)}b_4^{(0)}\Delta_T(\tilde{\omega}_{234}^1)\delta_{234}^1 \tag{68}$$

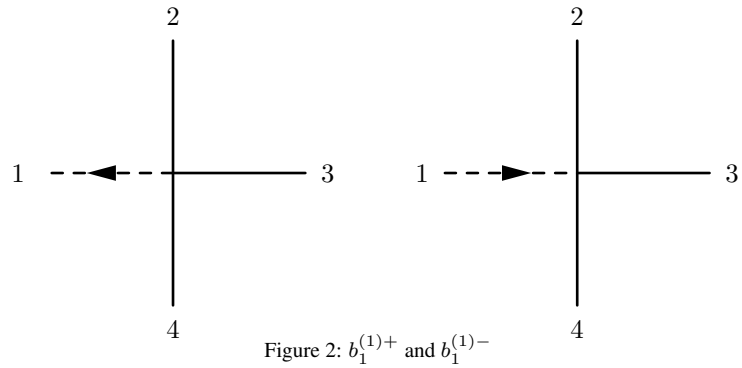

Figure 2: $b_1^{(1)+}$ and $b_1^{(1)-}$

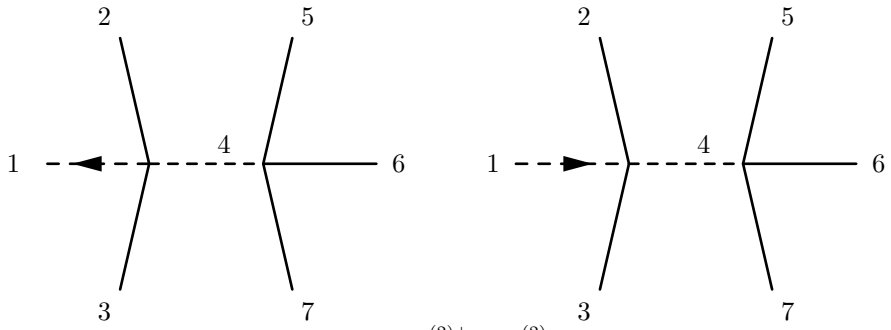

Figure 3: $b_1^{(2)+}$ and $b_1^{(2)-}$

$$b_1^{(2)}(T) = \sum_{234567}{}^{*} \mathcal{L}_{1234}\mathcal{L}_{4567}\, b_2^{(0)} b_3^{(0)} b_5^{(0)} b_6^{(0)} b_7^{(0)} \int_0^T \Delta_t(\tilde{\omega}_{567}^4) \exp\left(i\tilde{\omega}_{234}^1 t\right) dt \delta_{234}^1 \delta_{567}^4$$
$$+(4 \longleftrightarrow 3) + (4 \longleftrightarrow 2) + \int_0^T \mathcal{D}_1 b_1^{(0)} dt \tag{69}$$

Rule 2 **How to combine basic diagrams before phase-averaging**
Before averaging over phases, the various contributions (62)-(66) can be represented by diagrams (see next section), combining the tree diagrams in Figs. 1-3. The combination of two basic diagrams graphically represents the product of the two analytical terms to which the diagrams are associated, and this is performed by joining the trees with the same "root" indices, over which there must be a sum. Each of the integer labels indicates an index to be summed over independently of the others, except for the constraints imposed by Kronecker deltas at the vertices.

From now, we omit superscripts, as they are (0).

Rule 3 **Phase-averaging: diagrams closed by internal or external couplings**
The only contributions that survive the average over phases have phases summing to zero before averaging. Then, each $b^{(0)}$ either pairs with another $b^{(0)}$ so that their phases sum to zero or belong to a set of $b^{(0)}$'s that pair with a $\psi_{\mathbf{k}}^{(0)\mu_{\mathbf{k}}}$ making the sum of their phases vanish. The first is an internal coupling, represented by a solid line connecting the paired indices ij that contribute a factor $\delta_{\sigma_i+\sigma_j,0}\delta_{\mathbf{k}_i,\mathbf{k}_j}$ after phase averaging. The second is an external coupling, represented by joining all solid lines with indices $i_1, i_2, ..., i_p$ to a blob $\bullet$ labeled a, that represents the phase $\psi_{\mathbf{k}_a}^{(0)\mu_{\mathbf{k}_a}}$ which contributes a factor $\delta_{\sigma_{i_1}+\cdots\sigma_{i_p}+\mu_a,0}\prod_{j=1}^p \delta_{\mathbf{k}_j,\mathbf{k}_a}$ after phase averaging. We will say that the blob (Kronecker delta) makes the wavenumber $\mathbf{k}_j$ pinned to the value $\mathbf{k}_a$. Conventionally, we omit the letters labeling the blobs: factors such as $\delta_{\mathbf{k}_j,\mathbf{k}_a}\delta_{\mu_a+\sigma_j,0}$ are denoted by $\delta_{\mu_j+\sigma_j,0}$, meaning that $\mathbf{k}_j$ is constrained to the value $\mathbf{k}_a$ because of external coupling [19].

Call bridge the line connecting two vertices, labeled with just one number: e.g. the line labeled with 1 in presence of the factor $\mathcal{L}_{1234}^{+\sigma_2\sigma_3\sigma_4}\mathcal{L}_{1567}^{-\sigma_5\sigma_6\sigma_7}$. We distinguish between *in-internal coupling*, with two lines

starting from the same vertex closed together, and *cross-internal* coupling, when two lines starting from two different vertices are bound. Let the number of degrees of freedom (or number of free wavenumbers) be the number of summations over all N modes, cf. Appendix B.

Lemma *Let us assume the initial wavefield is an RP field. Consider the phase average*

$$\left\langle \prod_l \psi_l^{\mu_l} \psi_1 \cdots \psi_p \psi_{p+1}^* \cdots \psi_q^* \right\rangle$$

and all the possible associated diagrams giving non-null contributions. Then, the degrees of freedom of each closed diagram are equal to the total number of internal couplings in the diagram, no matter if "in-" or "cross-internal" couplings. No degrees of freedom must be counted for a bridge.

This implies a new rule for the phase-averaging method.

Rule 4 **Distinguishing leading order graphs**
The terms with a larger number of internal couplings are greater in order, so the leading contributions come from the terms with the maximum number of internal couplings. Therefore, we can subdivide the diagrams in four different types: type 0 diagrams with three free wavenumbers; type I diagrams two; type II diagrams with one; type III with no free wavenumbers. The leading contributions are then given by type 0 or type I diagrams and, in some cases, by type II diagrams.

The symbol $\sum^*$ expresses the fact that the combinations of $\mathbf{k}_i$'s and σ_i's giving linear terms inside the interaction term are separated. Then, the interaction representation (45) allows us to remove such linear terms from the interaction, implying:

Rule 5 **Diagram "eliminated" by frequency renormalization**
Definition (42) implies that the Kronecker delta's inside (41) vanish in $\sum^*_{234}$ for any allowed configuration. Definition (54) implies that the delta's inside (53) also vanish in the term $\sum^*_{2\ldots7}$. Thus, a diagram for $b_1^{(1)}$ implying the arguements of the delta's inside (41) to be simultaneously equal to zero is not contributing. The same holds for a graph for $b_1^{(2)}$ whose particular state requires null arguements for the delta's inside (53).

3.2.2. Contributions $\mathcal{J}_1 - \mathcal{J}_5$

The graph associated to $\mathcal{J}_1$ before phase-averaging is represented in Fig. 4, and analitically expressed by:

$$\begin{aligned} \mathcal{J}_1 \;=\; & \left\langle \prod_{\mathbf{k}} \psi_{\mathbf{k}}^{\mu_{\mathbf{k}}} \sum_{1234}^{*} \left(\lambda_1 + \frac{\mu_1}{2J_1}\right) \mathcal{L}_{1234}^{+\sigma_2\sigma_3\sigma_4} a_1^- a_2^{\sigma_2} a_3^{\sigma_3} a_4^{\sigma_4} \right. \\ & \left. \times \Delta_T \left(-\omega_1 + \sigma_2\omega_2 + \sigma_3\omega_3 + \sigma_4\omega_4\right) \delta_{\mathbf{k}_1,\sigma_2\mathbf{k}_2+\sigma_3\mathbf{k}_3+\sigma_4\mathbf{k}_4} \right\rangle_\psi \end{aligned} \tag{70}$$

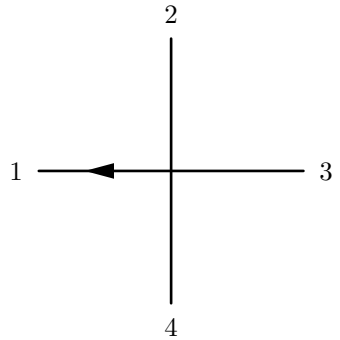

Figure 4: Diagram associated to $\mathcal{J}_1$ before phase-averaging

Substituting the action-angle variables, we have:

$$\begin{aligned}\mathcal{J}_1 &= \sum_{1234}{}^{*}\left(\lambda_1+\frac{\mu_1}{2J_1}\right)\sqrt{J_1J_2J_3J_4}\mathcal{L}_{1234}^{+\sigma_2\sigma_3\sigma_4}\left\langle\psi_1^{-1}\psi_2^{\sigma_2}\psi_3^{\sigma_3}\psi_4^{\sigma_4}\prod_{\mathbf{k}}\psi_{\mathbf{k}}^{\mu_{\mathbf{k}}}\right\rangle_{\psi}\\ &\quad\times\Delta_T\left(-\omega_1+\sigma_2\omega_2+\sigma_3\omega_3+\sigma_4\omega_4\right)\delta_{\mathbf{k}_1,\sigma_2\mathbf{k}_2+\sigma_3\mathbf{k}_3+\sigma_4\mathbf{k}_4}\end{aligned}\tag{71}$$

where only the term within angular brackets depends on phases. This term can be thought of as the sum of the contributions of all the possible closures (*Rule 3*) of the diagram in Fig. 4.

Figure 5: Diagram 1 (type I, vanishing) and diagram 2 (type II)

1. The contribution associated with diagram 1 in Fig. 5 may be directly written as

$$\sum_{\underline{\sigma}}\sum_{\underline{\mathbf{k}}}{}^{*}\left(\lambda_1+\frac{\mu_1}{2J_1}\right)\sqrt{J_1J_2J_3J_4}\mathcal{L}_{1234}^{+\sigma_2\sigma_2\sigma_4}\prod_m\delta_{\mu_m,0}\quad\Delta_T\left(0\right)\delta_{\mathbf{k}_1,\mathbf{k}_4}\delta_{\mathbf{k}_2,\mathbf{k}_3}\tag{72}$$

$$\underline{\sigma}=(1,\sigma_2,-\sigma_2,1)$$

   The two Kronecker delta's of the internal couplings make the vertex delta redundant. Applying *Rule 5*, one sees that this kind of graph is missing in the interaction. The physics of this diagram has already been included in the frequency renormalization and thus it must not been considered here. This implies that this is not a leading order term in $\mathcal{J}_1$.
2. For diagram 2 in Fig. 5, one has the following contribution to $\mathcal{J}_1$:

$$\begin{aligned}&\sum_{\underline{\sigma}}\sum_{\underline{\mathbf{k}}}{}^{'}\left(\lambda_1+\frac{\mu_1}{2J_1}\right)\sqrt{J_1J_2J_3J_4}\mathcal{L}_{1234}^{+\sigma_2\sigma_2\sigma_4}\delta_{\mu_1,1}\delta_{\mu_4,1}\delta_{\sigma_2,-\sigma_3}\\ &\qquad\times\prod_{m\neq1,-1}\delta_{\mu_m,0}\quad\Delta_T\left(-\omega_1-\omega_{-1}\right)\delta_{\mathbf{k}_2,\mathbf{k}_3}\delta_{\mathbf{k}_1,-\mathbf{k}_4}\end{aligned}\tag{73}$$

   Here $\underline{\sigma}=(1,\sigma_2,-\sigma_2,-1)$, because the internal coupling between 2 and 3 needs $\sigma_2=-\sigma_3$ for the phase of $\mathbf{k}_2$ to vanish. Then, $\mathbf{k}_1=\sigma_4\mathbf{k}_4=-\mathbf{k}_4$, as $\sigma_4=-1$.

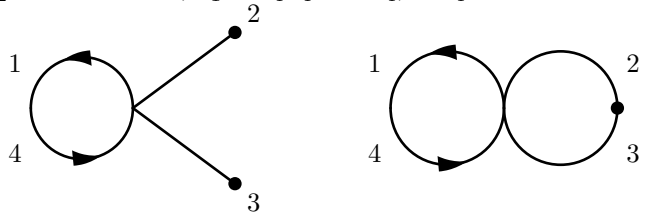

Figure 6: Diagram 3 (type II) and diagram 4 (type II, vanishing)

3. For diagram 3 in Fig. 6, the contribution to $\mathcal{J}_1$ reads:

$$\begin{aligned}&\sum_{\underline{\sigma}}\sum_{\underline{\mathbf{k}}}{}^{'}\left(\lambda_1+\frac{\mu_1}{2J_1}\right)\sqrt{J_1J_2J_3J_4}\mathcal{L}_{1234}^{+\sigma_2\sigma_2\sigma_4}\delta_{\mu_2,-\sigma_2}\delta_{\mu_3,-\sigma_2}\\ &\qquad\times\prod_{m\neq2,3}\delta_{\mu_m,0}\quad\Delta_T\left(\sigma_2\left(\omega_2+\omega_{-2}\right)\right)\delta_{\mathbf{k}_2,-\mathbf{k}_3}\delta_{\mathbf{k}_1,\mathbf{k}_4}\end{aligned}\tag{74}$$

   and $\underline{\sigma}=(1,\sigma_2,\sigma_2,1)$.

4. For diagram 4, the last Kronecker delta in (71), which represents momentum conservation at the vertex, implies $\mathbf{k}_2 = \mathbf{k}_3 = 0$. So this diagram does not represent an effective interaction. As a matter of fact, for spatially homogeneous WT fields there must be no coupling with the zero mode $\mathbf{k} = \mathbf{0}$ because such coupling would violate momentum conservation, cf. [1, 19]. If one of the arguments of $\mathcal{L}_{1234}$ vanishes, the matrix element is zero. That is to say that for any spatially homogeneous WT system $\mathcal{L}_{1234}$ is identically zero if one of $\mathbf{k}_1$, $\mathbf{k}_2$, $\mathbf{k}_3$ or $\mathbf{k}_4$ is zero. The situation is analogous for graphs obtained by permutations of the indices.

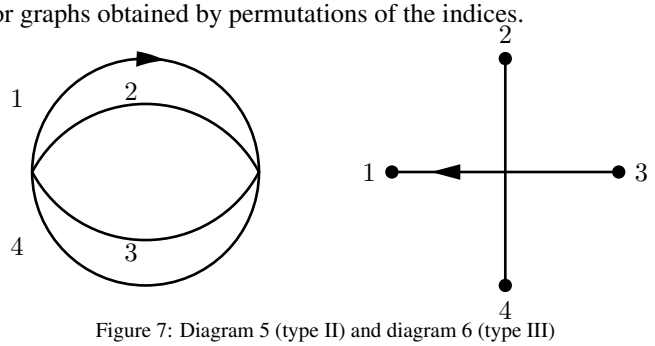

Figure 7: Diagram 5 (type II) and diagram 6 (type III)

5. Diagram 5 in Fig. 4 contributes as

$$\sum_{\underline{\sigma}} \sum_{\substack{\underline{\mathbf{k}}, \\ \mathbf{k}_1=\mathbf{k}_2=\mathbf{k}_3=\mathbf{k}_4}} \left(\lambda_1 + \frac{\mu_1}{2J_1}\right) \sqrt{J_1 J_2 J_3 J_4}\, \mathcal{L}_{1234}^{+\sigma_2\sigma_2\sigma_4} \delta_{\sigma_2+\sigma_3+\sigma_4,1} \prod_m \delta_{\mu_m,0}\, \Delta_T(0) \qquad (75)$$

$$\underline{\sigma} = (1, \sigma_2, \sigma_3, \sigma_4)$$

6. All other diagrams are type III (like *e.g.* diagram 6 in Fig. 4) and give subleading contributions.

Normalization of amplitudes: Let us introduce the change of variables

$$J_{\mathbf{k}} = \left(\frac{2\pi}{L}\right)^d \tilde{J}_{\mathbf{k}}, \qquad \lambda_{\mathbf{k}} = i\lambda(\mathbf{k}) \qquad (76)$$

Recalling [19], this substitution implies that the characteristic function be expressed by:

$$\mathcal{Z}_L[\lambda, \mu] \doteq \left\langle \exp\left(i \sum_{\mathbf{k}\in\Lambda_L^*} \left(\frac{2\pi}{L}\right)^d \lambda(\mathbf{k}) \tilde{J}_{\mathbf{k}} \right) \prod_{\mathbf{k}\in\Lambda_L^*} \psi_{\mathbf{k}}^{\mu_{\mathbf{k}}} \right\rangle \qquad (77)$$

where $\lambda(\mathbf{k})$ is a smooth test function and $\mu_{\mathbf{k}}$ are integers. Here we keep the time dependence implicit, for sake of notation. This characteristic function, after the transformation of the sum to an integral thanks to the large-L limit, becomes a characteristic functional [21].

Main contributions to $\mathcal{J}_1$: Diagram 2 is the only type II diagram with mode $\mathbf{k}_1$ pinned to an external blob, so that $\mu_1 \neq 0$. This graph contributes to $O(1)$, as it is order $O(L^d)$ (one free wavenumber, that is an unconstrained sum) multiplyed by order $O(L^{-d})$ (term proportional to μ_1, see (62)). A factor 3 appears to account the possible permutations of the indices. There is no other leading order term. The other graphs contribute to order $O(L^{-d})$ and vanish in the $L \to \infty$ limit. Summarizing, $\mathcal{J}_1$ may be written as:

$$\begin{aligned} \mathcal{J}_1 \;=\; & \frac{3}{2}\left(\frac{2\pi}{L}\right)^d \sum_{(1)} \left[\sqrt{\frac{\tilde{J}_2\tilde{J}_3\tilde{J}_4}{\tilde{J}_1}}\, \mathcal{L}_{1234}^{+\sigma_2\sigma_3\sigma_4} \delta_{\mu_1,1}\delta_{\mu_{-1},1} \prod_{m\neq\pm1} \delta_{\mu_m,0} \Delta_T\left(-2(\omega_1+\omega_{-1})\right) \right] \\ & + O\left(L^{-d}\right), \qquad \text{where} \quad \sum_{(1)} \doteq \sum_{\substack{\sigma_1=-\sigma_4=1, \\ \sigma_2=-\sigma_3}} \sum_{\mathbf{k}_2} \end{aligned} \qquad (78)$$

The contributions from the terms $\mathcal{J}_2$, ..., $\mathcal{J}_5$, are given in Appendix C.

Contribution of $\mathcal{J}_2$

$$\begin{aligned}\mathcal{J}_2 &= \frac{i}{2}\left(\frac{2\pi}{L}\right)^{3d}\delta_{\mu,0}\Big\{9\sum\nolimits_{(2)}\Big[\lambda\left(\mathbf{k}_1\right)\mathcal{L}_{1234}^{+\sigma_2\sigma_3\sigma_4}\mathcal{L}_{1567}^{-\sigma_5\sigma_6\sigma_7}\tilde{J}_2\tilde{J}_4\tilde{J}_5|\Delta_T\left(\tilde{\omega}_1+\tilde{\omega}_{-1}\right)|^2\Big] \\ &\quad +6\sum\nolimits_{(3)}\Big[\lambda\left(\mathbf{k}_1\right)|\mathcal{L}_{1234}^{+\sigma_2\sigma_3\sigma_4}|^2\tilde{J}_2\tilde{J}_3\tilde{J}_4|\Delta_T\left(\tilde{\omega}_{234}^1\right)|^2\Big]\Big\}+O\left(L^{-1}\right) \qquad (79)\end{aligned}$$

$$\sum\nolimits_{(2)} \doteq \sum_{\underline{\sigma}}\sum_{\underline{\mathbf{k}}}{}' \delta_{\mathbf{k}_4,-\mathbf{k}_1}\delta_{\mathbf{k}_4,\mathbf{k}_7}\delta_{\mathbf{k}_2,\mathbf{k}_3}\delta_{\mathbf{k}_5,\mathbf{k}_6},\ \underline{\sigma}=(1,\sigma_2,-\sigma_2,-1,\sigma_5,-\sigma_5,1) \qquad (80)$$

$$\sum\nolimits_{(3)} \doteq \sum_{\underline{\sigma}}\sum_{\underline{\mathbf{k}}}{}' \delta_{234}^1\delta_{\mathbf{k}_2,\mathbf{k}_5}\delta_{\mathbf{k}_4,\mathbf{k}_7}\delta_{\mathbf{k}_3,\mathbf{k}_6},\ \underline{\sigma}=(1,\sigma_2,\sigma_3,\sigma_4,-\sigma_2,-\sigma_3,-\sigma_4) \qquad (81)$$

Contribution of $\mathcal{J}_3$

$$\begin{aligned}\mathcal{J}_3 &= 18i\left(\frac{2\pi}{L}\right)^{3d}\delta_{\mu,0} \\ &\quad\times\Big\{\sum\nolimits_{(4)}\Big[\lambda\left(\mathbf{k}_1\right)\mathcal{L}_{1234}^{+\sigma_2\sigma_3\sigma_4}\mathcal{L}_{4567}^{\sigma_4\sigma_5\sigma_6\sigma_7}\tilde{J}_1\tilde{J}_3\tilde{J}_5E_T\left(0,\sigma_3\left(\omega_3+\omega_{-3}\right)\right)\Big] \\ &\quad+\frac{1}{2}\sum\nolimits_{(5)}\Big[\lambda\left(\mathbf{k}_1\right)\mathcal{L}_{1234}^{+\sigma_2\sigma_3\sigma_4}\mathcal{L}_{4567}^{\sigma_4\sigma_5\sigma_6\sigma_7}\tilde{J}_1\tilde{J}_3\tilde{J}_6E_T\left(0,-\left(\tilde{\omega}_1+\tilde{\omega}_{-1}\right)\right)\Big] \\ &\quad+\sum\nolimits_{(6)}\Big[\lambda\left(\mathbf{k}_1\right)\mathcal{L}_{1234}^{+\sigma_2\sigma_3\sigma_4}\mathcal{L}_{4567}^{\sigma_4\sigma_5\sigma_6\sigma_7}\tilde{J}_1\tilde{J}_2\tilde{J}_3E_T\left(0,\tilde{\omega}_{234}^1\right)\Big]\Big\} \\ &\quad+9\left(\frac{2\pi}{L}\right)^{2d}\Big\{\sum\nolimits_{(7)}\Big[\mathcal{L}_{1234}^{+\sigma_2\sigma_3\sigma_4}\mathcal{L}_{4567}^{\sigma_4\sigma_5\sigma_6\sigma_7}\sqrt{\frac{\tilde{J}_{-1}}{\tilde{J}_1}}\tilde{J}_3\tilde{J}_5\prod_{m\neq1,2}\delta_{\mu_m,0} \\ &\qquad\times E_T\big(-\left(\tilde{\omega}_1+\tilde{\omega}_{-1}\right),-\left(\tilde{\omega}_1+\tilde{\omega}_{-1}\right)+\sigma_3\tilde{\omega}_3+\sigma_4\tilde{\omega}_4\big)\Big] \\ &\qquad+\frac{1}{2}\sum\nolimits_{(8)}\Big[\mathcal{L}_{1234}^{+\sigma_2\sigma_3\sigma_4}\mathcal{L}_{4567}^{\sigma_4\sigma_5\sigma_6\sigma_7}\sqrt{\frac{\tilde{J}_7}{\tilde{J}_1}}\tilde{J}_3\tilde{J}_5\prod_{m\neq1,7}\delta_{\mu_m,0} \\ &\qquad\times E_T\big(-\left(\tilde{\omega}_1+\sigma_4\tilde{\omega}_4\right),-\left(\tilde{\omega}_1+\sigma_4\tilde{\omega}_4\right)\big)\Big] \\ &\qquad+\sum\nolimits_{(9)}\Big[\mathcal{L}_{1234}^{+\sigma_2\sigma_3\sigma_4}\mathcal{L}_{4567}^{\sigma_4\sigma_5\sigma_6\sigma_7}\sqrt{\frac{\tilde{J}_{-1}}{\tilde{J}_1}}\tilde{J}_3\tilde{J}_5\prod_{m\neq1,6}\delta_{\mu_m,0} \\ &\qquad\times E_T\big(-\left(\tilde{\omega}_1+\tilde{\omega}_{-1}\right),\tilde{\omega}_{234}^1\big)\Big]\Big\}+O\left(L^{-1}\right) \qquad (82)\end{aligned}$$

where

$$\begin{aligned}\sum\nolimits_{(4)} &\doteq \sum_{\underline{\sigma},\underline{\mathbf{k}}}{}' \delta_{\mathbf{k}_4,-\mathbf{k}_3}\delta_{\mathbf{k}_1,\mathbf{k}_2}\delta_{\mathbf{k}_3,\mathbf{k}_7}\delta_{\mathbf{k}_5,\mathbf{k}_6},\ \underline{\sigma}=(1,1,\sigma_3,\sigma_3,\sigma_5,-\sigma_5,-\sigma_3) \\ \sum\nolimits_{(5)} &\doteq \sum_{\underline{\sigma},\underline{\mathbf{k}}}{}' \delta_{\mathbf{k}_1,-\mathbf{k}_4}\delta_{\mathbf{k}_1,\mathbf{k}_5}\delta_{\mathbf{k}_3,\mathbf{k}_2}\delta_{\mathbf{k}_6,\mathbf{k}_7},\ \underline{\sigma}=(1,\sigma_2,-\sigma_2,-1,1,\sigma_6,-\sigma_6) \\ \sum\nolimits_{(6)} &\doteq \sum_{\underline{\sigma},\underline{\mathbf{k}}}{}' \delta_{234}^1\delta_{\mathbf{k}_1,\mathbf{k}_6}\delta_{\mathbf{k}_3,\mathbf{k}_7}\delta_{\mathbf{k}_5,\mathbf{k}_2},\ \underline{\sigma}=(1,\sigma_2,\sigma_3,\sigma_4,-\sigma_2,1,-\sigma_3) \\ \sum\nolimits_{(7)} &\doteq \sum_{\underline{\sigma},\underline{\mathbf{k}}}{}' \delta_{-\sigma_4\mathbf{k}_4,\sigma_3\mathbf{k}_3}\delta_{\mathbf{k}_1,-\mathbf{k}_2}\delta_{\mathbf{k}_3,\mathbf{k}_7}\delta_{\mathbf{k}_5,\mathbf{k}_6},\ \underline{\sigma}=(1,-1,\sigma_3,\sigma_4,\sigma_5,-\sigma_5,-\sigma_3) \\ \sum\nolimits_{(8)} &\doteq \sum_{\underline{\sigma},\underline{\mathbf{k}}}{}' \delta_{\mathbf{k}_1,\sigma_4\mathbf{k}_4}\delta_{\mathbf{k}_1,\sigma_7\mathbf{k}_7}\delta_{\mathbf{k}_3,\mathbf{k}_2}\delta_{\mathbf{k}_5,\mathbf{k}_6},\ \underline{\sigma}=(1,\sigma_2,-\sigma_2,\sigma_4,\sigma_5,-\sigma_5,\sigma_7) \\ \sum\nolimits_{(9)} &\doteq \sum_{\underline{\sigma},\underline{\mathbf{k}}}{}' \delta_{234}^1\delta_{\mathbf{k}_1,-\mathbf{k}_6}\delta_{\mathbf{k}_3,\mathbf{k}_7}\delta_{\mathbf{k}_5,\mathbf{k}_2},\ \underline{\sigma}=(1,\sigma_2,\sigma_3,\sigma_4,-\sigma_2,-1,-\sigma_3) \qquad (83)\end{aligned}$$

Contribution of $\mathcal{J}_4$
One finds that $\mathcal{J}_4 = O\left(L^{-d}\right)$, so it represents a subleading contribution.

Contribution of $\mathcal{J}_5$

$$\begin{aligned}\mathcal{J}_5 &= 3\left(\frac{2\pi}{L}\right)^{2d}\sum_{(10)}\frac{\mu_1\mu_2}{4J_1J_2}\mathcal{L}_{1345}^{+\sigma_3\sigma_4\sigma_5}\mathcal{L}_{2678}^{+\sigma_6\sigma_7\sigma_8}\sqrt{J_1J_2J_3J_4J_5J_6J_7J_8}\\ &\quad\times\delta_{\mu_1,1}\delta_{\mu_2,1}\prod_{m\neq1,2}\delta_{\mu_m,0}\,\Delta_T\left(\tilde{\omega}_{345}^1\right)\Delta_T\left(\tilde{\omega}^{(-1)345}\right)\\ &\quad+9\left(\frac{2\pi}{L}\right)^{2d}\sum_{(11)}\frac{\mu_1\mu_2}{4J_1J_2}\mathcal{L}_{1345}^{+\sigma_3\sigma_4\sigma_5}\mathcal{L}_{2678}^{+\sigma_6\sigma_7\sigma_8}\sqrt{J_1J_2J_3J_4J_5J_6J_7J_8}\\ &\quad\times\delta_{\mu_1,2}\delta_{\mu_2,2}\prod_{m\neq1,2}\delta_{\mu_m,0}\,\Delta_T\left(\tilde{\omega}_{(-1)44}^1\right)\Delta_T\left(\tilde{\omega}^{(-1)177}\right)+O\left(L^{-d}\right)\end{aligned}\tag{84}$$

$$\begin{aligned}\sum_{(10)} &\doteq \sum_{\underline{\sigma}}{\sum_{\underline{\mathbf{k}}}}'\delta_{\mathbf{k}_1,-\mathbf{k}_2}\delta_{\mathbf{k}_3,\mathbf{k}_6}\delta_{\mathbf{k}_4,\mathbf{k}_7}\delta_{\mathbf{k}_5,\mathbf{k}_8}\delta_{345}^1,\ \underline{\sigma}=(1,1,\sigma_3,\sigma_4,\sigma_5,-\sigma_3,-\sigma_4,-\sigma_5)\\ \sum_{(11)} &\doteq \sum_{\underline{\sigma}}{\sum_{\underline{\mathbf{k}}}}'\delta_{\mathbf{k}_1,-\mathbf{k}_2}\delta_{\mathbf{k}_1,-\mathbf{k}_3}\delta_{\mathbf{k}_1,\mathbf{k}_6}\delta_{\mathbf{k}_4,\mathbf{k}_5}\delta_{\mathbf{k}_7,\mathbf{k}_8},\ \underline{\sigma}=(1,1,-1,\sigma_4,-\sigma_4,-1,\sigma_7,-\sigma_7)\end{aligned}\tag{85}$$

3.3. Dynamical Multi-Mode Equation

In this section we turn Eq.(61) into a dynamical equation for the characteristic functional Z taking the $L\longrightarrow\infty$ and $\epsilon\longrightarrow 0$ limits. The two limits do not commute: the large-box limit must be taken first, the weak-nonlinearity limit after. The physical meaning of this operation is that there is a vast number of quasi-resonances (introduced by the large box limit, which leads to a continuous $\mathbf{k}$-space sending $\Lambda_L^*\longrightarrow\Lambda^*$), each of which is as important as the exact resonances [1].

3.3.1. Large-box limit

Let us introduce the large-L asymptotics standard substitutions, and

$$\left(\frac{2\pi}{L}\right)^d\sum_{\mathbf{k}}\Longrightarrow\int d^dk\,,\quad\left(\frac{L}{2\pi}\right)^d\delta_{\mathbf{k},\mathbf{k}'}\Longrightarrow\delta^d(\mathbf{k}-\mathbf{k}')\tag{86}$$

Recalling Eq.(60), using (78), (79), (82) and (84), and neglecting $O\left(L^{-d}\right)$ corrections, we can eventually write:

$$\begin{aligned}&\left\langle\exp\left[i\int d^dk\lambda(\mathbf{k})\tilde{J}_{\mathbf{k}}\right]\left\{24\epsilon\Big(\sum_{\mathbf{k}_1}\delta_{\mu_1,1}\delta_{\mu_{-1},1}\prod_{m\neq\pm1}\delta_{\mu_m,0}\Big)\right.\right.\\ &\qquad\times\sum_{\sigma_2}\int d^dk_2\tilde{J}_2\sqrt{\frac{\tilde{J}_{-1}}{\tilde{J}_1}}\mathcal{H}_{1224}^{-\sigma_2(-\sigma_2)-}\Delta_T\big(-2\left(\tilde{\omega}_1+\tilde{\omega}_{-1}\right)\big)+\\ &+8i\epsilon^2\delta_{\mu,0}\Big[9\sum_{\sigma_2,\sigma_5}\int d^dk_1d^dk_2d^dk_5\lambda\left(\mathbf{k}_1\right)\mathcal{H}_{122(-1)}^{-\sigma_2(-\sigma_2)-}\\ &\qquad\times\mathcal{H}_{155(-1)}^{+\sigma_5(-\sigma_5)+}\tilde{J}_{-1}\tilde{J}_2\tilde{J}_5|\Delta_T\left(\tilde{\omega}_1+\tilde{\omega}_{-1}\right)|^2\\ &\quad+6\sum_{\sigma_2,\sigma_3,\sigma_4}\int d^dk_1d^dk_2d^dk_3d^dk_4\lambda\left(\mathbf{k}_1\right)|\mathcal{H}_{1234}^{-\sigma_2\sigma_3\sigma_4}|^2\tilde{J}_2\tilde{J}_3\tilde{J}_4|\Delta_T\left(\tilde{\omega}_{234}^1\right)|^2\delta_{234}^1\Big]+\end{aligned}$$

$$
\begin{aligned}
&+288i\epsilon^2\delta_{\mu,0}\Big[\sum_{\sigma_4,\sigma_5}\int d^dk_1d^dk_4d^dk_5\,(-\sigma_4)\,\lambda\,(\mathbf{k}_1)\,\mathcal{H}^{-+\sigma_4\sigma_4}_{11(-4)4}\\
&\qquad\qquad\times\mathcal{H}^{(-\sigma_4)\sigma_5(-\sigma_5)(-\sigma_4)}_{455(-4)}\tilde{J}_1\tilde{J}_4\tilde{J}_5E_T\,(0,\sigma_4\,(\omega_4+\omega_{-4}))\\
&\quad+\frac{1}{2}\sum_{\sigma_2,\sigma_6}\int d^dk_1d^dk_2d^dk_6\lambda\,(\mathbf{k}_1)\,\mathcal{H}^{-\sigma_2(-\sigma_2)-}_{122(-1)}\\
&\qquad\qquad\times\mathcal{H}^{++\sigma_6-(\sigma_6)}_{(-1)166}\tilde{J}_1\tilde{J}_2\tilde{J}_6E_T\,(0,-\,(\tilde{\omega}_1+\tilde{\omega}_{-1}))\\
&\quad+\sum_{\sigma_2,\sigma_3,\sigma_4}\int d^dk_1d^dk_2d^dk_3d^dk_4\,(-\sigma_4)\,\lambda\,(\mathbf{k}_1)\,|\mathcal{H}^{-\sigma_2\sigma_3\sigma_4}_{1234}|^2\tilde{J}_1\tilde{J}_2\tilde{J}_3E_T\,\left(0,\tilde{\omega}^1_{234}\right)\delta^1_{234}\Big]+
\end{aligned}
$$

$$
\begin{aligned}
&+144\epsilon^2\Big[\Big(\sum_{\mathbf{k}_1}\delta_{\mu_1,1}\delta_{\mu_{-1},1}\prod_{m\neq\pm1}\delta_{\mu_m,0}\Big)\sum_{\sigma_3,\sigma_4,\sigma_5}\int d^dk_3d^dk_4d^dk_5\\
&\qquad\times(-\sigma_4)\,\mathcal{H}^{--\sigma_3\sigma_4}_{1(-1)34}\mathcal{L}^{(-\sigma_4)\sigma_5(-\sigma_3)(-\sigma_5)}_{4535}\sqrt{\frac{\tilde{J}_{-1}}{\tilde{J}_1}}\tilde{J}_3\tilde{J}_5\;\delta\,(\sigma_3\mathbf{k}_3+\sigma_4\mathbf{k}_4)\\
&\qquad\times E_T\big(-\,(\tilde{\omega}_1+\tilde{\omega}_{-1})\,,-\,(\tilde{\omega}_1+\tilde{\omega}_{-1})+\sigma_3\tilde{\omega}_3+\sigma_4\tilde{\omega}_4\big)\\
&\quad+\frac{1}{2}\sum_{\sigma_2,\sigma_4,\sigma_5,\sigma_7}\Big(\sum_{\mathbf{k}_1}\delta_{\mu_1,1}\sum_{\mathbf{k}_7}\delta_{\mu_7,-\sigma_7}\prod_{m\neq1,7}\delta_{\mu_m,0}\Big)\\
&\qquad\times\int d^dk_2d^dk_4d^dk_5d^dk_7\,(-\sigma_4)\,\mathcal{H}^{-\sigma_2(-\sigma_2)\sigma_4}_{1224}\mathcal{H}^{(-\sigma_4)\sigma_5(-\sigma_5)\sigma_7}_{4557}\sqrt{\frac{\tilde{J}_7}{\tilde{J}_1}}\tilde{J}_3\tilde{J}_5\\
&\qquad\times E_T\big(-\,(\tilde{\omega}_1+\sigma_4\tilde{\omega}_4)\,,-\,(\tilde{\omega}_1+\sigma_4\tilde{\omega}_4)\,\big)\delta(\mathbf{k}_1-\sigma_4\mathbf{k}_4)\delta(\mathbf{k}_1-\sigma_7\mathbf{k}_7)\\
&\quad+\Big(\sum_{\mathbf{k}_1}\delta_{\mu_1,1}\delta_{\mu_{-1},1}\prod_{m\neq\pm1}\delta_{\mu_m,0}\Big)\sum_{\sigma_2,\sigma_3,\sigma_4}\int d^dk_2d^dk_3d^dk_4\\
&\qquad\qquad\times(-\sigma_4)\,\mathcal{H}^{-\sigma_2\sigma_3\sigma_4}_{1234}\mathcal{H}^{(-\sigma_4)(-\sigma_2)-(-\sigma_3)}_{42(-1)3}\sqrt{\frac{\tilde{J}_{-1}}{\tilde{J}_1}}\tilde{J}_2\tilde{J}_3E_T\big(-\,(\tilde{\omega}_1+\tilde{\omega}_{-1})\,,\tilde{\omega}^1_{234}\big)\delta^1_{234}\Big]+
\end{aligned}
$$

$$
\begin{aligned}
&-12\epsilon^2\Big(\sum_{\mathbf{k}_1}\delta_{\mu_1,1}\delta_{\mu_{-1},1}\prod_{m\neq\pm1}\delta_{\mu_m,0}\Big)\sum_{\sigma_3,\sigma_4,\sigma_5}\\
&\qquad\qquad\times\int d^dk_3d^dk_4d^dk_5\mathcal{H}^{-\sigma_3\sigma_4\sigma_5}_{1345}\mathcal{H}^{-(-\sigma_3)(-\sigma_4)(-\sigma_5)}_{(-1)345}\frac{\tilde{J}_3\tilde{J}_4\tilde{J}_5}{\sqrt{\tilde{J}_1\tilde{J}_{-1}}}\Delta_T\big(\tilde{\omega}^1_{345}\big)\Delta_T\big(\tilde{\omega}^{(-1)345}\big)\delta^1_{345}
\end{aligned}
$$

$$
\begin{aligned}
&-36\epsilon^2\Big(\sum_{\mathbf{k}_1}\delta_{\mu_1,2}\delta_{\mu_{-1},2}\prod_{m\neq\pm1}\delta_{\mu_m,0}\Big)\sum_{\sigma_3,\sigma_4}\int d^dk_3d^dk_4\mathcal{H}^{--\sigma_3(-\sigma_3)}_{1(-1)33}\mathcal{H}^{--\sigma_4(-\sigma_4)}_{(-1)144}\tilde{J}_3\tilde{J}_4\\
&\qquad\qquad\times\tilde{J}_3\tilde{J}_4\Delta_T\big(\tilde{\omega}^1_{(-1)33}\big)\Delta_T\big(\tilde{\omega}^{(-1)144}\big)\Big\}\Big\rangle_J
\end{aligned}
\tag{87}
$$

3.3.2. Weak-nonlinearity limit

Recall that in section 3.1.2, we took $\frac{2\pi}{\tilde{\omega}_{\mathbf{k}}}\ll T\ll\frac{2\pi}{\epsilon^2\tilde{\omega}_{\mathbf{k}}}$, with T between the wave period and the nonlinear time. We can now take $T\sim\frac{2\pi}{\epsilon\tilde{\omega}_{\mathbf{k}}}$, so that $\lim_{\epsilon\to0}T=\infty$. Then, in (87) we must take the $T\to\infty$ limit, consistently with the large-T asymptotics of Δ_T and E_T [21, 27]:

$$
\Delta_T(x)\sim\widetilde{\Delta}(x)=\pi\delta(x)+iP\left(\frac{1}{x}\right),\;E_T(x;y)\sim\Delta_T(x)\Delta_T(y)\sim\widetilde{\Delta}(x)\widetilde{\Delta}(y),
$$

$$|\Delta_T(x)|^2 \sim 2\pi T\delta(x) + 2P\left(\frac{1}{x}\right)\frac{\partial}{\partial x},\ E_T(x;0) \sim \widetilde{\Delta}(x)\left(T - i\frac{\partial}{\partial x}\right), \tag{88}$$

Some considerations are in order.

1. in Eq.(87), only the terms containing $|\Delta_T(x)|^2$, $E_T(x;0)$ or $E_T(0;y)$ give secular contributions (proportional to T); the non-secular contributions are irrelevant in the $T \to \infty$ ($\epsilon \to 0$) limit. Thus, only the terms with $\delta_{\mu,0}$ survive the weak-nonlinearity assumption, while those with $\delta_{\mu_1,1}$ etc. are subleading.
2. The μ-dependent part of $\mathcal{Z}$ is constrained to be 1 by $\delta_{\mu,0}$. Then, using (76), switching to $i\lambda(\mathbf{k})$ and taking the large-box limit leads to the functional derivative
$$\left(\frac{L}{2\pi}\right)^d \frac{\partial}{\partial\lambda_{\mathbf{k}}} \Longrightarrow -i\frac{\delta}{\delta\lambda(\mathbf{k})} \tag{89}$$
3. Replace $(\mathcal{Z}[T] - \mathcal{Z}[0])/T$ with the time derivative $\dot{\mathcal{Z}}$. This can be done ([1],pg. 81) because time T is small compared to the characteristic time of averaged quantities such as $\mathcal{Z}$ (nonlinear time). Indeed, the istantaneous time derivative can be of same order or even greater than the rate of change described by our substitution, but such rapid changes are oscillatory and they drop out.
4. We introduce a new time variable $\tau \doteq \epsilon^2 T$.
5. Renaming indices, we split the integral with 4 wavenumbers into identical contributions

$$\begin{aligned}
\frac{d\mathcal{Z}[\lambda,\mu,\tau]}{d\tau} &= -192\pi\delta_{\mu,0}\sum_{\underline{\sigma}=(1,\sigma_2,\sigma_3,\sigma_4)}\int d^dk_1d^dk_2d^dk_3d^dk_4\lambda\left(\mathbf{k}_1\right)|\mathcal{H}_{1234}^{-\sigma_2\sigma_3\sigma_4}|^2 \\
&\quad \delta\left(\tilde{\omega}_{234}^1\right)\delta_{234}^1\left(\frac{\delta^3\mathcal{Z}}{\delta\lambda(\mathbf{k}_2)\delta\lambda(\mathbf{k}_3)\delta\lambda(\mathbf{k}_4)} - \sigma_2\frac{\delta^3\mathcal{Z}}{\delta\lambda(\mathbf{k}_1)\delta\lambda(\mathbf{k}_3)\delta\lambda(\mathbf{k}_4)}\right. \\
&\quad \left. -\sigma_3\frac{\delta^3\mathcal{Z}}{\delta\lambda(\mathbf{k}_1)\delta\lambda(\mathbf{k}_2)\delta\lambda(\mathbf{k}_4)} - \sigma_4\frac{\delta^3\mathcal{Z}}{\delta\lambda(\mathbf{k}_1)\delta\lambda(\mathbf{k}_2)\delta\lambda(\mathbf{k}_3)}\right) \\
&\quad -288\pi\delta_{\mu,0}\sum_{\underline{\sigma}=(1,\sigma_2,\sigma_3)}\int d^dk_1d^dk_2d^dk_3\lambda\left(\mathbf{k}_1\right) \\
&\quad \times\left[\mathcal{H}_{1(-1)22}^{--\sigma_2(-\sigma_2)}\mathcal{H}_{1(-1)33}^{++\sigma_3(-\sigma_3)}\delta\left(\tilde{\omega}_1 + \tilde{\omega}_{-1}\right)\right. \\
&\quad \sum_{\sigma=\pm1}\frac{\delta^3\mathcal{Z}}{\delta\lambda(\sigma\mathbf{k}_1)\delta\lambda(\mathbf{k}_2)\delta\lambda(\mathbf{k}_3)} - 2\sigma_2\mathcal{H}_{2(-2)11}^{\sigma_2\sigma_2+-} \\
&\quad \left.\mathcal{H}_{2(-2)33}^{(-\sigma_2)(-\sigma_2)\sigma_3(-\sigma_3)}\delta\left(\tilde{\omega}_2 + \tilde{\omega}_{-2}\right)\frac{\delta^3\mathcal{Z}}{\delta\lambda(\mathbf{k}_1)\delta\lambda(\mathbf{k}_2)\delta\lambda(\mathbf{k}_3)}\right]
\end{aligned} \tag{90}$$

3.3.3. Resonance condition

Recall definition $\tilde{\omega}_{\mathbf{k}} \doteq \omega_{\mathbf{k}} + \Omega_{\mathbf{k}}$. The definition of $\Omega_{\mathbf{k}}$ (44) and the thermodynamic limit imply:

$$\Omega_1 \overset{L\to\infty}{\longrightarrow} 24\epsilon\int_{\Lambda^*} d^dk_2\mathcal{H}_{1122}^{+-+-}\tilde{J}_2^{(0)}\ , \qquad \Omega_{-1} = 24\epsilon\int_{\Lambda^*} d^dk_2\mathcal{H}_{(-1)(-1)22}^{+-+-}\tilde{J}_2^{(0)} \tag{91}$$

Note: each component of $\mathbf{k}_2$, defined in the dual space Λ^*, ranges in the interval $[-k_{max}, k_{max}]$ and space isotropy implies that our system is symmetric under the $\mathbf{k} \to -\mathbf{k}$ transformation. Therefore:

$$\Omega_{-1} = 24\epsilon\int_{(-\Lambda^*)} d^d(-k_2)\mathcal{H}_{11(-2)(-2)}^{+-+-}\tilde{J}_{-2}^{(0)} \tag{92}$$

where $(-\Lambda^*)$ means that we are integrating over each component of $\mathbf{k}_2$ from $+k_{max}$ to $-k_{max}$ and not from $-k_{max}$ to $+k_{max}$ as it would be for Λ^*. However, the integration over $-\mathbf{k}_2 \in (-\Lambda^*)$ is equivalent to the integration over the variable $\mathbf{k}_3 \in \Lambda^*$, and this leads to:

$$\Omega_{-1} = 24\epsilon\int_{\Lambda^*} d^d(k_3)\mathcal{H}_{1133}^{+-+-}\tilde{J}_3^{(0)} \equiv \Omega_1 \tag{93}$$

Space isotropy also implies that $\omega_{\mathbf{k}} = \omega_{-\mathbf{k}}$ ($\omega_{\mathbf{k}}$ is positive for all $\mathbf{k} \in \Lambda^*$) and then:

$$\tilde{\omega}_{\mathbf{k}} + \tilde{\omega}_{-\mathbf{k}} = \omega_{\mathbf{k}} + \Omega_{\mathbf{k}} + \omega_{-\mathbf{k}} + \Omega_{-\mathbf{k}} = 2(\omega_{\mathbf{k}} + \Omega_{\mathbf{k}}) \tag{94}$$

Thus, the condition to fulfill for the resonance in the second term (last four lines) of equation (90) reads:

$$\omega_{\mathbf{k}} + \Omega_{\mathbf{k}} = 0 \tag{95}$$

Also, $\tilde{J}_2^{(0)}$ is positive, whereas the sign of $\mathcal{H}_{1122}^{+-+-}$ implies that it is impossible to generalize without looking at the specific problem we want to describe.

If we take as a paradigmatic example a relatively simple, 4-wave resonant system, namely the *Nonlinear Klein Gordon* system, we easily notice that the Hamiltonian coefficients are strictly positive, see also Ref.*vibrating elastic plate*. A more accurate analysis is needed in other cases, such as the deep water gravity waves, whose effective coefficients have been derived in [3]. If the Hamiltonian coefficients are positive, then $\Omega_{\mathbf{k}}$ is positive too.

Actually, many of the physical systems one usually considers have positive Hamiltonian coefficients. On the other hand, this last condition is not necessary to satisfy our weaker condition $\Omega_{\mathbf{k}} \geq 0, \forall \mathbf{k} \in \Lambda^*$. The reason to rely on such a condition is justified by the fact that those systems enjoy:

$$\tilde{\omega}_{\mathbf{k}} = \omega_{\mathbf{k}} + \Omega_{\mathbf{k}} \geq 0, \forall \mathbf{k} \in \Lambda^*. \tag{96}$$

Thus, condition (95) is never fulfilled, implying that the arguments of the two Dirac delta's $\delta\left(\tilde{\omega}_1 + \tilde{\omega}_{-1}\right)$ and $\delta\left(\tilde{\omega}_2 + \tilde{\omega}_{-2}\right)$ in equation (90) cannot vanish for any value of $\mathbf{k}$ except from $\mathbf{k} = 0$, but in that case the Hamiltonian coefficients are identically null. As a consequence, for "positive renormalized frequency" systems (*i.e.* satisfying (96)) the last four lines of equation (90) give zero identically and the dynamical multi-mode equation reduces to the really compact form (97) given below. Let us also note that the frequency $\Omega_{\mathbf{k}}$, Eq.(44), contains a factor ϵ and that the sum in (44) is expected to converge if the energy of the system is finite, then $\Omega_{\mathbf{k}}$ is of order $O(\epsilon)$. Therefore, $\Omega_{\mathbf{k}} \ll \omega_{\mathbf{k}}$. As a matter of fact, even for a system where $\Omega_{\mathbf{k}}$ can be negative, $\Omega_{\mathbf{k}}$ does not nullify the frequency $\omega_{\mathbf{k}}$. Thus, the relevant equation for 4-wave resonant systems is:

$$\begin{aligned}
\frac{d\mathcal{Z}[\lambda,\mu,\tau]}{d\tau} &= -192\pi\delta_{\mu,0} \sum_{\underline{\sigma}=(1,\sigma_2,\sigma_3,\sigma_4)} \int d^dk_1 d^dk_2 d^dk_3 d^dk_4 \lambda\left(\mathbf{k}_1\right) |\mathcal{H}_{1234}^{-\sigma_2\sigma_3\sigma_4}|^2 \\
&\quad \delta\left(\tilde{\omega}_{234}^1\right) \delta_{234}^1 \Bigg(\frac{\delta^3\mathcal{Z}}{\delta\lambda(\mathbf{k}_2)\delta\lambda(\mathbf{k}_3)\delta\lambda(\mathbf{k}_4)} - \sigma_2 \frac{\delta^3\mathcal{Z}}{\delta\lambda(\mathbf{k}_1)\delta\lambda(\mathbf{k}_3)\delta\lambda(\mathbf{k}_4)} \\
&\quad -\sigma_3 \frac{\delta^3\mathcal{Z}}{\delta\lambda(\mathbf{k}_1)\delta\lambda(\mathbf{k}_2)\delta\lambda(\mathbf{k}_4)} - \sigma_4 \frac{\delta^3\mathcal{Z}}{\delta\lambda(\mathbf{k}_1)\delta\lambda(\mathbf{k}_2)\delta\lambda(\mathbf{k}_3)} \Bigg)
\end{aligned} \tag{97}$$

which is a natural generalization to the 4-wave case of Eq.(94) in [21].

3.4. Derivation of the spectral hierarchy

We may now consider the characteristic functional of amplitudes only:[4]

$$\mathcal{Z}_L[\lambda, T] \doteq \left\langle \exp\left(\sum_{\mathbf{k}\in\Lambda_L^*} \lambda_{\mathbf{k}} J_{\mathbf{k}}(T) \right) \right\rangle \tag{98}$$

In analogy to [21], from (97) we derive a hierarchy of evolution equations for the M-mode spectral correlation functions defined in (30), in the kinetic limit:

$$\mathcal{N}^{(M)}(\mathbf{k}_1, ..., \mathbf{k}_M, \tau) = \lim_{\epsilon\to 0} \lim_{L\to\infty} \mathcal{N}_{L,\epsilon}^{(M)}(\mathbf{k}_1, ..., \mathbf{k}_M, \epsilon^{-2}\tau). \tag{99}$$

[4]Then, we can consider equation (97) without the $\delta_{\mu,0}$ term.

The hierarchy is easy to derive knowing the relation

$$\mathcal{N}^{(M)}(\mathbf{k}_1,...,\mathbf{k}_M,\tau) = (-i)^M \frac{\delta^M \mathcal{Z}[\lambda,\tau]}{\delta\lambda(\mathbf{k}_1)\cdots\delta\lambda(\mathbf{k}_M)}\bigg|_{\lambda=0}. \tag{100}$$

By taking M functional derivatives of (97) and setting $\lambda \equiv 0$, one obtains:

$$\begin{aligned}\dot{\mathcal{N}}^{(M)}(\mathbf{k}_1,...,\mathbf{k}_M,\tau) &= 192\pi \sum_{j=1}^{M}\sum_{\underline{\sigma}} \int d^d\overline{k}_2 d^d\overline{k}_3 d^d\overline{k}_4 \delta\left(\tilde{\omega}^1_{234}\right)\delta^1_{234}|H^{\underline{\sigma}}_{\mathbf{k}_j}|^2 \\ \Big[&\mathcal{N}^{(M+1)}(\mathbf{k}_1,...,\mathbf{k}_{j-1},\mathbf{k}_{j+1},...,\mathbf{k}_M,\overline{\mathbf{k}}_2,\overline{\mathbf{k}}_3,\overline{\mathbf{k}}_4\tau) - \sigma_2\mathcal{N}^{(M+1)}(\mathbf{k}_1,...,\mathbf{k}_M,\overline{\mathbf{k}}_3,\overline{\mathbf{k}}_4,\tau) \\ &- \sigma_3\mathcal{N}^{(M+1)}(\mathbf{k}_1,...,\mathbf{k}_M,\overline{\mathbf{k}}_2,\overline{\mathbf{k}}_4,\tau) - \sigma_4\mathcal{N}^{(M+1)}(\mathbf{k}_1,...,\mathbf{k}_M,\overline{\mathbf{k}}_2,\overline{\mathbf{k}}_3,\tau)\Big]\end{aligned} \tag{101}$$

We shall refer to this set of equations as to the *spectral hierarchy* of kinetic wave turbulence. It is exactly analogous to the hierarchy derived by Lanford from the BBGKY hierarchy in the low-density limit [23, 24]. If the spectral correlation functions satisfy bounds on their growth for large orders M that allow them to uniquely characterize the distribution of the empirical spectrum, then the spectral hierarchy (101) is not only a consequence of the equation (97) but is in fact equivalent to that equation. If the initial functional $\mathcal{Z}[\lambda,0]$ is of exponential form (28), as follows for an initial RP field with uncorrelated amplitudes, an exact solution of (97) is given by:

$$\mathcal{Z}[\lambda,\tau] = \exp\Big(i\int d^d\mathbf{k}\,\lambda(\mathbf{k})n(\mathbf{k},\tau)\Big), \tag{102}$$

where $n(\mathbf{k},\tau)$ satisfies the standard wave kinetic equation with initial condition $n(\mathbf{k},0) = n(\mathbf{k})$. Equivalently, factorized Mth-order correlation functions (31) as initial data, entail a factorized solution of the spectral hierarchy (101):

$$\mathcal{N}^{(M)}(\mathbf{k}_1,...,\mathbf{k}_M,\tau) = \prod_{m=1}^{M} n(\mathbf{k}_m,\tau). \tag{103}$$

Under suitable conditions [21] this is analogous to the propagation of chaos of Boltzmann's *Stosszahlansatz* [23, 24]. The results above have an important implication. As follows from our discussion in section 2, the conditions (102) or (103) imply a law of large numbers for the empirical spectrum at positive times. That is, with probability going to 1 in the kinetic limit (first $L\to\infty$, then $\epsilon\to 0$), it follows that

$$\widehat{n}_L(\mathbf{k},\epsilon^{-2}\tau) \simeq n(\mathbf{k},\tau), \quad \tau > 0 \tag{104}$$

where $n(\mathbf{k},\tau)$ is the solution of the wave kinetic equation. An interesting implication for laboratory and numerical experiments is that the wave kinetic equations hold for *typical* initial amplitudes and phases chosen from an RPA ensemble.

4. Derivation of the PDF equation

With respect to Section 3, we now consider a second possible limit involving only a fixed number of modes $\mathbf{k}_m$, $m = 1, 2, ..., M$, as the total number $N \to \infty$. As before, one must keep $\tilde{J}_{\mathbf{k}} = O(1)$ for all modes. We thus define the joint characteristic function:

$$\mathcal{Z}^{(M)}_L(\lambda_1,...,\lambda_M,\mu_1,...,T;\mathbf{k}_1,...) \doteq \left\langle \exp\left[i\sum_{m=1}^{M}\lambda_m\tilde{J}_{\mathbf{k}_M}(T)\right]\prod_{m=1}^{M}\psi^{\mu_m}_{\mathbf{k}_m}(T)\right\rangle \tag{105}$$

This is the characteristic function (110) of [21], which corresponds to the generating function (68) of [19] but with $\lambda_{\mathbf{k}_m} = i\left(\frac{L}{2\pi}\right)^d\lambda_m$, $\quad J_{\mathbf{k}_m} = \left(\frac{2\pi}{L}\right)^d\tilde{J}_{\mathbf{k}_m}$, $\quad m = 1,...,M$, and for all the other modes $\lambda_{\mathbf{k}} = 0$. It also corresponds to the generating functional (5.15) of [1], with same λ_m and $\tilde{J}_m$, but with an imaginary unit in the exponent, and with a finite number M of nonzero arguments.

The reason why λ_m is finite and $\lambda_{\mathbf{k}_m}$ is not is that the exponent of (105) contains finitely many terms $\lambda_m \tilde{J}_{\mathbf{k}_m}$, each of which is finite. Then, as $\tilde{J}_{\mathbf{k}_m}$ must be finite as $L \to \infty$, the same holds for λ_m.

We use the symbol $\mathcal{Z}_L^{(M)}(\lambda, \mu, T)$ when there is no possibility of confusion, and we use the perturbation expansion in ϵ giving (60) for the generating functions ($\forall M$), with the definitions (61) of $\chi_L(\lambda, \mu, T)$ and (62) - (66) of the $\mathcal{J}$'s. As λ_m is finite, different relations hold for the orders of the prefactors in the $\mathcal{J}$'s. In particular, for $\mathcal{J}_1$, $\mathcal{J}_2$, $\mathcal{J}_3$ we have:

$$\lambda_{\mathbf{k}_1} + \frac{\mu_{\mathbf{k}_1}}{2\tilde{J}_{\mathbf{k}_1}}, \;\; \lambda_{\mathbf{k}_1} + \lambda_{\mathbf{k}_1}^2 \tilde{J}_{\mathbf{k}_1} - \frac{\mu_{\mathbf{k}_1}^2}{4\tilde{J}_{\mathbf{k}_1}} = O\left(L^d\right) \tag{106}$$

and for $\mathcal{J}_4$, $\mathcal{J}_5$ we have:

$$\frac{1}{2}\lambda_{\mathbf{k}_1}^2 + \frac{\mu_{\mathbf{k}_1}}{4\tilde{J}_{\mathbf{k}_1}^2}\left(\frac{\mu_{\mathbf{k}_1}}{2} - 1\right) + \frac{\lambda_{\mathbf{k}_1}\mu_{\mathbf{k}_1}}{2\tilde{J}_{\mathbf{k}_1}}, \;\; \lambda_{\mathbf{k}_1}\lambda_{\mathbf{k}_2}, \;\; \left(\lambda_{\mathbf{k}_1} + \frac{\mu_{\mathbf{k}_1}}{4\tilde{J}_{\mathbf{k}_1}}\right)\frac{\mu_{\mathbf{k}_2}}{\tilde{J}_{\mathbf{k}_2}} = O\left(L^{2d}\right) \tag{107}$$

To calculate the leading order contributions, one must note that some wavenumbers are discrete and take only M values (mode 1 for $\mathcal{J}_1$ - $\mathcal{J}_4$, modes 1 and 2 for $\mathcal{J}_5$), whereas all the others are continuous in the infinite-box limit. This is important to distinguish $O(L^d)$ from $O(M)$ terms.

4.1. Derivation of the PDF hierarchy

Collecting the contributions of the $\mathcal{J}_1 - \mathcal{J}_5$ terms enumerated in Appendix D.1, we can neglect nonsecular terms. Furthermore, $\tilde{\omega}_{\mathbf{k}} + \tilde{\omega}_{-\mathbf{k}} = 0$ is never fulfilled, so we ignore the non-resonant terms with a $\delta(\tilde{\omega}_{\mathbf{k}} + \tilde{\omega}_{-\mathbf{k}})$ contribution. The two remaining contributions contain $\delta_{\mu,0}$, hence we can write:

$$\delta_{\mu,0}\langle \tilde{J}_j e^{\sum_m i\lambda_m \tilde{J}_m}\rangle_J = -i\delta_{\mu,0}\frac{\partial}{\partial\lambda_j}\mathcal{Z}^{(M)} \tag{108}$$

for wavenumber $\mathbf{k}_j, j = 1, ..., M$. Similarly, for mode $\mathbf{k} \neq \mathbf{k}_m, \forall m = 0, ..., M$ we have:

$$\delta_{\mu,0} i\langle \tilde{J}_{\mathbf{k}} e^{\sum_m i\lambda_m \tilde{J}_m}\rangle_J = \delta_{\mu,0}\left.\frac{\partial}{\partial\lambda_{\mathbf{k}}}\mathcal{Z}^{(M+1)}\right|_{\lambda_{\mathbf{k}}=0} \tag{109}$$

Subsequently, we consider an intermediate time between the linear time and the nonlinear time, cf. Section 3.3.2, $T \sim \frac{1}{\epsilon}$, and we take the $\epsilon \to 0$ limit. Because $\mathcal{Z}^{(M)}(\lambda, \mu, T) = \chi^{(M)}(\lambda, \mu, T) + \chi^{(M)*}(-\lambda, -\mu, T)$, while $\chi^{(M)}(\lambda, \mu, T) = \chi^{(M)*}(-\lambda, -\mu, T)$ and $\mathcal{Z}^{(M)}(\lambda, \mu, T) = 2\chi^{(M)}(\lambda, \mu, T)$, we get:

$$\frac{\mathcal{Z}^{(M)}(T) - \mathcal{Z}^{(M)}(0)}{\epsilon^2 T} \sim \frac{\partial\mathcal{Z}^{(M)}}{\epsilon^2\partial T}(\lambda, \mu, T) = \frac{\partial\mathcal{Z}^{(M)}}{\partial\tau}(\lambda, \mu, \tau) \tag{110}$$

where $\tau = \epsilon^2 T$ is the nonlinear time. This leads to:[5]

$$\begin{aligned}
&\frac{\partial\mathcal{Z}^{(M)}}{\partial\tau}(\lambda, \mu, \tau) = -192\pi\delta_{\mu,0} \\
&\times \sum_{j=1}^{M} \sum_{(1,\sigma_2,\sigma_3,\sigma_4)} \int d^d\overline{k}_2 d^d\overline{k}_3 d^d\overline{k}_4 \delta_{234}^j \delta\left(\tilde{\omega}_{234}^j\right) \left|\mathcal{H}_{j234}^{-\sigma_2\sigma_3\sigma_4}\right|^2 \\
&\times \left\{ \left(\lambda_j + \lambda_j^2 \frac{\partial}{\partial\lambda_j}\right) \left.\frac{\partial^3\mathcal{Z}^{(M+3)}}{\partial\overline{\lambda}_2\partial\overline{\lambda}_3\partial\overline{\lambda}_4}\right|_{\overline{\lambda}_2=\overline{\lambda}_3=\overline{\lambda}_4=0} - \sigma_2\lambda_j \left.\frac{\partial^3\mathcal{Z}^{(M+2)}}{\partial\lambda_j\partial\overline{\lambda}_3\partial\overline{\lambda}_4}\right|_{\overline{\lambda}_3=\overline{\lambda}_4=0} \right. \\
&\quad \left. - \sigma_3\lambda_j \left.\frac{\partial^3\mathcal{Z}^{(M+2)}}{\partial\lambda_j\partial\overline{\lambda}_2\partial\overline{\lambda}_4}\right|_{\overline{\lambda}_2=\overline{\lambda}_4=0} - \sigma_4\lambda_j \left.\frac{\partial^3\mathcal{Z}^{(M+2)}}{\partial\lambda_j\partial\overline{\lambda}_2\partial\overline{\lambda}_3}\right|_{\overline{\lambda}_2=\overline{\lambda}_3=0} \right\}
\end{aligned} \tag{111}$$

for $M = 1, 2, 3, ...$ An important fact is that $\delta_{\mu,0}$ implies that the RP property of the initial wavefield is preserved in time. By Fourier transformation in the λ variables, one can obtain an equivalent hierarchy of equations for the joint PDF's $\mathcal{P}^{(M)}(s_1, ..., s_M, \tau; \mathbf{k}_1, ..., \mathbf{k}_M)$, which appears more practical to implement boundary conditions on the amplitudes.

[5] The continuous quantities are identified by a bar, and symmetrization is made in the three continuous modes $\overline{\mathbf{k}}_2$, $\overline{\mathbf{k}}_3$, $\overline{\mathbf{k}}_4$.

4.2. The M-mode PDF equations

From the definition of the joint characteristic function of amplitudes, one has:

$$\begin{aligned}\mathcal{Z}^{(M)}(\lambda_1,...,\lambda_M) &= \left\langle e^{\sum_m i\lambda_m s_m}\right\rangle_J \\ &= \int ds_1...ds_M e^{\sum_m i\lambda_m s_m}\mathcal{P}^{(M)}(s_1,...,s_M)\end{aligned} \tag{112}$$

$\mathcal{P}^{(M)}$ is the Fourier transform of $\mathcal{Z}^{(M)}$, so that:

$$\mathcal{P}^{(M)}(s_1,...,s_M) = \frac{1}{2\pi}\int d\lambda_1...d\lambda_M e^{-\sum_m i\lambda_m s_m}\mathcal{Z}^{(M)}(\lambda_1,...,\lambda_M) \tag{113}$$

A straightforward Fourier transformation yields the following continuity equation:

$$\dot{\mathcal{P}}^{(M)} + \sum_{m=1}^{M}\frac{\partial}{\partial s_m}\mathcal{F}_m^{(M)} = 0, \tag{114}$$

$$\begin{aligned}\mathcal{F}_m^{(M)} = &-192\pi s_m \sum_{\underline{\sigma}=(1,\sigma_2,\sigma_3,\sigma_4)}\int d^d\overline{k}_2 d^d\overline{k}_3 d^d\overline{k}_4 \delta^m_{234}\delta\left(\tilde{\omega}^m_{234}\right)\left|\mathcal{H}^{-\sigma_2\sigma_3\sigma_4}_{m234}\right|^2 \\ &\times\Bigg[\int d\overline{s}_2 d\overline{s}_3 d\overline{s}_4 \overline{s}_2\overline{s}_3\overline{s}_4\frac{\partial\mathcal{P}^{(M+3)}}{\partial s_m} + \sigma_2\int d\overline{s}_3 d\overline{s}_4\overline{s}_3\overline{s}_4\mathcal{P}^{(M+2)} \\ &+ \sigma_3\int d\overline{s}_2 d\overline{s}_4\overline{s}_2\overline{s}_4\mathcal{P}^{(M+2)} + \sigma_4\int d\overline{s}_2 d\overline{s}_3\overline{s}_2\overline{s}_3\mathcal{P}^{(M+2)}\Bigg]\end{aligned} \tag{115}$$

This is not a closed equation for $\mathcal{P}^{(M)}$, as it contains $\mathcal{P}^{(M+2)}$ and $\mathcal{P}^{(M+3)}$, for $M = 1, 2, 3, ...$

4.3. The 1-mode PDF equation

It is interesting to note that factorized initial conditions (which is equivalent to RPA property at the initial time) imply factorized solutions for Eq.(115), $\forall\tau \geq 0$:

$$\mathcal{Z}^{(M)}(\lambda_1,...,\lambda_M,\tau;\mathbf{k}_1,...,\mathbf{k}_M) = \prod_{m=1}^{M}\mathcal{Z}(\lambda_m,\tau;\mathbf{k}_m), \quad \tau\geq 0 \tag{116}$$

with each $\mathcal{Z}(\lambda_{\mathbf{k}},\tau;\mathbf{k})$ satisfying

$$\frac{\partial\mathcal{Z}(\lambda_{\mathbf{k}},\tau;\mathbf{k})}{\partial\tau} = i\eta_{\mathbf{k}}\lambda_{\mathbf{k}}\Big(1+\lambda_{\mathbf{k}}\frac{\partial}{\partial\lambda_{\mathbf{k}}}\Big)\mathcal{Z}(\lambda_{\mathbf{k}},\tau;\mathbf{k}) - \gamma_{\mathbf{k}}\lambda_{\mathbf{k}}\frac{\partial\mathcal{Z}}{\partial\lambda_{\mathbf{k}}}(\lambda_{\mathbf{k}},\tau;\mathbf{k}) \tag{117}$$

where

$$\eta_{\mathbf{k}} \doteq 192\pi\sum_{\underline{\sigma}}\int d^d\mathbf{k}_2 d^d\mathbf{k}_3 d^d\mathbf{k}_4\delta^{\mathbf{k}}_{234}\delta\left(\tilde{\omega}^{\mathbf{k}}_{234}\right)\left|\mathcal{H}^{-\sigma_2\sigma_3\sigma_4}_{\mathbf{k}234}\right|^2 n(\mathbf{k}_2)n(\mathbf{k}_3)n(\mathbf{k}_4) \geq 0, \tag{118}$$

$$\begin{aligned}\gamma_{\mathbf{k}} \doteq 192\pi\sum_{\underline{\sigma}}&\int d^d\mathbf{k}_2 d^d\mathbf{k}_3 d^d\mathbf{k}_4\delta^{\mathbf{k}}_{234}\delta\left(\tilde{\omega}^{\mathbf{k}}_{234}\right)\left|\mathcal{H}^{-\sigma_2\sigma_3\sigma_4}_{\mathbf{k}234}\right|^2 \\ &\times\Big[\sigma_2 n(\mathbf{k}_3)n(\mathbf{k}_4) + \sigma_3 n(\mathbf{k}_2)n(\mathbf{k}_3) + \sigma_4 n(\mathbf{k}_2)n(\mathbf{k}_3)\Big]\end{aligned} \tag{119}$$

For the PDF hierarchy an analogous result holds. Substituting a factorized solution into Eq.(114) we get the equation for the one mode PDF:

$$\mathcal{P}^{(M)}(s_1,...,s_M,\tau;\mathbf{k}_1,...,\mathbf{k}_M) = \prod_{m=1}^{M}P(s_m,\tau;\mathbf{k}_m) \doteq \prod_{m=1}^{M}P_m, \quad \tau\geq 0 \tag{120}$$

Equation (114) transforms into:

$$\prod_{m\neq 1} P_m \frac{\partial P_1}{\partial \tau} + \prod_{m\neq 2} P_m \frac{\partial P_2}{\partial \tau} ... = \frac{\partial}{\partial s_1}\Big\{ 192\pi s_1 \sum_{\underline{\sigma}} \int d^dk_2 d^dk_3 d^dk_4 \delta^1_{234} \delta\left(\tilde{\omega}^1_{234}\right) \\ \times \left|\mathcal{H}^{-\sigma_2\sigma_3\sigma_4}_{1234}\right|^2 \prod_{m\neq 1} P_m \Big[\frac{\partial \mathcal{P}_1}{\partial s_1} \int d\overline{s}_2 \overline{s}_2 P_2 \int d\overline{s}_3 \overline{s}_3 P_3 \int d\overline{s}_4 \overline{s}_4 P_4 \\ + \Big(\sigma_2 P_1 \int d\overline{s}_3 \overline{s}_3 P_3 \int d\overline{s}_4 \overline{s}_4 P_4 + (2 \leftrightarrow 3) + (2 \leftrightarrow 4) \Big) \Big] + ... \Big\} \tag{121}$$

Recall that $\int ds_i s_i P(s_i, \tau; \mathbf{k}_i) = n(\mathbf{k}_i, \tau)$, because of the definition of the wave spectrum. Equation (121) is made of M independent parts, each of which can be written in the continuity equation form:

$$\frac{\partial P}{\partial \tau} = \frac{\partial}{\partial s}\Big[s\Big(\eta_{\mathbf{k}} \frac{\partial P}{\partial s} + \gamma_{\mathbf{k}} P \Big) \Big] \tag{122}$$

where $\eta_{\mathbf{k}}$ and $\gamma_{\mathbf{k}}$ are the same defined in (118) and (119). These are nonlinear Markov evolution equations in the sense of McKean, since the solutions satisfy the set of self-consistency conditions:

$$n(\mathbf{k}, \tau) = \int ds\ sP(s, \tau; \mathbf{k}) \tag{123}$$

where $n(\mathbf{k}, \tau)$ is the same spectrum that appears in the formulas for the coefficients (118) and (119).

These equations are the exact solutions of a model of "self-consistent Langevin equations". Here, the model equations take the form of the stochastic differential equations

$$ds_{\mathbf{k}} = (\eta_{\mathbf{k}} - \gamma_{\mathbf{k}} s_{\mathbf{k}}) d\tau + \sqrt{2\eta_{\mathbf{k}} s_{\mathbf{k}}} dW_{\mathbf{k}}, \tag{124}$$

interpreted in the Ito sense, with self-consistency determination of $n(\mathbf{k}, \tau)$ via (123). This generalizes the 3-wave case of Ref.[21] where, $P(s, \tau; \mathbf{k})$ relaxes to

$$Q(s, \tau; \mathbf{k}) = \frac{1}{n(\mathbf{k}, \tau)} \exp(-s/n(\mathbf{k}, \tau)), \tag{125}$$

which corresponds to a Gaussian distribution of the canonical variable $\tilde{b} = \left(\frac{2\pi}{L}\right)^{d/2} b$. For any solution $n(\mathbf{k}, \tau)$ of the wave kinetic equation, $Q(s, \tau; \mathbf{k})$ solves the 1-mode PDF equation (122). Also, the relaxation of a general solution P to Q is indicated by an H-theorem for the *relative entropy*

$$H(P|Q) = \int ds\ P(s) \ln\left(\frac{P(s)}{Q(s)}\right) = \int ds\ P(s) \ln P(s) + \ln n + 1. \tag{126}$$

This is a convex function of P, non-negative, and vanishing only for $P = Q$. Taking the time-derivative using (122), it is straightforward to derive

$$\frac{d}{d\tau} H(P(\tau)|Q(\tau)) = -\eta \int ds\ \frac{s|\partial_s P(s, \tau)|^2}{P(s, \tau)} + \frac{\eta}{n(\tau)}, \tag{127}$$

where

$$\int -s\partial_s P(s, \tau)\, ds = \int P(s, \tau)\, ds = 1 \tag{128}$$

is used to cancel terms involving γ. The self-consistency condition $n(\tau) = \int s\, P(s, \tau)\, ds$ implies

$$\frac{d}{d\tau} H(P(\tau)|Q(\tau)) = -\eta \left(\int ds\ \frac{s|\partial_s P(s, \tau)|^2}{P(s, \tau)} - \frac{1}{\int s\, P(s, \tau)\, ds} \right) \leq 0. \tag{129}$$

The inequality follows from the Cauchy-Schwartz inequality applied to (128)

$$1 = \int \sqrt{sP} \cdot \sqrt{\frac{s}{P}} (-\partial_s P)\, ds \leq \sqrt{\int sP(s)\, ds \cdot \int \frac{s|\partial_s P|^2}{P}\, ds}. \tag{130}$$

Equality holds and relative entropy production vanishes if and only if $\sqrt{sP} = c\sqrt{\frac{s}{P}}(-\partial_s P)$, or $P = -c\partial_s P$ for some c. The solution of this latter equation gives $P = Q$ with $n = 1/c$. Then, $P(\tau)$ relaxes to $Q(\tau)$ as τ increases, assuming that kinetic theory holds over the entire amplitudes range $s \in (0, \infty)$.

5. Conclusions

1. We have worked within the framework of WWT. We have considered a *Hamiltonian system* in d dimensions, with a quartic small perturbation implying *4-wave interactions*. From Hamilton equations, we have derived the equations of motion expressed in canonical normal variables.
2. To reach a closure for the problem, we have assumed that the canonical wavefield has the RP property at the initial time, allowing a statistical description of the field through its modes. We have averaged over phases using a method based on the *Feynman-Wyld diagrams*.
3. For the large-box limit, we have normalized the amplitudes to keep the wave spectrum finite, which is crucial for a correct evaluation of the contributions of the different diagrams [21]. This makes our results differ significantly from previous results for 4-wave resonant wave systems [1]. In particular, the equations we derive are simpler than previous ones and, as we shall see, they imply good properties for the solutions.
4. We have formally taken the large-box (*thermodynamic*) limit, followed by the small nonlinearity limit, obtaining the following closed equation:

$$\begin{aligned}\frac{d\mathcal{Z}[\lambda,\mu,\tau]}{d\tau} &= -192\pi\delta_{\mu,0}\sum_{\underline{\sigma}}\int d^dk_1d^dk_2d^dk_3d^dk_4\lambda\left(\mathbf{k}_1\right)|\mathcal{H}_{1234}^{-\sigma_2\sigma_3\sigma_4}|^2\delta(\tilde{\omega}_{234}^1)\\ &\times\delta_{234}^1\Bigg(\frac{\delta^3\mathcal{Z}}{\delta\lambda(\mathbf{k}_2)\delta\lambda(\mathbf{k}_3)\delta\lambda(\mathbf{k}_4)}-\sigma_2\frac{\delta^3\mathcal{Z}}{\delta\lambda(\mathbf{k}_1)\delta\lambda(\mathbf{k}_3)\delta\lambda(\mathbf{k}_4)}+\\ &-\sigma_3\frac{\delta^3\mathcal{Z}}{\delta\lambda(\mathbf{k}_1)\delta\lambda(\mathbf{k}_2)\delta\lambda(\mathbf{k}_4)}-\sigma_4\frac{\delta^3\mathcal{Z}}{\delta\lambda(\mathbf{k}_1)\delta\lambda(\mathbf{k}_2)\delta\lambda(\mathbf{k}_3)}\Bigg)\end{aligned}\tag{131}$$

   where τ is the nonlinear time. Note that:

   - Due to the $\delta_{\mu,0}$ factor, the RP property of the initial field is preserved as time goes on. This fact is crucial as it ensures the validity of the equation itself at $\tau>0$.
   - The stricter initial RPA property for the wavefield, and thus a factorized form for $\mathcal{Z}[\lambda,\mu,0]$, entails a solution preserving the factorized form in time.
   - Differentiating the characteristic functional in the variables $\lambda_{\mathbf{k}}$'s, one obtains the *spectral hierarchy*, which is analogous to the BBGKY hierarchy of Kinetic Theory. Assuming RPA for the initial field, the hierarchy is closed obtaining the kinetic wave equation for the spectrum. This connects our work with the literature that is mostly based on such equation. Furthermore, the general derivation for the 4-wave case for all possible interactions, and not only the $(2\to2)$ interactions, was hardly ever treated in the past.
5. We have defined a different *characteristic function*, for a *finite number of modes* M, and derived a hierarchy of equations for its time evolution for any value of M, which reads:

$$\begin{aligned}&\frac{\partial\mathcal{Z}^{(M)}}{\partial\tau}(\lambda,\mu,\tau)=-192\pi\delta_{\mu,0}\\ &\times\sum_{j=1}^{M}\sum_{(1,\sigma_2,\sigma_3,\sigma_4)}\int d^d\overline{k}_2d^d\overline{k}_3d^d\overline{k}_4\delta_{234}^j\delta\left(\tilde{\omega}_{234}^j\right)\left|\mathcal{H}_{j234}^{-\sigma_2\sigma_3\sigma_4}\right|^2\\ &\times\Bigg\{\left(\lambda_j+\lambda_j^2\frac{\partial}{\partial\lambda_j}\right)\frac{\partial^3\mathcal{Z}^{(M+3)}}{\partial\overline{\lambda}_2\partial\overline{\lambda}_3\partial\overline{\lambda}_4}\Bigg|_{\overline{\lambda}_2=\overline{\lambda}_3=\overline{\lambda}_4=0}-\sigma_2\lambda_j\left.\frac{\partial^3\mathcal{Z}^{(M+2)}}{\partial\lambda_j\partial\overline{\lambda}_3\partial\overline{\lambda}_4}\right|_{\overline{\lambda}_3=\overline{\lambda}_4=0}\\ &-\sigma_3\lambda_j\left.\frac{\partial^3\mathcal{Z}^{(M+2)}}{\partial\lambda_j\partial\overline{\lambda}_2\partial\overline{\lambda}_4}\right|_{\overline{\lambda}_2=\overline{\lambda}_4=0}-\sigma_4\lambda_j\left.\frac{\partial^3\mathcal{Z}^{(M+2)}}{\partial\lambda_j\partial\overline{\lambda}_2\partial\overline{\lambda}_3}\right|_{\overline{\lambda}_2=\overline{\lambda}_3=0}\Bigg\}\end{aligned}\tag{132}$$

6. By taking the Fourier transform of equation (132), we have derived a hierarchy for the M*-mode joint PDF's*, which can be written in *continuity equation* form:

$$\dot{\mathcal{P}}^{(M)}+\sum_{m=1}^{M}\frac{\partial}{\partial s_m}\mathcal{F}_m^{(M)}=0,\tag{133}$$

$$\mathcal{F}_m^{(M)} = -192\pi s_m \sum_{\underline{\sigma}=(1,\sigma_2,\sigma_3,\sigma_4)} \int d^d\overline{k}_2 d^d\overline{k}_3 d^d\overline{k}_4 \delta^m_{234} \delta\left(\tilde{\omega}^m_{234}\right) \left|\mathcal{H}^{-\sigma_2\sigma_3\sigma_4}_{m234}\right|^2$$
$$\times\Big[\int d\overline{s}_2 d\overline{s}_3 d\overline{s}_4 \overline{s}_2\overline{s}_3\overline{s}_4 \frac{\partial \mathcal{P}^{(M+3)}}{\partial s_m} + \sigma_2 \int d\overline{s}_3 d\overline{s}_4 \overline{s}_3\overline{s}_4 \mathcal{P}^{(M+2)}$$
$$+ \sigma_3 \int d\overline{s}_2 d\overline{s}_4 \overline{s}_2\overline{s}_4 \mathcal{P}^{(M+2)} + \sigma_4 \int d\overline{s}_2 d\overline{s}_3 \overline{s}_2\overline{s}_3 \mathcal{P}^{(M+2)}\Big]$$

where $\mathcal{F}_m^{(M)}$ is the flux for one of the M modes. As in the case of Eq.(131) we have:

- RP property for the wavefield at $\tau = 0$ remains fullfilled for the field at $\tau > 0$. So, equation (132) is valid for any nonlinear time $\tau \geq 0$.
- An initial RPA field remains RPA under the evolution of Eq.(133).
- Under RPA, the hierarchy (133) can be closed to yield the the 1-mode PDF equation:

$$\frac{\partial P}{\partial \tau} = \frac{\partial}{\partial s}\Big[s\Big(\eta_{\mathbf{k}} \frac{\partial P}{\partial s} + \gamma_{\mathbf{k}} P\Big)\Big], \tag{134}$$

$$\eta_{\mathbf{k}} \doteq 192\pi \sum_{\underline{\sigma}} \int d^d\mathbf{k}_2 d^d\mathbf{k}_3 d^d\mathbf{k}_4 \delta^{\mathbf{k}}_{234} \delta\left(\tilde{\omega}^{\mathbf{k}}_{234}\right) \left|\mathcal{H}^{-\sigma_2\sigma_3\sigma_4}_{\mathbf{k}234}\right|^2$$
$$\times n(\mathbf{k}_2) n(\mathbf{k}_3) n(\mathbf{k}_4) \geq 0, \tag{135}$$
$$\gamma_{\mathbf{k}} \doteq 192\pi \sum_{\underline{\sigma}} \int d^d\mathbf{k}_2 d^d\mathbf{k}_3 d^d\mathbf{k}_4 \delta^{\mathbf{k}}_{234} \delta\left(\tilde{\omega}^{\mathbf{k}}_{234}\right) \left|\mathcal{H}^{-\sigma_2\sigma_3\sigma_4}_{\mathbf{k}234}\right|^2$$
$$\times\Big[\sigma_2 n(\mathbf{k}_3) n(\mathbf{k}_4) + \sigma_3 n(\mathbf{k}_2) n(\mathbf{k}_3) + \sigma_4 n(\mathbf{k}_2) n(\mathbf{k}_3)\Big] \tag{136}$$

  that can be effciently treated numerically. The spectrum $n(\mathbf{k})$ in $\eta_{\mathbf{k}}$ and $\gamma_{\mathbf{k}}$ can be determined using the kinetic equation.
- Our Eq.(134) is more general than Eq.(6.51) of [1], as it contains all interactions, not only the $(2 \leftrightarrow 2)$ interactions.[6]
- An important solution to (137) is represented by the Rayleigh distribution:

$$Q(s, \tau; \mathbf{k}) = \frac{1}{n(\mathbf{k}, \tau)} e^{-s/n(\mathbf{k},\tau)} \tag{137}$$

  that corresponds to thermodynamic equilibrium. In absence of forcing and dissipation, it tends to the Rayleigh form (137) for any typical initial condition.

7. In the most general case, Eqs.(131,132,133) would have some supplementary terms (see equation (90)). However, as argued in Section 3.3.3, we think they are irrelevant for the known physical systems of wave turbulence, since the resonant condition is never fulfilled.
8. For any system where the leading nonlinear phenomena are N-wave resonances, our results suggest the conjecture that the coefficient preceding the right-hand side in Eq.(131) equals $12i^{2-N}A_N$, where A_N is a number and $A_3 = 3, A_4 = 16$. Integration over the N wavenumber variables, on which also the Hamiltonian coefficients and the two delta's depend yields:

$$\left(\frac{\delta^{N-1}\mathcal{Z}}{\delta\lambda(\mathbf{k}_2)\delta\lambda(\mathbf{k}_3)...\delta\lambda(\mathbf{k}_N)} - \sum_{i=2}^{N} \sigma_i \frac{\delta^{N-1}\mathcal{Z}}{\prod_{j\neq i}\delta\lambda(\mathbf{k}_i)}\right) \tag{138}$$

[6] Remarkably, see the system of vibrating elastic plates treated in [28].

Appendix A. Consistency with Choi et al. 2005 [18]

Let us assess the consistency of Eq.(50) with Eq.(3) in [18], which only concerns 2 waves -2 waves interactions. If Eq.(50) is to describe that particular case, the following factor has to be added:

$$(\delta_{\sigma_2,1}\delta_{\sigma_3,1}\delta_{\sigma_4,-1} + \delta_{\sigma_2,1}\delta_{\sigma_3,-1}\delta_{\sigma_4,1} + \delta_{\sigma_2,-1}\delta_{\sigma_3,1}\delta_{\sigma_4,1}) \tag{A.1}$$

turning (50) into:[7]

$$\begin{aligned} b_1^{(1)+}(T) &= {\sum_{\mathbf{k}_2\mathbf{k}_3\mathbf{k}_4}}^{*} \mathcal{L}_{1234}^{+++-} b_2^+ b_3^+ b_4^- \Delta_T(\tilde{\omega}_{34}^{12})\delta_{34}^{12} + (2 \leftrightarrow 4) + (3 \leftrightarrow 4) \\ &= 12i \sum_{\mathbf{k}_2\mathbf{k}_3\mathbf{k}_4} \mathcal{H}_{1234}^{-++-} b_2^+ b_3^+ b_4^- \Delta_T(\tilde{\omega}_{34}^{12})\delta_{34}^{12} \\ &\quad -6 \sum_{\mathbf{k}_3} \mathcal{L}_{1133}^{+++-} |b_3|^2 \Delta_T b_1^+ \end{aligned} \tag{A.2}$$

We used Eq.(42) and definition (12). Then, definition (44) yields:

$$ib_1^{(1)+}(T) = -12 \sum_{\mathbf{k}_2\mathbf{k}_3\mathbf{k}_4} \mathcal{H}_{1234}^{--++} b_2^- b_3^+ b_4^+ \Delta_T(\tilde{\omega}_{34}^{12})\delta_{34}^{12} + \frac{\Omega_1}{\epsilon} b_1^+ T \tag{A.3}$$

This can be compared with Eq.(3) of [18], which in our notation writes:

$$ib_1^{(1)+}(T) = \sum_{\mathbf{k}_2\mathbf{k}_3\mathbf{k}_4} \mathcal{W}_{34}^{12} b_2^- b_3^+ b_4^+ \Delta_T(\tilde{\omega}_{12}^{34})\delta_{12}^{34} - \frac{\Omega_1}{\epsilon} b_1^+ T \tag{A.4}$$

1. The two equations differ by a sign. This is due to a different definition of the initial field $A_{\mathbf{k}} \doteq \frac{1}{\sqrt{2}}(p_{\mathbf{k}} + iq_{\mathbf{k}})$, defined as $\frac{1}{\sqrt{2}}(q_{\mathbf{k}} + ip_{\mathbf{k}})$ in [18]. This also explains why in equation (A.4) there are the factors $\Delta_T(\tilde{\omega}_{12}^{34})\ \delta_{12}^{34}$ instead of our $\Delta_T(\tilde{\omega}_{34}^{12})\ \delta_{34}^{12}$ in (A.3).
2. Recall that $\mathcal{H}_{1234}^{--++} = \frac{1}{24}\mathcal{W}_{34}^{12}$, where $\frac{\mathcal{W}}{4}$ instead of $\frac{\mathcal{W}}{2}$ [18]. So, writing

   $$\mathcal{H}_{1234}^{--++} \doteq \frac{1}{2}\frac{1}{3}\frac{1}{2}\mathcal{W}_{34}^{12} = \frac{1}{12}\mathcal{W}_{34}^{12} \tag{A.5}$$

   one obtains

   $$12\ \mathcal{H}_{1234}^{--++} = \mathcal{W}_{34}^{12} \tag{A.6}$$

   Therefore, the first two terms in the right handside of equations (A.3) and (A.4) are consistent.
3. In [18] the linear terms inside the interaction term are grouped in Ω_1 this way[8]:

   $$\Omega_1 \doteq 2\epsilon \sum_{\mathbf{k}_2} \mathcal{W}_{12}^{12} |A_2(0)|^2 = 2\epsilon \sum_{\mathbf{k}_2} \mathcal{W}_{12}^{12} |b_2|^2 \tag{A.7}$$

   Then, from definition (44) and using (12) again, our Ω_1 obeys:

   $$\Omega_1 \doteq 24\epsilon \sum_{\mathbf{k}_3} \mathcal{H}_{1133}^{-++-} |b_3|^2 \tag{A.8}$$

   Replacing $12\ \mathcal{H}_{1133}^{-++-} = 12\ \mathcal{H}_{1313}^{--++}$ with $\mathcal{W}_{13}^{13}$ using (A.6) again, we obtain:

   $$\Omega_1 = 2\epsilon \sum_{\mathbf{k}_3} \mathcal{W}_{13}^{13} |b_3|^2 \tag{A.9}$$

   which is identical to (A.7).

[7] In this paragraph we omit the superscript (0) to simplify the notation.

[8] We recall that at time $t = 0$ the fields $A_{\mathbf{k}}$, $a_{\mathbf{k}}$ and $b_{\mathbf{k}}$ are equal, because they differ by an exponential factor with t in the exponent, which gives 1 at the initial time.

We can thus state that equations (A.3) and (A.4) are consistent, where (A.3) results from Eq.(50) for a Hamiltonian like the one of Ref.[18], containing only ($2 \to 2$) interactions. In other words, Eq.(3) of Ref.[18] is obtained as a particular case of our evolution equation (50) for the first-order term. This result is a check meant to assess the agreement of the formalism used in this paper with how 4-wave systems have already been treated in the past.

Appendix B. Proof of the *Lemma* in section 3.2.1

- *Role of couplings*
  The initial wavefield is an RP field and let us assume the k_i's are distinct. Then:

$$\Big\langle \prod_i \psi_i^{p_i} \Big\rangle_\psi = \prod_i \delta_{p_i,0}$$

  So, the phase average

$$\Big\langle \prod_l \psi_l^{\mu_l} \psi_1 \cdots \psi_p \psi_{p+1}^* \cdots \psi_q^* \Big\rangle$$

  is the sum of products of Kronecker delta's. Before phase-averaging each $\mathbf{k}_i \in \Lambda_L^*$, $i = 1, ..., q$ carries an independent degree of freedom. Each delta other than $\delta_{\mu_l,0}$ would cause the degrees of freedom to drop by one. The phase average is zero, unless either ψ_k's and ψ_m^*'s cancel each other (internal coupling) or they cancel with $\psi_l^{\mu_l}$ (external coupling).
  Every external coupling concerning $\mathbf{k}_i$ would lead to a Kronecker delta $\delta_{\mu_i,-1}$ or $\delta_{\mu_i,+1}$, which would cause the degrees of freedom to drop by one. Every internal coupling of pair $\mathbf{k}_i$, $\mathbf{k}_j$ (with $\sigma_i = +1, \sigma_j = -1$), would lead to a Kronecker delta $\delta_{\mathbf{k}_i,\mathbf{k}_j}$ which would cause the degrees of freedom to drop by one.
  Suppose a term has m internal couplings, so that $2m$ wavenumbers are internally coupled (each internal coupling concerns a pair of wavenumbers). Then, the term is non-zero only if the remaining $q-2m$ wavenumbers are externally coupled. Thus, the term totally drops by $m+(q-2m) = q-m$ degrees of freedom, that is the non-null contribution of the term is given by a product of $q - m$ Kronecker delta's different from $\delta_{\mu_l,0}$.
  Therefore, a diagram has m free wavenumbers, where m is the number of internal couplings.

- *Role of vertices*
  Consider the role of the momentum conservation delta's at the vertices and how they act with respect to the degrees of freedom.

  - *Diagrams with one vertex*
    The Kronecker delta of momentum conservation does not lower the degrees of freedom of the graph:

    1. if there are four external couplings there are no more degrees of freedom to reduce;
    2. if there are one internal coupling and two external couplings there is one degree of freedom, but in the momentum conservation delta the two internally coupled terms delete each other and thus one wavenumber remains free;
    3. if there are two internal couplings, two pairs of two wavenumbers delete each other in the momentum conservation delta, and then two free wavenumbers are preserved.

  - *Diagrams with two vertices*
    The bridge has initially one degree of freedom. Let us consider the three wavenumbers on one side of the bridge.

    1. *No cross-internal couplings*

       * If those three wavenumbers are pinned to a blob, the momentum conservation delta fixes the bridge to a value so that it does not bring any degree of freedom to the diagram;

∗ if one is pinned to a blob and two are in-internally coupled, the momentum conservation delta fixes the bridge to the value of the pinned wavenumber, because in the condition of the delta the two in-internally coupled wavenumbers delete each other.

2. *One cross-internal coupling*
   If only one wavenumber is cross-internally coupled with a wavenumber on the other side of the bridge, the two momentum conservation delta's (one is redundant) reduce from two to one the degrees of freedom of the bridge and the cross-internal coupling.
3. *Two cross-internal couplings*
   If two wavenumbers on one side are internally coupled with two wavenumbers on the other side (so the other two wavenumbers, one for each side, are externally coupled), the two delta's, giving the same condition, reduce the degrees of freedom of the bridge and the two cross-internal couplings from three to two.
4. *Three cross-internal couplings*
   If all the three wavenumbers on one side are cross-internally coupled with the other side, the two delta's reduce the total degrees of freedom from four to three.

In these four cases, with the only purpose of counting the degrees of freedom, it is as if the bridge never brings any degree of freedom to the diagram and each cross-internal coupling brings one, as a normal internal coupling.

We conclude, both for one vertex and two vertices diagrams, that the momentum conservation delta's only delete one degree of freedom when a bridge is present.

Collecting the contributions of the couplings and of the vertices, the lemma is proved.

Appendix C. Phase averaging with Feynman-Wyld diagrams

The expression of $\mathcal{J}_2$ in action-angle variables, changing variables in (63), is the following:

$$\begin{aligned}\mathcal{J}_2 \;=\; & \frac{1}{2}\sum_{1}\sum_{234}^{*}\sum_{567}^{*}\Big(\lambda_1+\lambda_1^2 J_1-\frac{\mu_1^2}{4J_1}\Big)\mathcal{L}_{1234}^{+\sigma_2\sigma_3\sigma_4}\mathcal{L}_{1567}^{-\sigma_5\sigma_6\sigma_7}\sqrt{J_2J_3J_4J_5J_6J_7}\\ & \times\Big\langle\psi_2^{\sigma_2}\psi_3^{\sigma_3}\psi_4^{\sigma_4}\psi_5^{\sigma_5}\psi_6^{\sigma_6}\psi_7^{\sigma_7}\prod_{\mathbf{k}}\psi_{\mathbf{k}}^{\mu_{\mathbf{k}}}\Big\rangle_{\psi}\Delta_T\left(\tilde{\omega}_{234}^{1}\right)\Delta_T\left(\tilde{\omega}_{1567}\right)\delta_{234}^{1}\delta_{1567}\end{aligned} \tag{C.1}$$

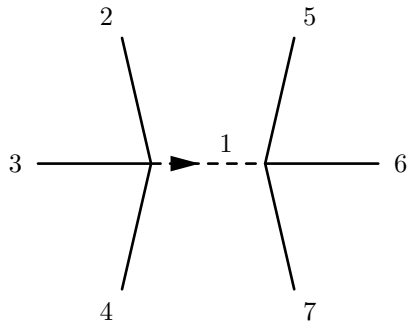

Figure C.8: Diagram associated to $\mathcal{J}_2$ before phase averaging

- Type 0 diagrams: having three free wavenumbers, these are the best candidates for the leading contributions to $\mathcal{J}_2$.

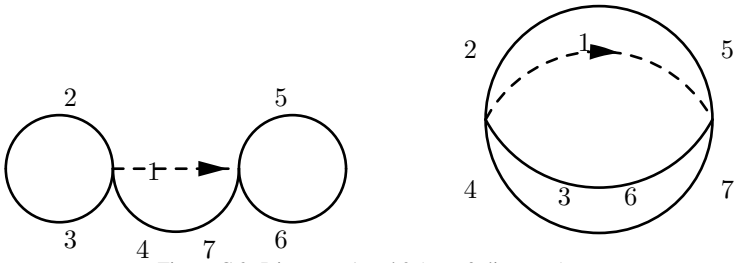

Figure C.9: Diagrams 1 and 2 (type 0 diagrams)

1. The contribution associated with diagram 1 in Fig. C.9 is the following:

$$\frac{1}{2}\sum_{1}\sum_{234}^{*'}\sum_{567}^{*'}\Big(\lambda_1+\lambda_1^2 J_1-\frac{\mu_1^2}{4J_1}\Big)\mathcal{L}_{1234}^{+\sigma_2\sigma_3\sigma_4}\mathcal{L}_{1567}^{-\sigma_5\sigma_6\sigma_7}\sqrt{J_2J_3J_4J_5J_6J_7}$$

$$\times\prod_m \delta_{\mu_m,0}\Delta_T\left(\sigma_4\tilde{\omega}_4-\tilde{\omega}_1\right)\Delta_T\left(\tilde{\omega}_1-\sigma_4\tilde{\omega}_4\right)\delta_{\mathbf{k}_1,\sigma_4\mathbf{k}_4}\delta_{\mathbf{k}_2,\mathbf{k}_3}\delta_{\mathbf{k}_4,\mathbf{k}_7}\delta_{\mathbf{k}_5,\mathbf{k}_6} \tag{C.2}$$

$$\underline{\sigma}=(1,\sigma_2,-\sigma_2,\sigma_4,\sigma_5,-\sigma_5,-\sigma_4)$$

The internal coupling between 2 and 3 and between 5 and 6 leads to Δ_T's and vertices δ's with just two terms each. Then, the $\delta_{\mathbf{k}_1,\sigma_4\mathbf{k}_4}$ term (left vertex) is the the only independent vertex condition, due to the internal coupling between 4 and 7. In turn, the $\prod_m \delta_{\mu_m,0}$ factor is due to the absence of external couplings. However, this graph does not entirely contribute to $\mathcal{J}_2$. Applying *Rule 5* one finds two cases in graph 1 (Fig. C.9):

- $\mathbf{k}_1=\mathbf{k}_4\Longrightarrow\sigma_4=1$ This term has been excluded from the interaction when frequency renormalization was done.
- $\mathbf{k}_1=-\mathbf{k}_4\Longrightarrow\sigma_4=-1$ Now, neither the left vertex nor the right one ($\mathbf{k}_7=-\mathbf{k}_1$) are in the configurations giving linear terms. We may conclude that this second case is effectively contributing to $\mathcal{J}_2$, so that diagram 1. finally gives:

$$\frac{1}{2}\sum_{\underline{\sigma}}\sum_{\underline{\mathbf{k}}}{}'\Big(\lambda_1+\lambda_1^2 J_1-\frac{\mu_1^2}{4J_1}\Big)\mathcal{L}_{1234}^{+\sigma_2\sigma_3\sigma_4}\mathcal{L}_{1567}^{-\sigma_5\sigma_6\sigma_7}\sqrt{J_2J_3J_4J_5J_6J_7}\;\delta_{\mu,0}$$

$$\times\Delta_T\left(-\tilde{\omega}_1-\tilde{\omega}_{-1}\right)\Delta_T\left(\tilde{\omega}_1+\tilde{\omega}_{-1}\right)\delta_{\mathbf{k}_4,-\mathbf{k}_1}\delta_{\mathbf{k}_4,\mathbf{k}_7}\delta_{\mathbf{k}_2,\mathbf{k}_3}\delta_{\mathbf{k}_5,\mathbf{k}_6} \tag{C.3}$$

$$\underline{\sigma}=(1,\sigma_2,-\sigma_2,-1,\sigma_5,-\sigma_5,1)$$

$$\underline{\mathbf{k}}=(\mathbf{k}_1,\mathbf{k}_2,\mathbf{k}_3,\mathbf{k}_4,\mathbf{k}_5,\mathbf{k}_6,\mathbf{k}_7)$$

2. The contribution to $\mathcal{J}_2$ of diagram 2 in Fig. C.9 is the following:

$$\frac{1}{2}\sum_{\underline{\sigma}}\sum_{\underline{\mathbf{k}}}{}'\Big(\lambda_1+\lambda_1^2 J_1-\frac{\mu_1^2}{4J_1}\Big)\mathcal{L}_{1234}^{+\sigma_2\sigma_3\sigma_4}\mathcal{L}_{1567}^{-\sigma_5\sigma_6\sigma_7}\sqrt{J_2J_3J_4J_5J_6J_7}$$

$$\times\prod_m \delta_{\mu_m,0}\Delta_T\left(\tilde{\omega}_{234}^{1}\right)\Delta_T\left(\tilde{\omega}_{1}^{234}\right)\delta_{234}^{1}\delta_{\mathbf{k}_2,\mathbf{k}_5}\delta_{\mathbf{k}_4,\mathbf{k}_7}\delta_{\mathbf{k}_3,\mathbf{k}_6} \tag{C.4}$$

$$\underline{\sigma}=(1,\sigma_2,\sigma_3,\sigma_4,-\sigma_2,-\sigma_3,-\sigma_4)$$

The Kronecker δ of the right vertex is redundant, the conditions of *Rule 5* for a graph to contribute are met, so there are no more simplifications in this case (we omit * on the sums).

- Type I diagrams: diagrams such as 3 and 4 in Fig.C.10 have two free wavenumbers, hence two unconstrained sums and, besided type 0 graphs, they represent the second choice for the leading order terms in $\mathcal{J}_2$. Together with those with permuted indices, they represent all type I diagrams.

Main contributions to $\mathcal{J}_2$. If present, the terms proportional to μ_1^2 carry a factor $O(L^{-2d})$ and are greater in order than the terms proportional to $\lambda(\mathbf{k}_1)$, which have a factor $O(L^{-3d})$.

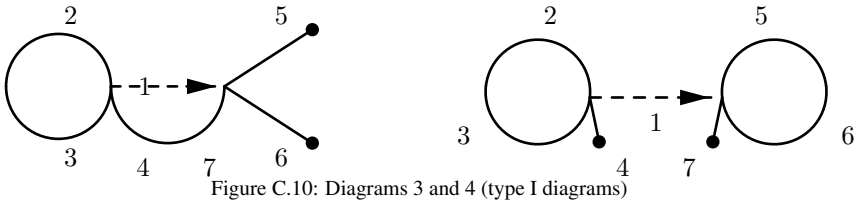

Figure C.10: Diagrams 3 and 4 (type I diagrams)

- Type 0 diagrams: the contributions of diagrams 1 and 2 are of order $O\left(L^{-3d}\right)$ because $\mathbf{k}_1$ is not pinned and so the average over phases gives a factor $\delta_{\mu,0}$, implying μ_1 is identically zero. These diagrams have three free summations, so they are of order $O\left(L^{-3d}\right) O\left(L^{3d}\right) = O(1)$. In total, there are 9 graphs similar to 1, because as far as the left vertex is concerned, the role of $\mathbf{k}_4$ can be played by $\mathbf{k}_2$, $\mathbf{k}_3$ and $\mathbf{k}_4$, and, as far as the right vertex is concerned, the role of $\mathbf{k}_7$ can be played by $\mathbf{k}_5$, $\mathbf{k}_6$ and $\mathbf{k}_7$. So there are 3×3 possibilities. There are 6 graphs similar to 2: one configuration has $\mathbf{k}_2$ coupled with one of the three different wavenumbers on the right side. In turn, $\mathbf{k}_3$ can be coupled with one of the two remaining wavenumbers and $\mathbf{k}_4$ has no more freedom to make a choice. So, there are $3\times2\times1$ different ways to "close" $\mathcal{J}_2$ with the shape of diagram 2.
- Type I diagrams: note that neither 3 nor 4 (our type I graphs) have $\mathbf{k}_1$ pinned. Thanks to an argument similar to the one used above, μ_1 is null because of the presence of the $\delta_{\mu,0}$. Thus, the two free summations of these graphs make their total contribution at most of order $O\left(L^{-3d}\right) O\left(L^{2d}\right) = O\left(L^{-d}\right)$, which is subleading with respect to the $O(1)$ terms.
- All the other types of diagrams represent subleading contributions.

Just keeping the terms of order $O(1)$, $\mathcal{J}_2$ takes the form of equation (79).[9]

Calculation of $\mathcal{J}_3$. Substituting the action-angle variables into the expression of $\mathcal{J}_3$ (64), we obtain

$$\mathcal{J}_3 = \sum_1 \Big[{\sum_{234567}}^{*} \Big(\lambda_1 + \frac{\mu_1}{2J_1}\Big) \mathcal{L}_{1234}^{+\sigma_2\sigma_3\sigma_4} \mathcal{L}_{4567}^{\sigma_4\sigma_5\sigma_6\sigma_7} \sqrt{J_1 J_2 J_3 J_5 J_6 J_7} \tag{C.5}$$

$$\times \Big\langle \psi_1^- \psi_2^{\sigma_2} \psi_3^{\sigma_3} \psi_5^{\sigma_5} \psi_6^{\sigma_6} \psi_7^{\sigma_7} \prod_{\mathbf{k}} \psi_{\mathbf{k}}^{\mu_{\mathbf{k}}} \Big\rangle_{\psi} E_T\left(\tilde{\omega}^1_{23567}, \tilde{\omega}^1_{234}\right) \delta^1_{234} \delta^4_{567}$$

$$+(4 \longleftrightarrow 2) + (4 \longleftrightarrow 3) + \int_0^T \mathcal{D}_1 b_1 dt \Big] \tag{C.6}$$

We start by taking into account the diagrams associated to $\mathcal{J}_3$, without the last term containing $\mathcal{D}_1$. Later, we will separately consider this term and its contribution. The first diagrams we consider are the

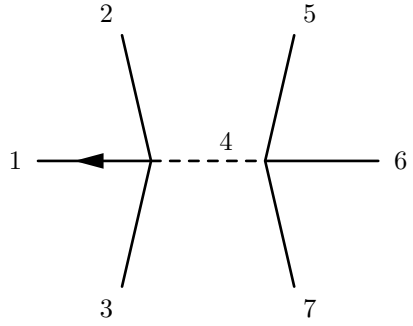

Figure C.11: Diagram associated to $\mathcal{J}_3$ before phase averaging

type 0 diagrams (3 free wavenumbers).

[9] Remember that these summations have to be intended with $\mathbf{k}_i \neq \mathbf{k}_j$, $i \neq j$, except when there is explicitly one $\delta_{\mathbf{k}_i,\mathbf{k}_j}$ term.

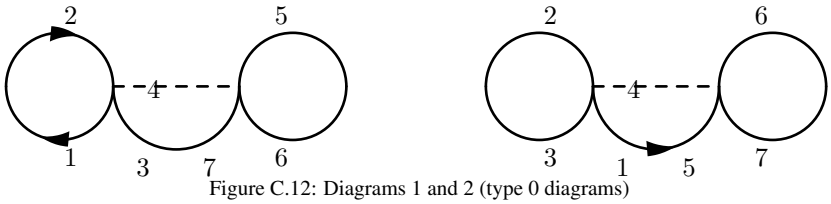

Figure C.12: Diagrams 1 and 2 (type 0 diagrams)

1. Diagram 1 in Fig. C.12 contributes to $\mathcal{J}_3$ as:

$$\sum_{1}\sum_{234567}^{*'}\Big(\lambda_1+\frac{\mu_1}{2J_1}\Big)\mathcal{L}_{1234}^{+\sigma_2\sigma_3\sigma_4}\mathcal{L}_{4567}^{\sigma_4\sigma_5\sigma_6\sigma_7}\sqrt{J_1J_2J_3J_5J_6J_7}\prod_m\delta_{\mu_m,0}$$
$$\times E_T\left(0,\sigma_3\tilde{\omega}_3+\sigma_4\tilde{\omega}_4\right)\delta_{\sigma_4\mathbf{k}_4,-\sigma_3\mathbf{k}_3}\delta_{\mathbf{k}_1,\mathbf{k}_2}\delta_{\mathbf{k}_3,\mathbf{k}_7}\delta_{\mathbf{k}_5,\mathbf{k}_6} \tag{C.7}$$
$$\underline{\sigma}=(1,1,\sigma_3,\sigma_4,\sigma_5,-\sigma_5,-\sigma_3)$$

The internal couplings between 1 and 2, between 5 and 6 and between 3, 4 and 7 result into a great simplification inside the arguments of E_T and the vertices delta's (both of which give the same condition). The term $\prod_m\delta_{\mu_m,0}$ is due to the fact that there are no external couplings. Similarly to the case of graph 1 of $\mathcal{J}_2$ (Fig. C.9), this graph is not entirely contributing to $\mathcal{J}_3$. Applying *Rule 5* of our phase-averaging method, in graph 1 there are two cases:

- $\mathbf{k}_3=\mathbf{k}_4=\mathbf{k}_7\Longrightarrow\sigma_3=-\sigma_4=-\sigma_7$, non contributing;
- $\mathbf{k}_4=-\mathbf{k}_3=-\mathbf{k}_7\Longrightarrow\sigma_4=\sigma_3=-\sigma_7$, contributing and giving:

$$18\sum_{\underline{\sigma}}\sum_{\underline{\mathbf{k}}}{}'\Big(\lambda_1+\frac{\mu_1}{2J_1}\Big)\mathcal{L}_{1234}^{+\sigma_2\sigma_3\sigma_4}\mathcal{L}_{4567}^{\sigma_4\sigma_5\sigma_6\sigma_7}\sqrt{J_1J_2J_3J_5J_6J_7}\prod_m\delta_{\mu_m,0}$$
$$\times E_T\left(0,\sigma_3\left(\omega_3+\omega_{-3}\right)\right)\delta_{\mathbf{k}_4,-\mathbf{k}_3}\delta_{\mathbf{k}_1,\mathbf{k}_2}\delta_{\mathbf{k}_3,\mathbf{k}_7}\delta_{\mathbf{k}_5,\mathbf{k}_6} \tag{C.8}$$
$$\underline{\sigma}=(1,1,\sigma_3,\sigma_3,\sigma_5,-\sigma_5,-\sigma_3)$$
$$\underline{\mathbf{k}}=(\mathbf{k}_1,\mathbf{k}_2,\mathbf{k}_3,\mathbf{k}_4,\mathbf{k}_5,\mathbf{k}_6,\mathbf{k}_7)$$

As a matter of fact, there are 18 graphs similar to 1, because the role of $\mathbf{k}_4$ can be played by $\mathbf{k}_2$, $\mathbf{k}_3$ and $\mathbf{k}_4$, and they all give equivalent results.

2. The contribution to $\mathcal{J}_3$ of diagram 2 in Fig. C.12 is the following:

$$\sum_{1}\sum_{234567}^{*'}\Big(\lambda_1+\frac{\mu_1}{2J_1}\Big)\mathcal{L}_{1234}^{+\sigma_2\sigma_3\sigma_4}\mathcal{L}_{4567}^{\sigma_4\sigma_5\sigma_6\sigma_7}\sqrt{J_1J_2J_3J_5J_6J_7}\prod_m\delta_{\mu_m,0}$$
$$\times E_T\left(0,-\tilde{\omega}_1+\sigma_4\tilde{\omega}_4\right)\delta_{\mathbf{k}_1,\sigma_4\mathbf{k}_4}\delta_{\mathbf{k}_2,\mathbf{k}_3}\delta_{\mathbf{k}_1,\mathbf{k}_5}\delta_{\mathbf{k}_6,\mathbf{k}_7} \tag{C.9}$$
$$\underline{\sigma}=(1,\sigma_2,-\sigma_2,\sigma_4,1,\sigma_6,-\sigma_6)$$

The proof of the above expression is anologous to diagram 1, with two cases:

- $\mathbf{k}_1=\mathbf{k}_4=\mathbf{k}_5\Longrightarrow\sigma_4=1=\sigma_5$, non contributing;
- $\mathbf{k}_4=-\mathbf{k}_1=-\mathbf{k}_5\Longrightarrow\sigma_4=-1=-\sigma_5$, contributing and giving:

$$9\sum_{\underline{\sigma}}\sum_{\underline{\mathbf{k}}}{}'\Big(\lambda_1+\frac{\mu_1}{2J_1}\Big)\mathcal{L}_{1234}^{+\sigma_2\sigma_3\sigma_4}\mathcal{L}_{4567}^{\sigma_4\sigma_5\sigma_6\sigma_7}\sqrt{J_1J_2J_3J_5J_6J_7}\prod_m\delta_{\mu_m,0}$$
$$\times E_T\left(0,-\left(\tilde{\omega}_1+\tilde{\omega}_{-1}\right)\right)\delta_{\mathbf{k}_1,-\mathbf{k}_4}\delta_{\mathbf{k}_2,\mathbf{k}_3}\delta_{\mathbf{k}_1,\mathbf{k}_5}\delta_{\mathbf{k}_6,\mathbf{k}_7} \tag{C.10}$$
$$\underline{\sigma}=(1,\sigma_2,-\sigma_2,-1,1,\sigma_6,-\sigma_6)$$

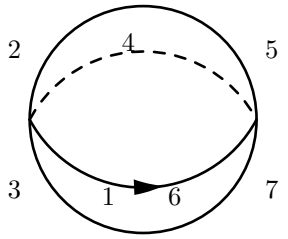

Figure C.13: Diagram 3 (type 0)

3. The contribution to $\mathcal{J}_3$ of diagram 3 in Fig. C.13 is the following:

$$18\sum_{\underline{\sigma}}\sum_{\underline{\mathbf{k}}}{}'\Big(\lambda_1+\frac{\mu_1}{2J_1}\Big)\mathcal{L}^{+\sigma_2\sigma_3\sigma_4}_{1234}\mathcal{L}^{\sigma_4\sigma_5\sigma_6\sigma_7}_{4567}\sqrt{J_1J_2J_3J_5J_6J_7}\prod_m\delta_{\mu_m,0}$$
$$\times E_T\left(0,\tilde{\omega}^1_{234}\right)\delta^1_{234}\delta_{\mathbf{k}_2,\mathbf{k}_5}\delta_{\mathbf{k}_1,\mathbf{k}_6}\delta_{\mathbf{k}_3,\mathbf{k}_7} \tag{C.11}$$
$$\underline{\sigma}=(1,\sigma_2,\sigma_3,\sigma_4,-\sigma_2,1,-\sigma_3)$$

In this case, the pinning between wavenumbers of the same vertex is not done. So, with the condition that the wavenumbers of each vertex are different from each other ($\sum'$), this graph does not vanish because of *Rule 5*. Multiplicity is 18 also here.

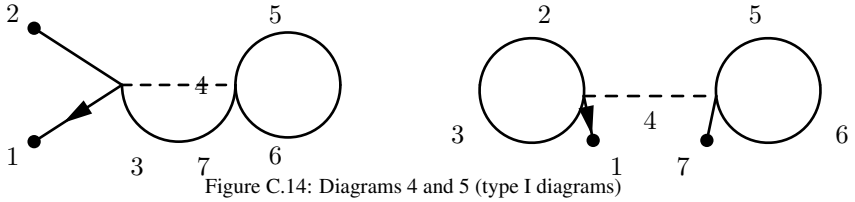

Figure C.14: Diagrams 4 and 5 (type I diagrams)

4. From graph 4 (Fig.C.14), we analyze type I diagrams,[10] to write the contribution to $\mathcal{J}_3$. The right-vertex δ becomes $\delta_{\sigma_4\mathbf{k}_4,\sigma_7\mathbf{k}_7}\Longrightarrow\delta_{\sigma_4\mathbf{k}_4,-\sigma_3\mathbf{k}_3}$. In the left-vertex condition, this yields $\delta_{\mathbf{k}_1,\sigma_2\mathbf{k}_2}$; but $\mathbf{k}_1\neq\mathbf{k}_2$ in this graph, so $\mathbf{k}_1=-\mathbf{k}_2$ and $\sigma_2=-1$. Considering the number of equivalent diagrams obtained by permutation of the indices, this contribution writes:

$$18\sum_{\underline{\sigma}}\sum_{\underline{\mathbf{k}}}{}'\Big(\lambda_1+\frac{\mu_1}{2J_1}\Big)\mathcal{L}^{+\sigma_2\sigma_3\sigma_4}_{1234}\mathcal{L}^{\sigma_4\sigma_5\sigma_6\sigma_7}_{4567}\sqrt{J_1J_2J_3J_5J_6J_7}\,\delta_{\mu_1,1}\delta_{\mu_2,-\sigma_2}$$
$$\times\prod_{m\neq1,2}\delta_{\mu_m,0}E_T\big(-(\tilde{\omega}_1+\tilde{\omega}_{-1}),-(\tilde{\omega}_1+\tilde{\omega}_{-1})+\sigma_3\tilde{\omega}_3+\sigma_4\tilde{\omega}_4\big)$$
$$\times\delta_{\mathbf{k}_1,-\mathbf{k}_2}\delta_{-\sigma_3\mathbf{k}_3,\sigma_4\mathbf{k}_4}\delta_{\mathbf{k}_3,\mathbf{k}_7}\delta_{\mathbf{k}_5,\mathbf{k}_6} \tag{C.12}$$
$$\underline{\sigma}=(1,-1,\sigma_3,\sigma_4,\sigma_5,-\sigma_5,-\sigma_3)$$

5. Diagram 5 in Fig. C.14 gives this contribution to $\mathcal{J}_3$ (proof similar to above):

$$9\sum_{\underline{\sigma}}\sum_{\underline{\mathbf{k}}}{}'\Big(\lambda_1+\frac{\mu_1}{2J_1}\Big)\mathcal{L}^{+\sigma_2\sigma_3\sigma_4}_{1234}\mathcal{L}^{\sigma_4\sigma_5\sigma_6\sigma_7}_{4567}\sqrt{J_1J_2J_3J_5J_6J_7}\,\delta_{\mu_1,1}\delta_{\mu_7,-\sigma_7}$$
$$\times\prod_{m\neq1,7}\delta_{\mu_m,0}E_T\big(-(\tilde{\omega}_1+\sigma_4\tilde{\omega}_4),-(\tilde{\omega}_1+\sigma_4\tilde{\omega}_4)\big)\delta_{\mathbf{k}_1,\sigma_4\mathbf{k}_4}\delta_{\mathbf{k}_1,\sigma_7\mathbf{k}_7}\delta_{\mathbf{k}_2,\mathbf{k}_3}\delta_{\mathbf{k}_5,\mathbf{k}_6}$$
$$\underline{\sigma}=(1,\sigma_2,-\sigma_2,\sigma_4,\sigma_5,-\sigma_5,\sigma_7) \tag{C.13}$$

[10] We only draw the type I diagrams with $\mathbf{k}_1$ pinned, knowing that they give a leading contribution as $L\to\infty$, since they allow $\mu_1\neq0$ and so they get an extra factor L^d with respect to the other graphs.

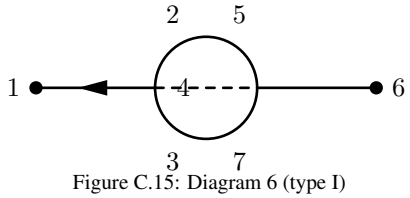

Figure C.15: Diagram 6 (type I)

6. The contribution to $\mathcal{J}_3$ of diagram 6 (Fig. C.15) is:

$$
\begin{aligned}
18 \sum_{\underline{\sigma}} \sum_{\underline{\mathbf{k}}}{}' \Big(\lambda_1 + \frac{\mu_1}{2J_1}\Big) \mathcal{L}_{1234}^{+\sigma_2\sigma_3\sigma_4} \mathcal{L}_{4567}^{\sigma_4\sigma_5\sigma_6\sigma_7} \sqrt{J_1 J_2 J_3 J_5 J_6 J_7}\; \delta_{\mu_1,1}\delta_{\mu_6,-\sigma_6} \\
\prod_{m\neq 1,6} \delta_{\mu_m,0} E_T\big(-(\tilde{\omega}_1+\tilde{\omega}_{-1}), -\tilde{\omega}_1+\sigma_2\tilde{\omega}_2+\sigma_3\tilde{\omega}_3+\sigma_4\tilde{\omega}_4\big) \\
\times \delta_{\mathbf{k}_1,\sigma_2\mathbf{k}_2+\sigma_3\mathbf{k}_3+\sigma_4\mathbf{k}_4} \delta_{\mathbf{k}_1,-\mathbf{k}_6} \delta_{\mathbf{k}_2,\mathbf{k}_5} \delta_{\mathbf{k}_3,\mathbf{k}_7} \qquad \text{(C.14)} \\
\underline{\sigma} = (1,\sigma_2,\sigma_3,\sigma_4,-\sigma_2,-1,-\sigma_3)
\end{aligned}
$$

Calculation of diagrams corresponding to $\int_0^T \mathcal{D}_1 b_1 dt$. Starting from definition (55), such term can be written in the equivalent form:

$$
\begin{aligned}
\int_0^T \mathcal{D}_1 b_1 dt \;=\; & 3 \sum_{\sigma_3=\pm 1} \sum_{\mathbf{k}_2\mathbf{k}_3\mathbf{k}_4} \sum_{567}{}^{*} \Big(\lambda_1 + \frac{\mu_1}{2J_1}\Big) \mathcal{L}_{1234}^{++\sigma_3-\sigma_3} \mathcal{L}_{3567}^{\sigma_3\sigma_5\sigma_6\sigma_7} \\
& \times b_2^{+} b_4^{-\sigma_3} b_5^{\sigma_5} b_6^{\sigma_6} b_7^{\sigma_7} \Delta_T\left(\tilde{\omega}_{567}^3\right) \delta_{567}^3 \delta_{\mathbf{k}_1,\mathbf{k}_2} \delta_{\mathbf{k}_3,\mathbf{k}_4} \qquad \text{(C.15)}
\end{aligned}
$$

The diagram associated to this expression before phase averaging is given in Fig.C.16, with the constraint $\mathbf{k}_3 = \mathbf{k}_4$ to keep in mind, because it cannot be represented in the graph.

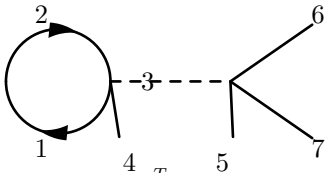

Figure C.16: Diagram associated to $\int_0^T \mathcal{D}_1 b_1 dt$, with the condition that $\mathbf{k}_3 = \mathbf{k}_4$

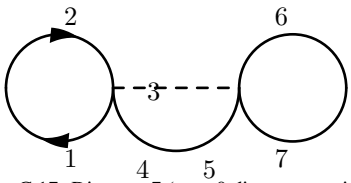

Figure C.17: Diagram 7 (type 0 diagram, vanishing)

7. The graph in Fig. C.16 is closed preserving the maximum number of free wavenumbers as in diagram 7 in Fig. C.17. However, $\delta_{\mathbf{k}_5,\mathbf{k}_3}$ and $\delta_{\mathbf{k}_6,\mathbf{k}_7}$ imply that such diagram does not contribute.

Other two type I graphs (8 and 9, Fig. C.18) are obtained closing the diagram in Fig. C.16 with two external pinnings. These diagrams have two free wavenumbers, but $\mathbf{k}_1$ is not pinned so they vanish identically because of the $\delta_{\mu_1,0}$. Then, the term with $\mathcal{D}_1$ inside $\mathcal{J}_3$ (equation (C.6)) can be neglected.
Main contributions to $\mathcal{J}_3$. If present, the terms proportional to μ_1 carry a factor $O(L^{-2d})$ and are greater in order than the terms proportional to $\lambda(\mathbf{k}_1)$, which are of order $O(L^{-3d})$. As usual, we must be careful when a $\delta_{\mu,0}$ is present, since that implies the terms in μ_1 to identically vanish. Among type 0 diagrams, the contributions of diagrams 1, 2 and 3 take with them an $O\left(L^{-3d}\right)$ because $\mathbf{k}_1$ is not pinned

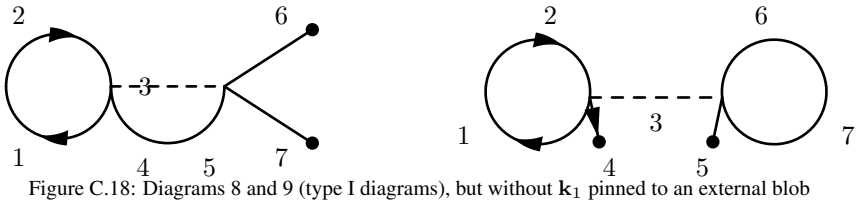

Figure C.18: Diagrams 8 and 9 (type I diagrams), but without $\mathbf{k}_1$ pinned to an external blob

and so the average over phases gives a factor $\delta_{\mu,0}$, implying μ_1 to be identically zero. These diagrams have 3 free summations, so the resulting terms turn out to be of order $O\left(L^{-3d}\right) O\left(L^{3d}\right) = O(1)$. As far as type I diagrams are concerned, thanks to the external coupling of $\mathbf{k}_1$, diagrams 4, 5 and 6 have μ_1 constrained to the value 1. Their leading contribution brings an $O\left(L^{-2d}\right)$ and therefore their two free summations are sufficient to make the total contribution $O(1)$. The other type I diagrams contribute with an $O\left(L^{-d}\right)$ and so are neglected in our work. All the other diagrams (type II and type III) represent subleading contributions.

Calculation of $\mathcal{J}_4$

$$\begin{aligned}\mathcal{J}_4 \;=\; & \sum_{1}\Big(\frac{1}{2}\lambda_1^2+\frac{\mu_1}{4J_1^2}\Big(\frac{\mu_1}{2}-1\Big)+\frac{\lambda_1\mu_1}{2J_1}\Big)\sum_{234}^{*}\sum_{567}^{*}\mathcal{L}_{1234}^{+\sigma_2\sigma_3\sigma_4}\mathcal{L}_{1567}^{+\sigma_5\sigma_6\sigma_7}\\ & \times J_1\sqrt{J_2J_3J_4J_5J_6J_7}\Big\langle\psi_1^{-2}\psi_2^{\sigma_2}\psi_3^{\sigma_3}\psi_4^{\sigma_4}\psi_5^{\sigma_5}\psi_6^{\sigma_6}\psi_7^{\sigma_7}\prod_{\mathbf{k}}\psi_{\mathbf{k}}^{\mu_{\mathbf{k}}}\Big\rangle_{\psi}\\ & \times\Delta_T\left(\tilde{\omega}_{234}^1\right)\Delta_T\left(\tilde{\omega}_{567}^1\right)\delta_{234}^1\delta_{567}^1 \qquad \text{(C.16)}\end{aligned}$$

$\mathbf{k}_1$ must be pinned to a blob so that $\mu_1 - 2 = 0$. Let us begin with type I diagrams, with two free

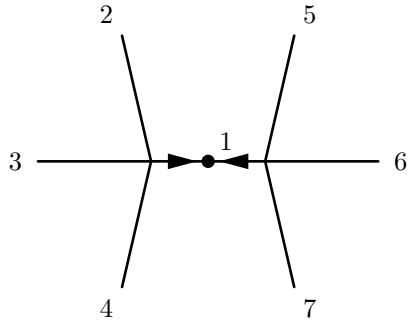

Figure C.19: Diagram associated to $\mathcal{J}_4$ before phase averaging

wavenumbers.

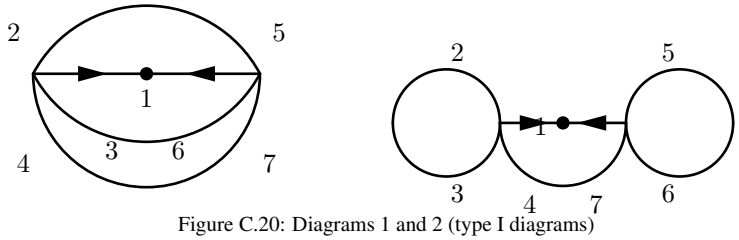

Figure C.20: Diagrams 1 and 2 (type I diagrams)

1. (Fig. C.20) The two conditions at the vertices imply $\mathbf{k}_1 = \mathbf{k}_{-1} = 0$, so the contribution to $\mathcal{J}_4$ is null. Due to the internal coupling between wavenumbers, we have:

$$\mathbf{k}_1 = \sigma_2\mathbf{k}_2 + \sigma_3\mathbf{k}_3 + \sigma_4\mathbf{k}_4\ , \quad \mathbf{k}_1 = -\sigma_2\mathbf{k}_2 - \sigma_3\mathbf{k}_3 - \sigma_4\mathbf{k}_4 \qquad \text{(C.17)}$$

2. (Fig. C.20) As for the previous graph, the two conditions at the vertices imply $\mathbf{k}_1 = \mathbf{k}_{-1} = 0$, so also this contribution to $\mathcal{J}_4$ is null. Due to the internal coupling between wavenumbers, we have

$$\mathbf{k}_1 = \sigma_4 \mathbf{k}_4 \ , \quad \mathbf{k}_1 = -\sigma_4 \mathbf{k}_4$$

and $\mathbf{k}_1 = 0$ follows.

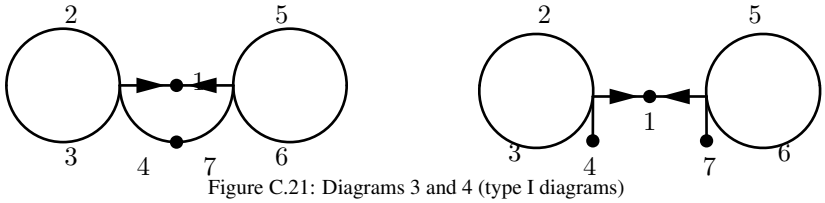

Figure C.21: Diagrams 3 and 4 (type I diagrams)

3. (Fig. C.21) This diagram gives one of the non-zero leading contributions to $\mathcal{J}_4$ and we keep in mind that it has two free wavenumbers implying two free sums.

$$\mathbf{k}_1 = \sigma_4 \mathbf{k}_4 \, , \mathbf{k}_1 = \sigma_7 \mathbf{k}_7 \ , \quad \Longrightarrow \sigma_4 = -\sigma_7, \quad \mathbf{k}_4 = -\mathbf{k}_7 \tag{C.18}$$

because $\mathbf{k}_4$ must be different from $\mathbf{k}_7$.
4. (Fig. C.21) Diagram 4 gives the other non-zero leading contribution to $\mathcal{J}_4$ and it implies two free sums too, $\sigma_4 = \sigma_7, \quad \mathbf{k}_4 = \mathbf{k}_7$.

Main contributions to $\mathcal{J}_4$. The term $\frac{1}{J_1^2}$ has a $\left(\frac{\mu_1}{2} - 1\right)$ factor which vanishes with μ_1 pinned to the value $\mu_1 = 2$. The term $\frac{1}{J_1}$ gives the leading contribution, $O(L^{-3d})$, coming from the J_i's. This can at most reach order $O(L^{-d})$ thanks to the two free sums of graphs 3 and 4. Type II and type III graphs cannot give larger contributions, having at most one free summation. Finally, $\mathcal{J}_4$ is of order $O(L^{-d})$ for large L, and hence negligible with respect to $\mathcal{J}_2$ and $\mathcal{J}_3$.
Calculation of $\mathcal{J}_5$. Before starting, here, we remark that $\mathbf{k}_2$ has to be treated like $\mathbf{k}_1$;[11] so, as for $\mathbf{k}_1$ there is no σ_2 degeneration in the following formulas. Let us rewrite (66) in the form:

$$\mathcal{J}_5 = \frac{1}{2} \sum_{\mathbf{k}_1 \neq \mathbf{k}_2} \Big[\lambda_1 \lambda_2 (B_1 + B_2) + \Big(\frac{\lambda_1 \mu_2}{J_2} + \frac{\mu_1 \mu_2}{4 J_1 J_2} \Big) (B_1 - B_3) \Big] \tag{C.19}$$

where, substituting the action-angle variables, (66) gives

$$\begin{aligned} B_1 \ = \ & \sum_{345}^{*} \sum_{678}^{*} \mathcal{L}_{1345}^{+\sigma_3\sigma_4\sigma_5} \mathcal{L}_{2678}^{+\sigma_6\sigma_7\sigma_8} \sqrt{J_1 J_2 J_3 J_4 J_5 J_6 J_7 J_8} \Big\langle \psi_1^- \psi_2^- \psi_3^{\sigma_3} \psi_4^{\sigma_4} \\ & \psi_5^{\sigma_5} \psi_6^{\sigma_6} \psi_7^{\sigma_7} \psi_8^{\sigma_8} \prod_{\mathbf{k}} \psi_{\mathbf{k}}^{\mu_{\mathbf{k}}} \Big\rangle_{\psi} \Delta_T \left(\tilde{\omega}_{345}^1 \right) \Delta_T \left(\tilde{\omega}_{678}^2 \right) \delta_{345}^1 \delta_{678}^2 \end{aligned} \tag{C.20}$$

$$\begin{aligned} B_2 \ = \ & \sum_{345}^{*} \sum_{678}^{*} \mathcal{L}_{1345}^{-\sigma_3\sigma_4\sigma_5} \mathcal{L}_{2678}^{+\sigma_6\sigma_7\sigma_8} \sqrt{J_1 J_2 J_3 J_4 J_5 J_6 J_7 J_8} \Big\langle \psi_1^+ \psi_2^- \psi_3^{\sigma_3} \psi_4^{\sigma_4} \\ & \psi_5^{\sigma_5} \psi_6^{\sigma_6} \psi_7^{\sigma_7} \psi_8^{\sigma_8} \prod_{\mathbf{k}} \psi_{\mathbf{k}}^{\mu_{\mathbf{k}}} \Big\rangle_{\psi} \Delta_T \left(\tilde{\omega}_{1345} \right) \Delta_T \left(\tilde{\omega}_{678}^2 \right) \delta_{1345} \delta_{678}^2 \end{aligned} \tag{C.21}$$

$$\begin{aligned} B_3 \ = \ & \sum_{345}^{*} \sum_{678}^{*} \mathcal{L}_{1345}^{+\sigma_3\sigma_4\sigma_5} \mathcal{L}_{2678}^{-\sigma_6\sigma_7\sigma_8} \sqrt{J_1 J_2 J_3 J_4 J_5 J_6 J_7 J_8} \Big\langle \psi_1^- \psi_2^+ \psi_3^{\sigma_3} \psi_4^{\sigma_4} \\ & \psi_5^{\sigma_5} \psi_6^{\sigma_6} \psi_7^{\sigma_7} \psi_8^{\sigma_8} \prod_{\mathbf{k}} \psi_{\mathbf{k}}^{\mu_{\mathbf{k}}} \Big\rangle_{\psi} \Delta_T \left(\tilde{\omega}_{345}^1 \right) \Delta_T \left(\tilde{\omega}_{2678} \right) \delta_{345}^1 \delta_{2678} \end{aligned} \tag{C.22}$$

The three B_i's can be drawn like in Figs. C.22, C.23 and C.24. Then, B_2 and B_3 have the same diagram under permutation $(1, 3, 4, 5) \leftrightarrow (2, 6, 7, 8)$. Consider type 0 diagrams with 3 free wavenumbers.

[11] We can see this looking back to (66).

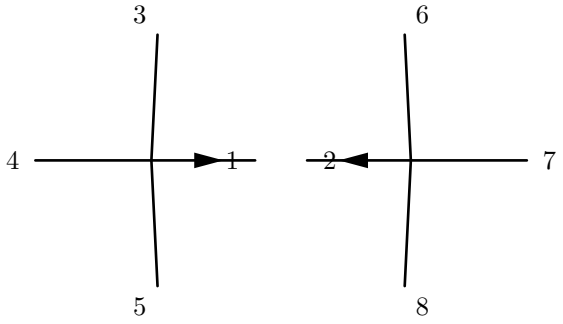

Figure C.22: Diagram associated to B_1

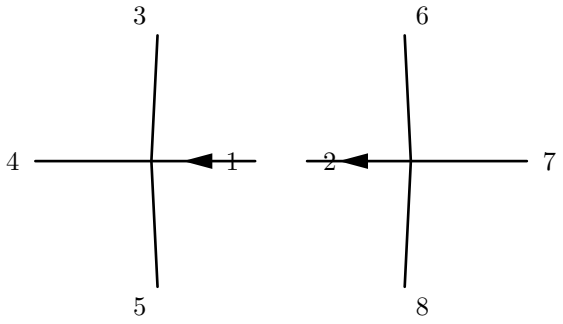

Figure C.23: Diagram associated to B_2

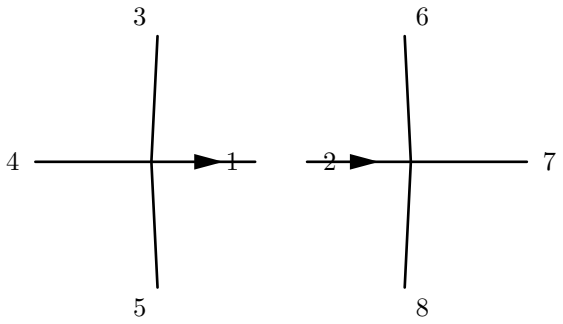

Figure C.24: Diagram associated to B_3

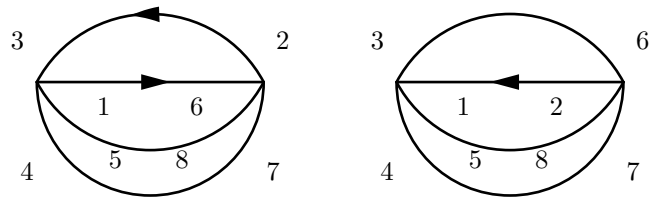

Figure C.25: Diagram 1 (for B_1) and diagram 2 (for B_2); both are type 0 diagrams

1. (Fig. C.25) This graph and similar ones for B_2 and B_3 (with $\mathbf{k}_1$ coupled with $\mathbf{k}_6$ too) contribute, but they imply $\mu_1 = \mu_2 = 0$, so they are subleading.
2. (Fig. C.25) This graph and a similar one for B_3 (with $\mathbf{k}_1$ coupled with $\mathbf{k}_2$) are not allowed due to the condition $\mathbf{k}_1 \neq \mathbf{k}_2$ in (C.19). Such a diagram for B_1 is not allowed because the internal coupling between $\mathbf{k}_1$ and $\mathbf{k}_2$ would lead to $\sigma_1 = -\sigma_2$, but B_1 already has $\sigma_1 = \sigma_2$.

Consider type I diagrams, illustrated in Figs. C.26 and C.27.

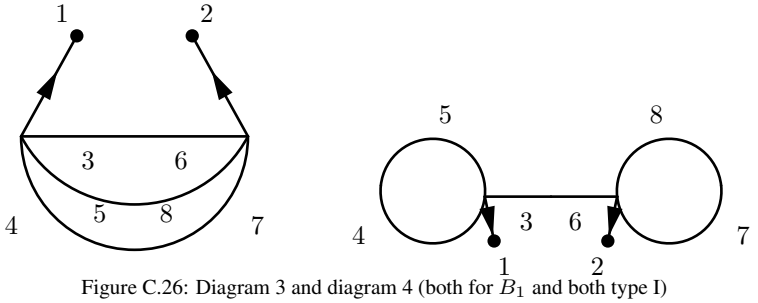

Figure C.26: Diagram 3 and diagram 4 (both for B_1 and both type I)

3. (Fig. C.26) The internal couplings yield: $\mathbf{k}_3 = \mathbf{k}_6$, $\mathbf{k}_4 = \mathbf{k}_7$, $\mathbf{k}_5 = \mathbf{k}_8$, $\sigma_3 = -\sigma_6$, $\sigma_4 = -\sigma_7$, $\sigma_5 = -\sigma_8$. The two deltas at the vertices imply the conditions

$$\begin{aligned} \mathbf{k}_1 &= \sigma_3\mathbf{k}_3 + \sigma_4\mathbf{k}_4 + \sigma_5\mathbf{k}_5 \; ; \quad \mathbf{k}_2 = \sigma_6\mathbf{k}_6 + \sigma_7\mathbf{k}_7 + \sigma_8\mathbf{k}_8 \\ \Longrightarrow \mathbf{k}_2 &= -\sigma_3\mathbf{k}_3 - \sigma_4\mathbf{k}_4 - \sigma_5\mathbf{k}_5 \quad \text{and so} \quad \mathbf{k}_2 = -\mathbf{k}_1 \end{aligned}$$

This holds for B_1, because for B_2 and B_3 the δ's at the vertices would lead to $\mathbf{k}_1 = \mathbf{k}_2$, which is forbidden by (C.19). The contribution of diagram 3 to $\mathcal{J}_5$ (only due to $\frac{1}{2}\sum_{1\neq 2}(...)B_1$) reads:

$$\begin{aligned} &\frac{1}{2}\sum_{\underline{\sigma}}\sum_{\underline{\mathbf{k}}}{}'(...)\mathcal{L}^{+\sigma_3\sigma_4\sigma_5}_{1345}\mathcal{L}^{+\sigma_6\sigma_7\sigma_8}_{2678}\sqrt{J_1J_2J_3J_4J_5J_6J_7J_8}\;\delta_{\mu_1,1}\delta_{\mu_2,1} \\ &\times\prod_{m\neq 1,2}\delta_{\mu_m,0}\,\delta_{\mathbf{k}_1,-\mathbf{k}_2}\delta_{\mathbf{k}_3,\mathbf{k}_6}\delta_{\mathbf{k}_4,\mathbf{k}_7}\delta_{\mathbf{k}_5,\mathbf{k}_8}\delta^1_{345}\Delta_T\big(\tilde{\omega}^1_{345}\big)\Delta_T\big(\tilde{\omega}^{(-1)345}\big) \end{aligned} \tag{C.23}$$

$$\underline{\sigma} = (1, 1, \sigma_3, \sigma_4, \sigma_5, -\sigma_3, -\sigma_4, -\sigma_5)$$

4. (Fig. C.26) For the same reason as above, this kind of contribution is only present for B_1. The left-vertex condition gives $\mathbf{k}_1 = \sigma_3\mathbf{k}_3$; the right-vertex condition gives $\mathbf{k}_2 = -\sigma_3\mathbf{k}_3$. So, $\mathbf{k}_2 = -\mathbf{k}_1$. Due to *Rule 5*, the right-vertex here is null and then the contribution vanishes. So, finally diagram 4 does not contribute to $\mathcal{J}_5$.

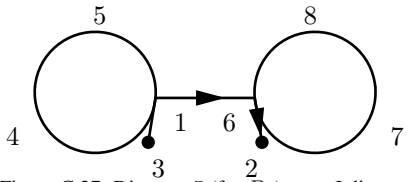

Figure C.27: Diagram 5 (for B_1); type I diagram

5. (Fig. C.27) An analogous kind of graph also exists for B_2 and B_3. There are two free wavenumbers; however, $\mu_1 = 0$ identically and then, as we are going to see, the contribution to $\mathcal{J}_5$ is not leading order. Similar graphs with $\mathbf{k}_2$ internally coupled are possible, but with $\mu_2 = 0$ their contributions to $\mathcal{J}_5$ are even smaller.

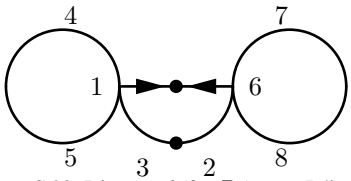

Figure C.28: Diagram 6 (for B_1); type I diagram

6. (Fig. C.28) One last contribution comes from the type I graph referred to B_1.

$$\sigma_6 = -1, \quad \sigma_3 = -1, \quad \mathbf{k}_1 = -\mathbf{k}_3, \quad \mathbf{k}_1 = \mathbf{k}_6, \quad \mathbf{k}_2 = \sigma_6 \mathbf{k}_6 = -\mathbf{k}_1$$

The contribution of diagram 6 to $\mathcal{J}_5$ (only due to $\frac{1}{2}\sum_{1\neq 2}(...)B_1$) is the following:

$$\begin{aligned}\frac{1}{2}\sum_{\underline{\sigma}}\sum_{\underline{\mathbf{k}}}{}'(...)\mathcal{L}_{1345}^{+\sigma_3\sigma_4\sigma_5}\mathcal{L}_{2678}^{+\sigma_6\sigma_7\sigma_8}\sqrt{J_1J_2J_3J_4J_5J_6J_7J_8}\,\delta_{\mu_1,2}\delta_{\mu_2,2}\prod_{m\neq 1,2}\delta_{\mu_m,0}\\ \times\delta_{\mathbf{k}_1,-\mathbf{k}_2}\delta_{\mathbf{k}_1,-\mathbf{k}_3}\delta_{\mathbf{k}_1,\mathbf{k}_6}\delta_{\mathbf{k}_4,\mathbf{k}_5}\delta_{\mathbf{k}_7,\mathbf{k}_8}\Delta_T\left(\tilde{\omega}^1_{(-1)44}\right)\Delta_T\left(\tilde{\omega}^{(-1)177}\right) \qquad \text{(C.24)}\\ \underline{\sigma} = (1,1,-1,\sigma_4,-\sigma_4,-1,\sigma_7,-\sigma_7)\end{aligned}$$

Type II diagrams (with one free wavenumber) and type III (with no free wavenumbers) certainly give subleading contributions and so it is not worth looking at them in detail.

Main contributions to $\mathcal{J}_5$. Consider the order of the various terms for growing L, using the variables $\tilde{J}_{\mathbf{k}}$ and $\lambda(\mathbf{k})$, cf. Eq.(76).

- For $\frac{1}{2}\sum_{1\neq 2}\lambda_1\lambda_2\,(B_1+B_2)$, the leading contribution is of order $O\left(L^{-d}\right) = O\left(L^{3d}\right)O\left(L^{-4d}\right)$ (3 free sums and 8 factors $\sqrt{J}$).
- For $\frac{1}{2}\sum_{1\neq 2}\frac{\lambda_1\mu_2}{J_2}\,(B_1-B_3)$, the leading contribution is of order $O\left(L^{-d}\right) = O\left(L^{2d}\right)O\left(L^{-4d}\right)O\left(L^{d}\right)$ (2 free sums, 8 factors $\sqrt{J}$ and J_2 at denominator).
- For $\frac{1}{2}\sum_{1\neq 2}\frac{\mu_1\mu_2}{4J_1J_2}B_1$, graph 3 contribution (Fig. C.26) is of order $O\left(L^{2d}\right)O\left(L^{-4d}\right)O\left(L^{2d}\right)$ (2 free sums, 8 factors $\sqrt{J}$ and J_1J_2 at denominator). This graph has multiplicity 6. Graph 6 in Fig.(C.28) and permutations contribute to same order. The multiplicity is 18.
- For $\frac{1}{2}\sum_{1\neq 2}\frac{\mu_1\mu_2}{4J_1J_2}B_3$, the leading contribution is given by type II diagrams (type I do not exist for B_3, cf. diagram 3, Fig. C.25) and is of order $O\left(L^{-d}\right) = O\left(L^{d}\right)O\left(L^{-4d}\right)O\left(L^{2d}\right)$ (1 free sum, 8 factors $\sqrt{J}$ and J_1J_2 at denominator).

The final expression of $\mathcal{J}_5$ is the one given in equation (84).

Appendix D. The PDF hierarchy

Appendix D.1. The five contributions $\mathcal{J}_1 - \mathcal{J}_5$

- $\mathcal{J}_1$ As seen in Section 3.2.2, the leading order graph is diagram 2 (Fig. 5), a type II diagram with one free wavenumber. This free wavenumber is continuous, as resulting from the internal coupling of $\mathbf{k}_2$ and $\mathbf{k}_3$; so, it brings an $O\left(L^{d}\right)$ factor. Then, we have an $O\left(L^{d}\right)$ from the prefactor and an $O\left(L^{-2d}\right)$ from the factor $\sqrt{J_1...J_4}$. Thus, the contribution is $O(1)$ and it looks like (78):

$$\begin{aligned}\left\langle e^{\sum_{\mathbf{k}} i\lambda_{\mathbf{k}}J_{\mathbf{k}}}\mathcal{J}_1\right\rangle_J \sim \left(\frac{2\pi}{L}\right)^d\sum_{(1)}\left\langle\left[i\lambda_j\sqrt{\tilde{J}_j}+\frac{1}{2\sqrt{\tilde{J}_j}}\right]\sqrt{\tilde{J}_2\tilde{J}_3\tilde{J}_4}e^{\sum_{m=1}^M i\lambda_m\tilde{J}_m}\right\rangle_J\\ \times\mathcal{L}_{j22(-j)}^{+\sigma_2\sigma_2-}\delta_{\mu_j,1}\delta_{\mu_{-j},1}\prod_{m\neq\pm j}\delta_{\mu_m,0}\Delta_T\left(-2(\tilde{\omega}_j+\tilde{\omega}_{-j})\right)\Big] \qquad \text{(D.1)}\end{aligned}$$

$$\text{with} \quad \sum_{(1)} \doteq \sum_{j=1}^{M} \sum_{\sigma_2=\pm 1} \sum_{\mathbf{k}_2} \tag{D.2}$$

- $\mathcal{J}_{\mathbf{2}}$ The prefactor $O\left(L^d\right)$ and the $\sqrt{J_1 ...}$ term ($O\left(L^{-3d}\right)$) give $O\left(L^{-2d}\right)$. The leading order graphs are diagrams 1 and 2 in Fig. C.9 (type 0).
  - In diagram 1 we have three free wavenumbers, but the one given by $\mathbf{k}_1$ (and consequently by $\mathbf{k}_4$ and $\mathbf{k}_7$, dependent on $\mathbf{k}_1$) is discrete. So, the total contribution is $O(1)$.
  - In diagram 2 the situation is similar: $\mathbf{k}_1$ is discrete and the δ^1_{234} allows other two wavenumbers to be continuous, so it is $O(1)$ too.
  - Diagrams 3 and 4 (type I) in Fig.C.10 only have one continuous free wavenumber and thus they are subleading (of order $O\left(L^{-d}\right)$).

  The total contribution to $\mathcal{J}_2$ reads:

$$\begin{aligned}\left\langle e^{\sum_{\mathbf{k}} i\lambda_{\mathbf{k}} J_{\mathbf{k}}} \mathcal{J}_2 \right\rangle_J \sim \frac{1}{2}\delta_{\mu,0}\Bigg\{ & 9 \sum_{(2)} \left(\frac{2\pi}{L}\right)^{2d} \left\langle \left[i\lambda_j - \lambda_j^2 \tilde{J}_j \right] \tilde{J}_2 \tilde{J}_5 \tilde{J}_{-j} e^{\sum_m i\lambda_m \tilde{J}_m} \right\rangle_J \\ & \mathcal{L}^{+\sigma_2(-\sigma_2)-}_{j22(-j)} \mathcal{L}^{-\sigma_5(-\sigma_5)+}_{j55(-j)} \left|\Delta_T\left(\tilde{\omega}_1 + \tilde{\omega}_{-1}\right)\right|^2 + \\ & + 6 \sum_{(3)} \left(\frac{2\pi}{L}\right)^{2d} \left\langle \left[i\lambda_j - \lambda_j^2 \tilde{J}_j \right] \tilde{J}_2 \tilde{J}_3 \tilde{J}_4 e^{\sum_m i\lambda_m \tilde{J}_m} \right\rangle_J \\ & \mathcal{L}^{+\sigma_2\sigma_3\sigma_4}_{j234} \mathcal{L}^{-(-\sigma_2)(-\sigma_3)(-\sigma_4)}_{j234} \left|\Delta_T\left(\tilde{\omega}^1_{234}\right)\right|^2 \Bigg\}\end{aligned} \tag{D.3}$$

  where similar definitions to those given in Section 3.2.2 hold:

$$\sum\nolimits_{(2)} \doteq \sum_{j=1}^{M} \sum_{\underline{\sigma}=(1,\sigma_2,-\sigma_2,-1,\sigma_5,-\sigma_5,1)} {\sum_{\mathbf{k}_2 \ldots \mathbf{k}_7}}' \delta_{\mathbf{k}_4,-\mathbf{k}_1} \delta_{\mathbf{k}_4,\mathbf{k}_7} \delta_{\mathbf{k}_2,\mathbf{k}_3} \delta_{\mathbf{k}_5,\mathbf{k}_6} \tag{D.4}$$

$$\sum\nolimits_{(3)} \doteq \sum_{j=1}^{M} \sum_{\underline{\sigma}=(1,\sigma_2,\sigma_3,\sigma_4,-\sigma_2,-\sigma_3,-\sigma_4)} {\sum_{\mathbf{k}_2 \ldots \mathbf{k}_7}}' \delta^1_{234} \delta_{\mathbf{k}_2,\mathbf{k}_5} \delta_{\mathbf{k}_4,\mathbf{k}_7} \delta_{\mathbf{k}_3,\mathbf{k}_6} \tag{D.5}$$

- $\mathcal{J}_{\mathbf{3}}$ The prefactor is $O(L^d)$ and the $\sqrt{J_1 ...}$ term is $O\left(L^{-3d}\right)$. The leading order graphs are diagrams 1, 2, 3, 4, 5 and 6.
  - In diagrams 1, 2 and 3 we have three free wavenumbers, but $\mathbf{k}_1$ is discrete and so there are two free wavenumbers, making the contributions $O(1)$.
  - In diagrams 4, 5 and 6 $\mathbf{k}_1$ is discrete too but it is pinned. Two degrees of freedom remain, due to two free continuous wavenumbers.
  - All the other graphs are subleading.

The following contributions for $\mathcal{J}_3$ result:

$$
\begin{aligned}
&\left\langle e^{\sum_{\mathbf{k}} i\lambda_{\mathbf{k}} J_{\mathbf{k}}} \mathcal{J}_3 \right\rangle_J \sim \left(\frac{2\pi}{L}\right)^{2d} \delta_{\mu,0} \\
&\times \Bigg\{ 18 \sum_{(4)} \left\langle i\lambda_j \tilde{J}_j \tilde{J}_j \tilde{J}_3 \tilde{J}_5 e^{\Sigma \cdots} \right\rangle_J \mathcal{L}^{++\sigma_3\sigma_3}_{jj3(-3)} \mathcal{L}^{\sigma_3\sigma_5(-\sigma_5)(-\sigma_3)}_{(-3)553} E_T\left(0, \sigma_3(\tilde{\omega}_3 + \tilde{\omega}_{-3})\right) \\
&\quad + 9 \sum_{(5)} \left\langle i\lambda_j \tilde{J}_j \tilde{J}_3 \tilde{J}_6 e^{\Sigma \cdots} \right\rangle_J \mathcal{L}^{+\sigma_2(-\sigma_2)-}_{j22(-j)} \mathcal{L}^{-+\sigma_6(-\sigma_6)}_{(-j)j66} E_T\left(0, -(\tilde{\omega}_j + \tilde{\omega}_{-j})\right) \\
&\quad + 18 \sum_{(6)} \left\langle i\lambda_j \tilde{J}_j \tilde{J}_2 \tilde{J}_3 e^{\Sigma \cdots} \right\rangle_J \mathcal{L}^{+\sigma_2\sigma_3\sigma_4}_{j234} \mathcal{L}^{\sigma_4(-\sigma_2)+(-\sigma_3)}_{42j3} E_T\left(0, \tilde{\omega}^j_{234}\right) \Bigg\} \\
&+ \left(\frac{2\pi}{L}\right)^{2d} \Bigg\{ 18 \sum_{(7)} \left\langle \left[i\lambda_j + \frac{1}{2\tilde{J}_j} \right] \sqrt{\tilde{J}_j \tilde{J}_{-j}}\, \tilde{J}_3 \tilde{J}_5 e^{\Sigma \cdots} \right\rangle_J \mathcal{L}^{+-\sigma_3\sigma_4}_{j(-j)34} \\
&\qquad \times \mathcal{L}^{\sigma_4\sigma_5(-\sigma_5)(-\sigma_3)}_{4553} \prod_{m \neq \pm j} \delta_{\mu_m,0} \delta_{\mu_j,1} \delta_{\mu_{-j},1} \delta_{\mu_7,-\sigma_7} \\
&\qquad \times E_T\left(-(\tilde{\omega}_j + \tilde{\omega}_{-j}, -(\tilde{\omega}_j + \tilde{\omega}_{-j} + \sigma_3\tilde{\omega}_3 + \sigma_4\tilde{\omega}_4)\right) \\
&\qquad + 9 \sum_{(8)} \left\langle \left[i\lambda_j + \frac{1}{2\tilde{J}_j} \right] \sqrt{\tilde{J}_7 \tilde{J}_j}\, \tilde{J}_3 \tilde{J}_5 e^{\Sigma \cdots} \right\rangle_J \mathcal{L}^{+\sigma_2(-\sigma_2)\sigma_4}_{j224} \\
&\qquad \times \mathcal{L}^{\sigma_4\sigma_5(-\sigma_5)\sigma_7}_{4557} \prod_{m \neq j,7} \delta_{\mu_m,0} \delta_{\mu_j,1} \delta_{\mu_7,-\sigma_7} \\
&\qquad \times E_T\left(-\tilde{\omega}_j + \sigma_4\tilde{\omega}_4, -\sigma_4\tilde{\omega}_4 + \sigma_7\tilde{\omega}_7)\right) \\
&\qquad + 18 \sum_{(9)} \left\langle \left[i\lambda_j + \frac{1}{2\tilde{J}_j} \right] \sqrt{\tilde{J}_j \tilde{J}_{-j}}\, \tilde{J}_3 \tilde{J}_5 e^{\Sigma \cdots} \right\rangle_J \mathcal{L}^{+\sigma_2\sigma_3\sigma_4}_{j234} \\
&\qquad \times \mathcal{L}^{\sigma_4(-\sigma_2)-(-\sigma_3)}_{42(-j)3} \prod_{m \neq \pm j} \delta_{\mu_m,0} \delta_{\mu_j,1} \delta_{\mu_{-j},1} \\
&\qquad \times E_T\left(-(\tilde{\omega}_j + \tilde{\omega}_{-j}, -\sigma_4\tilde{\omega}_4 + \sigma_7\tilde{\omega}_7)\right) \Bigg\}
\end{aligned}
\tag{D.6}
$$

where the definitions given in Section 3.2.2 still hold for the summations, with slight variation:

$$
\begin{aligned}
\sum\nolimits_{(4)} &\doteq \sum_{j=1}^{M} \sum_{\underline{\sigma}=(1,1,\sigma_3,\sigma_3,\sigma_5,-\sigma_5,-\sigma_3)} \sum_{\mathbf{k}_2 \ldots \mathbf{k}_7}{}' \delta_{\mathbf{k}_4,-\mathbf{k}_3} \delta_{\mathbf{k}_j,\mathbf{k}_2} \delta_{\mathbf{k}_3,\mathbf{k}_7} \delta_{\mathbf{k}_5,\mathbf{k}_6} \\
\sum\nolimits_{(5)} &\doteq \sum_{j=1}^{M} \sum_{\underline{\sigma}=(1,\sigma_2,-\sigma_2,-1,1,\sigma_6,-\sigma_6)} \sum_{\mathbf{k}_2 \ldots \mathbf{k}_7}{}' \delta_{\mathbf{k}_j,-\mathbf{k}_4} \delta_{\mathbf{k}_j,\mathbf{k}_5} \delta_{\mathbf{k}_3,\mathbf{k}_2} \delta_{\mathbf{k}_6,\mathbf{k}_7} \\
\sum\nolimits_{(6)} &\doteq \sum_{j=1}^{M} \sum_{\underline{\sigma}=(1,\sigma_2,\sigma_3,\sigma_4,-\sigma_2,1,-\sigma_3)} \sum_{\mathbf{k}_2 \ldots \mathbf{k}_7}{}' \delta^j_{234} \delta_{\mathbf{k}_j,\mathbf{k}_6} \delta_{\mathbf{k}_3,\mathbf{k}_7} \delta_{\mathbf{k}_5,\mathbf{k}_2} \\
\sum\nolimits_{(7)} &\doteq \sum_{j=1}^{M} \sum_{\underline{\sigma}=(1,-1,\sigma_3,\sigma_4,\sigma_5,-\sigma_5,-\sigma_3)} \sum_{\mathbf{k}_2 \ldots \mathbf{k}_7}{}' \delta_{-\sigma_4\mathbf{k}_4,\sigma_3\mathbf{k}_3} \delta_{\mathbf{k}_j,-\mathbf{k}_2} \delta_{\mathbf{k}_3,\mathbf{k}_7} \delta_{\mathbf{k}_5,\mathbf{k}_6} \\
\sum\nolimits_{(8)} &\doteq \sum_{j=1}^{M} \sum_{\underline{\sigma}=(1,\sigma_2,-\sigma_2,\sigma_4,\sigma_5,-\sigma_5,\sigma_7)} \sum_{\mathbf{k}_2 \ldots \mathbf{k}_7}{}' \delta_{\mathbf{k}_j,\sigma_4\mathbf{k}_4} \delta_{\mathbf{k}_j,\sigma_7\mathbf{k}_7} \delta_{\mathbf{k}_3,\mathbf{k}_2} \delta_{\mathbf{k}_5,\mathbf{k}_6} \\
\sum\nolimits_{(9)} &\doteq \sum_{j=1}^{M} \sum_{\underline{\sigma}=(1,\sigma_2,\sigma_3,\sigma_4,-\sigma_2,-1,-\sigma_3)} \sum_{\mathbf{k}_2 \ldots \mathbf{k}_7}{}' \delta^j_{234} \delta_{\mathbf{k}_j,-\mathbf{k}_6} \delta_{\mathbf{k}_3,\mathbf{k}_7} \delta_{\mathbf{k}_5,\mathbf{k}_2}
\end{aligned}
\tag{D.7}
$$

- $\mathcal{J}_4$ The prefactor is of order $O(L^{2d})$ and $\sqrt{J_1...}$ is $O\left(L^{-4d}\right)$. One needs at least a type I diagram with two continuous free wavenumbers to make $\mathcal{J}_4$ order $O(1)$. All other diagrams are subleading. In the graph of $\mathcal{J}_4$ in Fig.C.19, $\mathbf{k}_1$ is pinned to an external blob ($\mu_1 = 2$). The leading order diagrams are type I, with two free wavenumbers (Figs. C.20 and C.21).

  - Diagrams 1 and 2 in Fig. C.20 are vanishing, as already shown.
  - Diagrams 3 and 4 (Fig. C.21) have two free continuous wavenumbers, responsible for two degrees of freedom. Considering the prefactor ($\frac{1}{2}\lambda_1^2 + \frac{\lambda_1\mu_1}{2\tilde{J}_1}$, because here $\frac{\mu_1}{2} - 1 = 0$), the $\sqrt{J_1...}$ term and the two free sums, both diagrams give an $O(1)$ contribution to $\mathcal{J}_4$.

    Diagram 3: $\mathbf{k}_1 = \sigma_2\mathbf{k}_2 + \sigma_3\mathbf{k}_3 + \sigma_4\mathbf{k}_4$, $\mathbf{k}_2 = \mathbf{k}_3$, $\sigma_3 = -\sigma_2 \Rightarrow \mathbf{k}_1 = \sigma_4\mathbf{k}_4$, $\mathbf{k}_1 = \sigma_7\mathbf{k}_7 \Rightarrow \sigma_4\mathbf{k}_4 = \sigma_7\mathbf{k}_7$, $\mathbf{k}_4 = \mathbf{k}_7$, $\sigma_4 = \sigma_7$. If $\sigma_4 = +1$, then $\mathbf{k}_1 = \mathbf{k}_4$. Because of *Rule 5*, the left vertex is vanishing and so the diagram is not contributing. If $\sigma_4 = -1$, then $\mathbf{k}_4 = -\mathbf{k}_1$, $\sigma_7 = -1$ and $\mathbf{k}_7 = \mathbf{k}_4 = -\mathbf{k}_1$. There are 9 graphs equivalent to diagram 3, obtained substituting 4 with 2 and 3 and substituting 7 with 5 and 6, cf. (D.8).

    Diagram 4. If $\sigma_4 = -1$, then $\mathbf{k}_4 = -\mathbf{k}_1$, $\sigma_7 = 1$ and $\mathbf{k}_7 = \mathbf{k}_1$. Because of *Rule 5*, the right vertex is vanishing and the diagram does not contribute. If $\sigma_4 = +1$, then $\mathbf{k}_4 = \mathbf{k}_1$. The left vertex vanishes. Therefore, this graph does not contribute. Therefore:

$$\begin{aligned}\left\langle e^{\sum_{\mathbf{k}} i\lambda_{\mathbf{k}} J_{\mathbf{k}}}\mathcal{J}_4\right\rangle_J \sim \left(\frac{2\pi}{L}\right)^{2d} 9\sum_{(10)}\left\langle\Big[-\frac{1}{2}\lambda_j^2 + i\frac{\lambda_j}{\tilde{J}_j}\Big]\tilde{J}_j\tilde{J}_{-j}\tilde{J}_2\tilde{J}_5 e^{\sum_m i\lambda_m\tilde{J}_m}\right\rangle_J \\ \times\mathcal{L}_{j234}^{+\sigma_2\sigma_3\sigma_4}\mathcal{L}_{j567}^{+\sigma_5\sigma_6\sigma_7}\delta_{\mu_j,2}\delta_{\mu_{-j},2}\prod_{m\neq\pm j}\delta_{\mu,0} \\ \times\Delta_T\left(-\tilde{\omega}_j - \tilde{\omega}_{-j}\right)\Delta_T\left(-\tilde{\omega}_j - \tilde{\omega}_{-j}\right) \qquad \text{(D.8)}\end{aligned}$$

$$\sum\nolimits_{(10)} \doteq \sum_{j=1}^{M}\sum_{\underline{\sigma}=(1,\sigma_2,-\sigma_2,-1,\sigma_5,-\sigma_5,-1)}\sum_{\mathbf{k}_2...\mathbf{k}_7}{}' \delta_{\mathbf{k}_1,-\mathbf{k}_4}\delta_{\mathbf{k}_4,\mathbf{k}_7}\delta_{\mathbf{k}_5,\mathbf{k}_6}\delta_{\mathbf{k}_2,\mathbf{k}_3} \qquad \text{(D.9)}$$

- $\mathcal{J}_5$ The order $O(L^{2d})$ from the prefactor and the $O\left(L^{-4d}\right)$ from the $\sqrt{J_1...}$ term lead to a global $O\left(L^{-2d}\right)$. So, we have to seek graphs with two free continuous wavenumbers, cf. (D.10).

  - Diagram 1 in Fig. C.25 (for $B1$) and a similar one for B_2, with the arrow referred to 1 reversed, have two free discrete wavenumbers. μ_1 and μ_2 are identically null due to the internal couplings of $\mathbf{k}_1$ and $\mathbf{k}_2$. At each vertex, the sum of the two discrete wavenumbers is discrete. Then, because of the vertex condition ("momentum conservation") only one continuous free wavenumber remains (so as in one dimension, if the sum of the discrete wavenumbers is an integer n, the two continuous wavenumbers can be chosen as a real x and the constrained $-n - x$, so that $n + x + (-n - x) = 0$). Thus, diagram 1 does not contribute to the leading order of $\mathcal{J}_5$.
  - Diagram 3 in Fig. C.26 (referred to B_1) has two continuous free wavenumbers (in one dimension, the three continuous wavenumbers are x, y, $-x-y-n$, if the discrete wavenumber is n, so that $n + x + y + (-x - y - n) = 0$ at each vertex). This diagram is leading order and its multiplicity is 6.
  - Let us turn our attention to diagram 5 in Fig. C.27. The condition of the left vertex delta gives $\mathbf{k}_1 = \sigma_3\mathbf{k}_3$. There are two cases:
    if $\sigma_3 = +1 \Rightarrow \mathbf{k}_1 = \mathbf{k}_3$, because of *Rule 5* this contribution is vanishing;
    if $\sigma 3 = -1 \Rightarrow \mathbf{k}_1 = -\mathbf{k}_3$, $\mathbf{k}_1 = \mathbf{k}_6$, $\sigma_6 = +1$, the right vertex conditions says: $\mathbf{k}_2 = \sigma_6\mathbf{k}_6 = -\mathbf{k}_6 = -\mathbf{k}_1$. This is forbidden by the condition on the sum, stating that $\mathbf{k}_1 \neq \mathbf{k}_2$. Thus, this graph does not represent any physical interaction.

– A diagram analogous to 5 in Fig. C.27, but with the "1" arrow reversed, is possible for B_2. One has that $-\mathbf{k}_1 = \sigma_3 \mathbf{k}_3$.
If $\sigma_3 = -1$: $\mathbf{k}_1 = \mathbf{k}_3$, $\sigma_3 = -1$, we have a vanishing contribution;
If $\sigma_3 = +1$: $\mathbf{k}_3 = -\mathbf{k}_1$, $\mathbf{k}_6 = \mathbf{k}_1$, $\sigma_6 = -1$. The right vertex condition gives: $\mathbf{k}_1 = \sigma_6 \mathbf{k}_6 \Rightarrow \mathbf{k}_2 = -\mathbf{k}_6 = -\mathbf{k}_1 \ (\neq \mathbf{k}_1)$. We notice that $\mathbf{k}_2 = \mathbf{k}_3$, and $\mathbf{k}_2$ is a sink while $\mathbf{k}_3$ is a source. The total momentum is conserved. The multiplicity of such a graph is 9.

– A graph analogous to 5 in Fig. C.27 is also possible for B_3, if one reverses the "2" arrow. The case $\sigma_3 = +1$ requires $\mathbf{k}_1 = \mathbf{k}_3$, we have a vanishing contribution;
If $\sigma_3 = -1$, $\mathbf{k}_3 = -\mathbf{k}_1$, $\mathbf{k}_6 = \mathbf{k}_1$,
$\sigma_6 = 1$, $\sigma_6 \mathbf{k}_6 = -\mathbf{k}_2 \Rightarrow \mathbf{k}_2 = -\mathbf{k}_6 \ (\neq \mathbf{k}_1)$. We have that $\mathbf{k}_2 = \mathbf{k}_3$, but now $\mathbf{k}_2$ is the source and $\mathbf{k}_3$ is the sink. It is the simmetric of the situation previously described for B_2. The multiplicity of this contribution is 9.

– One more contribution comes from a graph analogous to diagram 5 in Fig. C.27 but with 1 and 2 exchanged. In such a case $\mu_2 = 0$, so it is useless to compute the contribution from B_3. Then, one can easily notice that the contribution from B_2 is exacly the same as that just calculated for B_3 at the previous point, but permuting 1 with 2 and using the right prefactor. The multiplicity of this graph is 9 too.

– The last non-zero contribution comes from diagram 6 in Fig. C.28. Here, $\sigma_6 = -1$, $\sigma_3 = -1$, $\mathbf{k}_1 = -\mathbf{k}_3$, $\mathbf{k}_6 = \mathbf{k}_1$ and $\mathbf{k}_2 = \sigma_6 \mathbf{k}_6 = -\mathbf{k}_1$. There is also an identical contribution permuting 1 with 2, so we add a factor 2 to the multiplicity, which become equal to 18.

Finally, the $\mathcal{J}_5$ total contribution is the following:

$$
\begin{aligned}
\left\langle e^{\sum_{\mathbf{k}} i\lambda_{\mathbf{k}} J_{\mathbf{k}}} \mathcal{J}_5 \right\rangle_J \sim \frac{1}{2}\left(\frac{2\pi}{L}\right)^{2d} & \\
\times \Bigg\{ 6 \sum_{(11)} \Big\langle \Big[-\lambda_j \lambda_{-j} + i\frac{\lambda_j}{\tilde{J}_{-j}} + \frac{1}{4\tilde{J}_j \tilde{J}_{-j}} + \Big] \sqrt{\tilde{J}_j \tilde{J}_{-j}}\, \tilde{J}_3 \tilde{J}_4 \tilde{J}_5 & \\
\times e^{\sum_m i\lambda_m \tilde{J}_m} \Big\rangle_J \mathcal{L}^{+\sigma_3\sigma_4\sigma_5}_{j345} \mathcal{L}^{-(-\sigma_6)(-\sigma_7)(-\sigma_8)}_{(-j)345} \delta_{\mu_j,1} \delta_{\mu_{-j},1} & \\
\times \prod_{m \neq \pm j} \delta_{\mu,0} \Delta_T \left(\tilde{\omega}^j_{345}\right) \Delta_T \left(\tilde{\omega}^{(-j)345}\right) & \\
- 9 \sum_{(12)} \Big\langle \lambda_j \lambda_{-j} \tilde{J}_j \tilde{J}_{-j} \tilde{J}_4 \tilde{J}_7 e^{\Sigma \cdots} \Big\rangle_J \mathcal{L}^{-+\sigma_4(-\sigma_4)}_{j(-j)44} \mathcal{L}^{+-\sigma_7(-\sigma_7)}_{(-j)j77} & \\
\times \delta_{\mu_{-j},1} \prod_{m \neq -j} \delta_{\mu,0} \ \left|\Delta_T \left(-\tilde{\omega}_{-j} - \tilde{\omega}_j\right)\right|^2 & \\
+ 9 \sum_{(13)} \Big\langle \frac{\lambda_j}{\tilde{J}_{-j}} \tilde{J}_j \tilde{J}_{-j} \tilde{J}_4 \tilde{J}_7 e^{\Sigma \cdots} \Big\rangle_J \mathcal{L}^{+-\sigma_4(-\sigma_4)}_{j(-j)44} \mathcal{L}^{-+\sigma_7(-\sigma_7)}_{(-j)j77} & \\
\times \delta_{\mu_{-j},-1} \prod_{m \neq l} \delta_{\mu,0} \ \left|\Delta_T \left(\tilde{\omega}_j + \tilde{\omega}_{-j}\right)\right|^2 & \\
- 9 \sum_{(14)} \Big\langle \lambda_j \lambda_{-j} \tilde{J}_j \tilde{J}_{-j} \tilde{J}_4 \tilde{J}_7 e^{\Sigma \cdots} \Big\rangle_J \mathcal{L}^{-+\sigma_4(-\sigma_4)}_{jj44} \mathcal{L}^{+-\sigma_7(-\sigma_7)}_{(-j)(-j)77} & \\
\times \delta_{\mu_j,-1} \prod_{m \neq j} \delta_{\mu,0} \ \left|\Delta_T \left(\tilde{\omega}_j + \tilde{\omega}_{-j}\right)\right|^2 & \\
+ 18 \sum_{(15)} \Big\langle \Big[-\lambda_j \lambda_{-j} + i\frac{2\lambda_j}{\tilde{J}_{-j}} + \frac{1}{\tilde{J}_j \tilde{J}_{-j}} \Big] e^{\Sigma \cdots} \Big\rangle_J \tilde{J}_j \tilde{J}_{-j} \tilde{J}_4 \tilde{J}_7 & \\
\times \mathcal{L}^{+-\sigma_4(-\sigma_4)}_{j(-j)44} \mathcal{L}^{-+\sigma_7(-\sigma_7)}_{(-j)j77} \delta_{\mu_j,2} \delta_{\mu_{-j},2} \prod_{m \neq j,l} \delta_{\mu,0} \left(\Delta_T \left(-\tilde{\omega}_j - \tilde{\omega}_{-j}\right)\right)^2 \Bigg\} &
\end{aligned}
\tag{D.10}
$$

$$
\begin{aligned}
\sum\nolimits_{(11)} &\doteq \sum_{j\neq l} \sum_{\underline{\sigma}=(1,1,\sigma_3,\sigma_4,\sigma_5,-\sigma_3,-\sigma_4,-\sigma_5)} \sum_{\mathbf{k}_3\ldots\mathbf{k}_8}{}' \delta_{\mathbf{k}_j,-\mathbf{k}_l}\delta_{\mathbf{k}_3,\mathbf{k}_6}\delta_{\mathbf{k}_4,\mathbf{k}_7}\delta_{\mathbf{k}_5,\mathbf{k}_8} \\
\sum\nolimits_{(12)} &\doteq \sum_{j\neq l} \sum_{\underline{\sigma}=(1,1,1,\sigma_4,-\sigma_4,-1,\sigma_7,-\sigma_7)} \sum_{\mathbf{k}_3\ldots\mathbf{k}_8}{}' \delta_{\mathbf{k}_j,-\mathbf{k}_l}\delta_{\mathbf{k}_3,-\mathbf{k}_j}\delta_{\mathbf{k}_6,\mathbf{k}_j}\delta_{\mathbf{k}_7,\mathbf{k}_8}\delta_{\mathbf{k}_4,\mathbf{k}_5} \\
\sum\nolimits_{(13)} &\doteq \sum_{j\neq l} \sum_{\underline{\sigma}=(1,-1,-1,\sigma_4,-\sigma_4,1,\sigma_7,-\sigma_7)} \sum_{\mathbf{k}_3\ldots\mathbf{k}_8}{}' \delta_{\mathbf{k}_j,-\mathbf{k}_l}\delta_{\mathbf{k}_3,-\mathbf{k}_j}\delta_{\mathbf{k}_6,\mathbf{k}_j}\delta_{\mathbf{k}_7,\mathbf{k}_8}\delta_{\mathbf{k}_4,\mathbf{k}_5} \\
\sum\nolimits_{(14)} &\doteq \sum_{j\neq l} \sum_{\underline{\sigma}=(-1,1,1,\sigma_4,-\sigma_4,-1,\sigma_7,-\sigma_7)} \sum_{\mathbf{k}_3\ldots\mathbf{k}_8}{}' \delta_{\mathbf{k}_j,-\mathbf{k}_l}\delta_{\mathbf{k}_6,-\mathbf{k}_l}\delta_{\mathbf{k}_3,\mathbf{k}_j}\delta_{\mathbf{k}_7,\mathbf{k}_8}\delta_{\mathbf{k}_4,\mathbf{k}_5} \\
\sum\nolimits_{(15)} &\doteq \sum_{j\neq l} \sum_{\underline{\sigma}=(1,1,-1,\sigma_4,-\sigma_4,-1,\sigma_7,-\sigma_7)} \sum_{\mathbf{k}_3\ldots\mathbf{k}_8}{}' \delta_{\mathbf{k}_j,-\mathbf{k}_3}\delta_{\mathbf{k}_j,-\mathbf{k}_l}\delta_{\mathbf{k}_6,\mathbf{k}_j}\delta_{\mathbf{k}_7,\mathbf{k}_8}\delta_{\mathbf{k}_4,\mathbf{k}_5}
\end{aligned}
\tag{D.11}
$$

References

[1] S. Nazarenko, Wave Turbulence, Vol. 825 of Lecture Notes in Physics, Springer, 2011.

[2] A. C. Newell, B. Rumpf, Wave turbulence, Annual Review of Fluid Mechanics 43 (2011) 59–78.

[3] V. E. Zakharov, V. S. L'vov, G. Falkovich, Kolmogorov spectra of turbulence I. Wave turbulence, Springer series in nonlinear dynamics, Springer Berlin, 1992.

[4] G. J. Komen, L. Cavaleri, M. Donelan, K. Hasselmann, S. Hasselmann, P. Janssen, Dynamics and modelling of ocean waves, Cambridge University Press, 1996.

[5] E. Falcon, C. Laroche, S. Fauve, Observation of gravity-capillary wave turbulence, Phys. Rev. Lett. 98 (9) (2007) 094503.

[6] M. Onorato, A. R. Osborne, M. Serio, S. Bertone, Freak waves in random oceanic sea states, Phys. Rev. Lett. 86 (25) (2001) 5831.

[7] V. Zakharov, N. Filonenko, Zh. Prikl. Mekh. I Tekn. Fiz. 5 (1967) 62.

[8] A. Pushkarev, Z. V.E., Turbulence of capillary waves, Phys. Rev. Lett. 76 (18) (1996) 3320–3323.

[9] C. Falcon, E. Falcon, U. Bortolozzo, S. Fauve, Capillary wave turbulence on a spherical fluid surface in low gravity, Europhys. Lett. 86 (2009) 14002.

[10] S. Galtier, S. Nazarenko, A. C. Newell, A. Pouquet, A weak turbulence theory for incompressible magnetohydrodynamics, J. Plasma Phys. 63 (05) (2000) 447–488.

[11] A. Picozzi, J. Garnier, T. Hansson, P. Suret, S. Randoux, G. Millot, D. Christodoulides, Optical wave turbulence: Towards a unified nonequilibrium thermodynamic formulation of statistical nonlinear optics, Phys. Rep. 542 (2014) 1–132.

[12] G. Düring, C. Josserand, S. Rica, Weak turbulence for a vibrating plate: Can one hear a kolmogorov spectrum?, Phys. Rev. Lett. 97 (2) (2006) 25503.

[13] A. Boudaoud, O. Cadot, B. Odille, C. Touzé, Observation of wave turbulence in vibrating plates, Phys. Rev. Lett. 100 (23) (2008) 234504.

[14] N. Mordant, Are there waves in elastic wave turbulence?, Phys. Rev. Lett. 100 (23) (2008) 234505.

[15] U. Frisch, Turbulence: the legacy of AN Kolmogorov, Cambridge university press, 1995.

[16] E. Falcon, S. Roux, C. Laroche, On the origin of intermittency in wave turbulence, Europhys. Lett. 90 (3) (2010) 34005.

[17] R. Meyrand, K. Kiyani, S. Galtier, Weak magnetohydrodynamic turbulence and intermittency, Journal of Fluid Mechanics 770 (2015) R1.

[18] Y. Choi, Y. V. Lvov, S. Nazarenko, B. Pokorni, Anomalous probability of large amplitudes in wave turbulence, Phys. Lett. A 339 (2005) 361–369.

[19] Y. Choi, Y. V. Lvov, S. Nazarenko, Joint statistics of amplitudes and phases in wave turbulence, Physica D 201 (2005) 121–149.

[20] P. Jakobsen, A. C. Newell, Invariant measures and entropy production in wave turbulence, J. Stat. Mech.-Theory E. 2004 (2004) L10002.

[21] G. L. Eyink, Y.-K. Shi, Kinetic wave turbulence, Physica D: Nonlinear Phenomena 241 (2012) 1487–1511.

[22] O. Kurbanmuradov, Convergence of numerical models for the Gaussian fields, Russ. J. Numer. Anal. M. 10 (1995) 311–323.

[23] O. E. Lanford, Time evolution of large classical systems, in: J. Moser (Ed.), Dynamical Systems, Theory and Applications, Vol. 38 of Lecture Notes in Physics, Springer Berlin / Heidelberg, 1975, pp. 1–111.

[24] O. E. Lanford, On the derivation of the Boltzmann equation, Asterisque 40 (1976) 117–137.

[25] H. W. Wyld, Ann. Phys. 14 (1961) 143.

[26] V. E. Zakharov, V. S. L'vov, Statistical description of nonlinear wave fields, Radiophys. Quantum El. 18 (1975) 1084–1097.

[27] D. J. Benney, A. C. Newell, Random wave closures, Stud. Appl. Math. 48 (1969) 29–53.

[28] G. Düring, C. Josserand, S. Rica, Weak turbulence for a vibrating plate: can one hear a kolmogorov spectrum?, Phys. Rev. Lett. 97.2 (2006) 025503.